



**HAL**  
open science

## **A multi-proxy approach to Late Holocene fluctuations of Tungnahryggsjökull glaciers in the Tröllaskagi peninsula (northern Iceland)**

José M. Fernández-Fernández, David Palacios, Nuria Andrés, Irene Schimmelpfennig, Skafti Brynjólfsson, Leopoldo Sancho, Jose Zamorano, Starri Heiðmarsson, Þorsteinn Sæmundsson

### ► To cite this version:

José M. Fernández-Fernández, David Palacios, Nuria Andrés, Irene Schimmelpfennig, Skafti Brynjólfsson, et al.. A multi-proxy approach to Late Holocene fluctuations of Tungnahryggsjökull glaciers in the Tröllaskagi peninsula (northern Iceland). *Science of the Total Environment*, 2019, 664, pp.499-517. 10.1016/j.scitotenv.2019.01.364 . hal-02013550

**HAL Id: hal-02013550**

**<https://hal.science/hal-02013550>**

Submitted on 13 May 2022

**HAL** is a multi-disciplinary open access archive for the deposit and dissemination of scientific research documents, whether they are published or not. The documents may come from teaching and research institutions in France or abroad, or from public or private research centers.

L'archive ouverte pluridisciplinaire **HAL**, est destinée au dépôt et à la diffusion de documents scientifiques de niveau recherche, publiés ou non, émanant des établissements d'enseignement et de recherche français ou étrangers, des laboratoires publics ou privés.

## A multi-proxy approach to Late Holocene fluctuations of Tungnahryggsjökull glaciers in the Tröllaskagi peninsula (northern Iceland).

José M. Fernández-Fernández<sup>(1)</sup>, David Palacios<sup>(1)</sup>, Nuria Andrés<sup>(1)</sup>, Irene Schimmelpfennig<sup>(2)</sup>, Skafti Brynjólfsson<sup>(3)</sup>, Leopoldo G. Sancho<sup>(4)</sup>, José J. Zamorano<sup>(5)</sup>, Starri Heiðmarsson<sup>(3)</sup>, Þorsteinn Sæmundsson<sup>(6)</sup>, ASTER Team<sup>(2, 7)</sup>.

<sup>(1)</sup> High Mountain Physical Geography Research Group. Department of Geography, Faculty of Geography and History, Universidad Complutense de Madrid, 28040 Madrid, Spain.

<sup>(2)</sup> Aix-Marseille Université, CNRS, IRD, Coll. France, UM 34 CEREGE, Technopôle de l'Environnement Arbois-Méditerranée, BP 80, 13545 Aix-en-Provence, France.

<sup>(3)</sup> Icelandic Institute of Natural History, Borgum við Norðurslóð, Box 180, 602 Akureyri, Iceland.

<sup>(4)</sup> Departament of Vegetal Biology II, Faculty of Pharmacology, Universidad Complutense de Madrid, 28040, Madrid, Spain.

<sup>(5)</sup> Instituto de Geografía, Universidad Nacional Autónoma de México, Ciudad Universitaria, 04510 Ciudad de México, Mexico.

<sup>(6)</sup> Faculty of Life and Environmental Science, University of Iceland, Öskju, Sturlugötu 7, 101 Reykjavík, Iceland.

<sup>(7)</sup> Consortium: Georges Aumaître, Didier Bourlès, Karim Keddadouche.

### Corresponding author:

José M. Fernández-Fernández, [josemariafernandez@ucm.es](mailto:josemariafernandez@ucm.es)  
High Mountain Physical Geography Research Group.  
Department of Geography.  
Faculty of Geography and History, Universidad Complutense de Madrid  
Profesor Aranguren St., 28040 – Madrid, SPAIN

## 1 Abstract

2 The Tröllaskagi Peninsula in northern Iceland hosts more than a hundred small glaciers  
3 that have left a rich terrestrial record of Holocene climatic fluctuations in their  
4 forelands. Traditionally, it has been assumed that most of the Tröllaskagi glaciers  
5 reached their Late Holocene maximum extent during the Little Ice Age (LIA). However,  
6 there is evidence of slightly more advanced pre-LIA positions. LIA moraines from  
7 Iceland have been primary dated mostly through lichenometric dating, but the limitations  
8 of this technique do not allow dating of glacial advances prior to the 18<sup>th</sup> or 19<sup>th</sup>  
9 centuries. The application of <sup>36</sup>Cl Cosmic-Ray Exposure (CRE) dating to  
10 Tungnahryggsjökull moraine sequences in Vesturdalur and Austurdalur (central  
11 Tröllaskagi) has revealed a number of pre-LIA glacial advances at ~400 and ~700 CE,  
12 and a number of LIA advances in the 15<sup>th</sup> and 17<sup>th</sup> centuries, the earliest LIA advances  
13 dated so far in Tröllaskagi. This technique hence shows that the LIA chronology in  
14 Tröllaskagi agrees with that of other European areas such as the Alps or the  
15 Mediterranean mountains. The combined use of lichenometric dating, aerial  
16 photographs, satellite images and fieldwork shows that the regional colonization lag of  
17 the commonly used lichen species *Rhizocarpon geographicum* is longer than previously  
18 assumed. For exploratory purposes, an alternative lichen species (*Porpidia soredizodes*)  
19 has been tested for lichenometric dating, estimating a tentative growth rate of 0.737 mm  
20 yr<sup>-1</sup>.

## 21 1. Introduction

22 The Tröllaskagi Peninsula (northern Iceland) hosts over 160 small alpine cirque glaciers  
23 (Björnsson, 1978; see synthesis in Andrés et al., 2016). Only a few of these small  
24 glaciers do not have supraglacial debris cover that allows them to react quickly to small  
25 climatic fluctuations (Caseldine, 1985b; Häberle, 1991; Kugelmann, 1991), compared to

26 the reduced dynamism of the predominant rock glaciers and debris-covered glaciers  
27 ([Martin et al., 1991](#); [Andrés et al., 2016](#); [Tanarro et al., 2019](#)). As a result of their high  
28 sensitivity to climatic changes, the few debris-free glaciers in Tröllaskagi fluctuated  
29 repeatedly in the past, forming a large number of moraines in front of their termini (see  
30 [Caseldine, 1983, 1985b, 1987](#); [Kugelmann, 1991](#) amongst others). However, the  
31 relation between glacier fluctuations and the climate is complicated due to: (i) the well-  
32 known surging potential activity in Tröllaskagi ([Brynjólfsson et al., 2012](#); [Ingólfsson et](#)  
33 [al., 2016](#)); (ii) the possibility of glaciers being debris-covered in the past, with the  
34 subsequent change of their climate sensitivity over time; (iii) the intense and dynamic  
35 slope geomorphological activity, paraglacial to a great extent ([Jónsson, 1976](#); [Whalley](#)  
36 [et al., 1983](#); [Mercier et al., 2013](#); [Cossart et al., 2014](#); [Feuillet et al., 2014](#); [Decaulne and](#)  
37 [Sæmundsson, 2006](#); [Sæmundsson et al., 2018](#)) that hides and erases the previous glacial  
38 features.

39 In Iceland, a great part of the research on glacial fluctuations during the late Holocene,  
40 LIA ([Grove, 1988](#); 1250-1850 CE, see [Solomina et al., 2016](#)) and later stages has been  
41 approached through application of radiocarbon dating of organic material, analyzing  
42 lake sediment varves ([Larsen et al., 2011](#); [Striberger et al., 2012](#)), dead vegetation  
43 remnants ([Harning et al., 2018](#)) and threshold lake sediment records ([Harning et al.,](#)  
44 [2016b](#); [Schomacker et al., 2016](#)). These provide high-resolution records of glacier  
45 variability. In Tröllaskagi, very few reliable dates exist at present, obtained from  
46 radiocarbon and tephrochronology ([Häberle, 1991, 1994](#); [Stötter, 1991](#); [Stötter et al.,](#)  
47 [1999](#); [Wastl and Stötter, 2005](#)). They suggest that late Holocene glaciers were slightly  
48 more advanced than during the LIA maximum in Tröllaskagi. However, these  
49 techniques only provide minimum or maximum ages for Holocene glacier history in  
50 northern Iceland ([Wastl and Stötter, 2005](#)). In addition, at Tröllaskagi most of the

51 moraines are at 600-1000 m a.s.l., where the applicability of tephrochronology is very  
52 limited (Caseldine, 1990) due to the great intensity of slope geomorphological  
53 processes.

54 In any case, most of the moraine datings of Tröllaskagi –especially those of the last  
55 millenium– comes from lichenometry (see synthesis in Decaulne, 2016). However, the  
56 ages derived from this technique tend to be younger if they are compared to those  
57 estimated from tephra layers (Kirkbride and Dugmore, 2001). Generally, there is  
58 disagreement about the validity of the results provided by lichenometry, due to the  
59 difficulty of the lichen species identification in the field, the complexity and reliability  
60 of the sampling and measurement strategies, the uncertainty estimates, the nature of the  
61 ages provided as relative, as well as the relative reliability at producing lichen growth  
62 curves of the different species, with an extreme dependence on local environmental  
63 factors (see Osborn et al., 2015).

64 In fact, these problems had already been detected in northern Iceland, where in spite of  
65 the time elapsed since the first applications of this technique (Jaksch, 1970, 1975, 1984;  
66 Gordon and Sharp, 1983; Maizels and Dugmore, 1985) and contrasting with its  
67 widespread use in the south and southeast of the island (Thompson and Jones, 1986;  
68 Evans et al., 1999; Russell et al., 2001; Kirkbride and Dugmore, 2001; Bradwell, 2001,  
69 2004a; Harris et al., 2004; Bradwell and Armstrong, 2006; Orwin et al., 2008; Chenet et  
70 al., 2010 and others), there are still very few established growth rates for the lichen  
71 group *Rhizocarpon geographicum* (Roca-Valiente et al., 2016) from Tröllaskagi  
72 (Caseldine, 1983; Häberle, 1991; Kugelmann, 1991; Caseldine and Stötter, 1993; see  
73 synthesis in Decaulne, 2016). In general, the growth curves from Tröllaskagi suffer  
74 from a few control points (i.e. surfaces of known age) for calibration. This leads to  
75 considerable underestimation when lichen thalli sizes are beyond the calibration growth

76 curve (Caseldine, 1990; see e.g. Caseldine, 1985b; Caseldine and Stötter, 1993;  
77 Kugelmann, 1991). That is to say, the extrapolation does not account for the decreasing  
78 growth rate with increasing age (i.e. non-linear growth). Kugelmann's (1991) growth  
79 curve has the highest number of control points to date (19 in total). In addition, the  
80 colonization lag in Tröllaskagi is poorly defined, although 10-15 years have been  
81 assumed for the *Rhizocarpon geographicum* (Caseldine, 1983; Kugelmann, 1991).  
82 Other issues, such as the absence of large thalli (Maizels and Dugmore, 1985), lichen  
83 saturation (e.g. Wiles et al., 2010), and other environmental factors (Innes, 1985 and  
84 references included; Hamilton and Whalley, 1995) contribute to appreciable age  
85 underestimations when dating surfaces using this approach. Snow is also a major  
86 environmental factor for lichenometry in Iceland due to its long residence time on the  
87 ground (Dietz et al., 2012) and the avalanching frequency –especially in Tröllaskagi–,  
88 whose effect restricts the growth rate of lichens, and even destroys them (Sancho et al.,  
89 2017). These problems considerably limit the quality (reliability) of the lichenometric  
90 dating range of utility for applying lichenometric dating in Iceland, where the oldest  
91 ages estimated so far are between 160 and 220 years (Maizels and Dugmore, 1985;  
92 Thompson and Jones, 1986; Evans et al., 1999), thus preventing the dating of glacial  
93 advances prior to the 18<sup>th</sup> century.

94 In spite of the high uncertainty of the lichenometric dating, many authors working in  
95 Tröllaskagi have treated their lichenometric results as absolute ages (see Caseldine,  
96 1983, 1985b, 1987; Kugelmann, 1991; Häberle, 1991; Caseldine and Stötter, 1993,  
97 amongst others). In fact, previously considered dates of LIA maximum glacier  
98 culmination are restricted to the very late 18<sup>th</sup> and early 19<sup>th</sup> centuries (Caseldine, 1983,  
99 1985b, 1987; Kugelmann, 1991; Caseldine and Stötter, 1993; Caseldine, 1991; Martin  
100 et al., 1991), very close to the applicability threshold of this method. Consequently, no

101 evidence of previous advances during phases of the LIA that were more conducive to  
102 glacier expansion (probably colder; see e.g. [Ogilvie, 1984, 1996](#); [Ogilvie and Jónsdóttir,](#)  
103 [2000](#); [Ogilvie and Jónsson, 2001](#)) has been found ([Kirkbride and Dugmore, 2001](#)).

104 In the recent years, dating methods based on the Exposure to the Cosmic-Rays (CRE)  
105 have been introduced successfully to date moraines of the last millennium, and even  
106 formed during the LIA ([Schimmelpfennig et al., 2012, 2014](#); [Le Roy et al., 2017](#);  
107 [Young et al., 2015](#); [Jomelli et al., 2016](#); [Li et al., 2016](#); [Dong et al., 2017](#); [Palacios et](#)  
108 [al., 2018](#)). The cosmogenic nuclides  $^{36}\text{Cl}$  and  $^3\text{He}$  have been applied previously in  
109 northern Iceland to date the Pleistocene deglaciation. [Principato et al. \(2006\)](#) studied the  
110 deglaciation of Vestfirðir combining  $^{36}\text{Cl}$  CRE dating of moraine boulders and bedrock  
111 surfaces with marine records and tephra marker beds. [Andrés et al. \(2018\)](#) reconstructed  
112 the deglaciation at the Late Pleistocene to Holocene transition at Skagafjörður through  
113  $^{36}\text{Cl}$  CRE dating applied to polished surfaces along a transect from the highlands to the  
114 mouth of the fjord. [Brynjólfsson et al. \(2015b\)](#) applied the same isotope to samples  
115 coming from the highlands and the fjords to reconstruct the glacial history of the  
116 Drangajökull region. The other cosmogenic isotope used is  $^3\text{He}$ , applied to helium-  
117 retentive olivine phenocrysts by [Licciardi et al. \(2007\)](#) to determine eruption ages of  
118 Icelandic table mountains and to reconstruct the volcanic history and the thickness  
119 evolution of the Icelandic Ice Sheet during the last glacial cycle. However, CRE dating  
120 has not yet been applied to the late Holocene glacial landforms both in Iceland as a  
121 whole and the Tröllaskagi Peninsula. CRE dating is an alternative to the use of high-  
122 resolution continuous lacustrine records in northern Iceland, given the rarity of lakes in  
123 this peninsula, which limits the application of radiocarbon to date the deglaciation  
124 processes ([Striberger et al., 2012](#); [Harning et al., 2016b](#)).

125 Nevertheless, CRE dating methods approach the nuclides' detection limit when applied  
126 to very recent moraines (Marrero et al., 2016; Jomelli et al., 2016). This issue precludes  
127 the application of CRE dating to the abundant post-LIA moraines existing in some of  
128 the Tröllaskagi valleys whose headwalls are occupied by climate-sensitive debris-free  
129 glaciers (Caseldine and Cullingford, 1981; Caseldine, 1983,1985b; Kugelmann, 1991;  
130 Fernández-Fernández et al., 2017). Dating these post-LIA moraines allows to  
131 reconstruct recent climate evolution, and even to match and assess the climate  
132 reconstructions with the instrumental climate records (see Dahl and Nesje, 1992;  
133 Caseldine and Stötter, 1993; Fernández-Fernández et al., 2017). Furthermore, improving  
134 the knowledge of the recent evolution of alpine mountain glaciers, such as those of  
135 Tröllaskagi, is fundamental in the assessment of present global warming (Marzeion et  
136 al., 2014)

137 The use of aerial photographs from different dates is a reliable approach to the glacier  
138 evolution during the last decades (Fernández-Fernández et al., 2017; Tanarro et al.,  
139 2019). The main advantage of this technique is the possibility of studying the evolution  
140 of glacier snouts in recent dates with high accuracy. In fact, there is no dependence on  
141 the glacial features (i.e. moraines), which circumvents moraine deterioration issues  
142 derived by the geomorphological activity of the slopes. However, the main shortcoming  
143 of the aerial photo imagery is the availability only on few dates, at least in Tröllaskagi.  
144 This circumstance makes it impossible to obtain the glacier fluctuations with a high  
145 time resolution (i.e. only the periods between the available aerial photos; Fernández-  
146 Fernández et al., 2017; Tanarro et al., 2019), and hence to match them to short-term  
147 (decadal scale) climate fluctuations that are known to exert a major control especially  
148 on small mountain glaciers with short time responses (see Caseldine, 1985b;  
149 Sigurðsson, 1998; Sigurðsson et al., 2007; Fernández-Fernández et al., 2017). The only

150 way to fill the gap between two dates with available aerial photos is through applying  
151 lichenometric dating (Sancho et al., 2011), as there is no tree species suitable to apply  
152 dendrochronology. In addition, the information provided by the aerial photo imagery  
153 (i.e. glacier snout position) constrains the period when the lichens appear and begin to  
154 grow, which circumvents many of the criticisms made on lichenometry (see Osborn et  
155 al., 2015).

156 Moreover, a detailed geomorphological mapping allows for identification of stable  
157 moraines, not remobilized or destroyed by glacier advances or slope processes  
158 (avalanches, slope deformations, debris-flows, etc.) and also to reconstruct the glacier  
159 snout geometry throughout different phases (see Caseldine, 1981; Bradwel, 2004b;  
160 Principato et al., 2006 amongst others). The analysis of the moraine morphology and the  
161 glacial features on the forelands is a key tool to confirm whether the glaciers were  
162 debris-free or debris-covered in the past (Kirkbride, 2011; Janke et al., 2015; Knight, et  
163 al., 2018, amongst others) as this issue determines their climate sensitivity (see  
164 Fernández-Fernández et al., 2017; Tanarro et al., 2019).

165 The western and eastern Tungnahryggsjökull glaciers, in the Vesturdalur and  
166 Austurdalur Valleys (central Tröllaskagi), respectively (Fig. 1), are two of the few  
167 debris-free glaciers –or almost debris-free in the case of the western glacier– of the  
168 peninsula that are both small and highly sensitive to climatic fluctuations (Fernández-  
169 Fernández et al., 2017). This makes them ideal for studying glacial and climatic  
170 evolution during last last millennia.

171 The aim of our work was to apply the best methodology possible to analyze the glacial  
172 evolution of western and eastern Tungnahryggsjökull glaciers during the last millennia  
173 to the present. Applying for the first time a number of dating techniques to study the  
174 Late Holocene evolution of the two glaciers, the objectives of this paper are:

175 (i) To carry out a detailed geomorphological survey of the glacier forelands in order to  
176 map accurately well-preserved glacial features. This mapping is used both to devise the  
177 sampling strategy for dating, and also to reconstruct the palaeoglaciers in 3D in order to  
178 obtain glaciologic climate indicators such as the Equilibrium-Line Altitudes (ELAs).  
179 These can be used as a proxy to infer palaeoclimatic information (see [Dahl and Nesje,](#)  
180 [1992](#); [Caseldine and Stötter, 1993](#); [Brugger, 2006](#); [Hughes et al., 2010](#); [Fernández-](#)  
181 [Fernández et al., 2017](#) amongst others).

182 (ii) To use aerial photographs / satellite imagery post-dating 1946 to map the glacier  
183 extent in each available date in order to improve the information of ELA evolution in  
184 the recent decades. Aerial photographs will be used to constrain the possible periods of  
185 lichen colonization and growth over stable boulders, and will be useful to identify  
186 phases of advance, stagnation or retreat of the glacier snouts. By this way we will  
187 complete the glacier evolution from pre-instrumental glacial stages (identified from  
188 geomorphological evidence, i.e. moraines) to their current situation.

189 (iii) To apply CRE dating when possible depending on the preservation degree of the  
190 glacial features, and when moraines were too old to be dated by lichenometry.

191 (iv) To apply lichenometric relative dating to recent moraines or those where CRE  
192 dating might not be suitable (i.e. limit of applicability) and provided that: 1) the  
193 geomorphological criteria evidence a good preservation of glacial features; and 2) aerial  
194 photographs constrain the earliest and oldest possible lichen ages. This approach will  
195 also allow to check the growth rates and colonization lags of the lichen species usually  
196 used in Iceland for lichenometric dating purposes.

197 The experimentation and validation of this methodological purpose will help to improve  
198 the knowledge of the recent climate evolution of northern Iceland. This is of maximum

199 interest if we consider its location within the current atmospheric and oceanic setting,  
200 strongly linked to the evolution of the Meridional Overturning Circulation ([Andrews](#)  
201 [and Giraudeau, 2003](#); [Xiao et al., 2017](#)), a key factor in the studies for the assessment of  
202 the global climate change effects ([Barker et al., 2010](#); [Chen et al., 2015](#) amongst others).  
203 Moreover, if this proposal is valid, it could be applied to the research on the recent  
204 evolution of other mountain glaciers similar to those of Tröllaskagi. This aspect is a  
205 main research objective at present, as these glaciers represent the greatest contribution  
206 to the current sea-level rise ([Jacob et al., 2012](#); [Gardner et al., 2013](#) amongst others).

## 207 **2. Regional setting**

208 The Tröllaskagi Peninsula extends into the Atlantic Ocean at 66°12' N from the central  
209 highland plateau (65°23' N) of Iceland ([Fig. 1](#)). The fjords of Skagafjörður (19°30' W)  
210 and Eyjafjörður (18°10' W) separate it from the Skagi and Flateyjarskagi peninsulas,  
211 respectively. Tröllaskagi is an accumulation of successive Miocene basalt flows,  
212 interspersed with reddish sedimentary strata ([Sæmundsson et al., 1980](#); [Jóhannesson](#)  
213 [and Sæmundsson, 1989](#)). The plateau culminates at altitudes of 1000-1500 m a.s.l. (with  
214 the highest peak Kerling at 1536 m a.s.l.) and is dissected by deep valleys with steep  
215 slopes whose headwaters are currently glacial cirques. These cirques host more than 160  
216 small glaciers, mostly north-facing, resulting from the leeward accumulation of snow  
217 from the plateau ([Caseldine and Stötter, 1993](#)) and reduced exposure to solar radiation.  
218 In fact, deposits caused by rock-slope failure are common in Tröllaskagi valley slopes  
219 and have been considered a result of the final deglaciation during the early Holocene  
220 ([Jónsson, 1976](#); [Feuillet et al., 2014](#); [Cossart et al., 2014](#); [Coquin et al., 2015](#)). Most of  
221 the glaciers are rock or debris-covered glaciers, due to the intense paraglacial activity  
222 affecting the walls that minimizes cosmogenic nuclide concentrations from earlier  
223 exposure periods on the cirque headwalls ([Andrés et al, 2018](#)).

224 The climate in Tröllaskagi is characterized by a mean annual air temperature (MAAT;  
225 1901-1990 series) of 2 to 4 °C at sea level, dropping to between -2 and -4 °C at the  
226 summits (Etzelmüller et al., 2007). At the town of Akureyri, located in the east of the  
227 peninsula at the mouth of Eyjafjarðardalur (Fig. 1), the MAAT is 3.4 °C and the average  
228 temperature in the three summer months is about 9 to 10 °C (Einarsson, 1991). Annual  
229 precipitation (1971-2000) ranges from 400 mm at lower altitudes to 2500 mm at the  
230 summits (Crochet et al., 2007).

231 The frontier location of Icelandic glaciers in relation to atmosphere and ocean systems  
232 (warm/moist Subtropical and cold/dry Arctic air masses; and the warm Irminger and  
233 cold East Greenland sea currents) makes them exceptionally sensitive to climate  
234 oscillations (Bergþórsson, 1969; Flowers et al., 2008; Geirsdóttir et al., 2009), and these  
235 debris-free glaciers are thus reliable indicators of climatic evolution and the impact of  
236 climate change on the cryosphere (see Jóhannesson and Sigurðsson, 1998; Bradwell,  
237 2004b; Sigurðsson, 2005; Geirsdóttir et al., 2009; Fernández-Fernández et al., 2017).

238 The glaciers studied here are the western (6.5 km<sup>2</sup>) and eastern (3.9 km<sup>2</sup>)  
239 Tungnahryggsjökull, located in the Vesturdalur and Austurdalur valleys respectively,  
240 separated from each other by the crest of Tungnaryggur, and tributaries of the  
241 Kolbeinsdalur Valley (Fig. 1).

### 242 **3. Methodology**

#### 243 *3.1 Geomorphological mapping and glacier geometry mapping*

244 Four summer field campaigns (2012, 2013, 2014 and 2015) were conducted in  
245 Vesturdalur and Austurdalur, with the objective of identifying moraines that clearly  
246 provided evidence of various glacial culminations of the western and eastern  
247 Tungnahryggsjökull glaciers. We identified the palaeo-positions of the glacier snouts,

248 the glacier geometry and extent through photo interpretation of stereoscopic pairs and  
249 previous fieldwork. Mapping of glacial and non-glacial landforms was conducted on  
250 two enlarged 50-cm-resolution aerial orthophotos ([National Land Survey of Iceland,](#)  
251 [2015](#)) plotted at scale  $\approx 1:7000$ . These maps were imported into an ArcGIS 1.4.1  
252 database after geo-referencing. Finally, all the glacial linear landforms were digitized,  
253 and where the moraines were prominent, continuous, or well-preserved, they were  
254 assumed to represent major culminations, and hence, glacial stages. In addition to the  
255 geomorphological evidence, glacier variations in recent years were mapped, based on  
256 the photo interpretation of four historical aerial photographs from 1946, 1985, 1994 and  
257 2000 ([National Land Survey of Iceland, 2015](#)), and also one SPOT satellite image  
258 (2005), previously geo-referenced in ArcGIS. For more details of the aerial photograph  
259 processing, see [Fernández-Fernández and Andrés \(2018\)](#). As the glacier headwalls are  
260 ice diffluences in both cases, it was assumed that: (i) the ice divides are the upper  
261 boundaries of the glaciers for the different stages, and (ii) the ice divide is invariant for  
262 the different stages/dates, following [Koblet et al. \(2010\)](#) as changes in the extent of the  
263 accumulation zone are smaller than the outlining differences derived from the operator  
264 mapping. Likewise, in the case of the upper glacier edge constrained by the cirque wall,  
265 the glacier geometry was also assumed to be invariant from stage to stage unless the  
266 aerial photographs showed otherwise.

### 267 *3.2 Glacier reconstruction and equilibrium-line altitude (ELA) calculation*

268 [Benn and Hulton's \(2010\)](#) glacier reconstruction approach using a physical-based model  
269 describing ice rheology and glacier flow ([Van der Veen, 1999](#)) was preferred to  
270 arbitrary hand-drawn contouring (e.g. [Sissons, 1974](#)) in order to achieve more robust  
271 reconstructions ([Fernández-Fernández and Andrés, 2018](#)). This model operates on  
272 deglaciated areas with non-extant glaciers. As this is not the case in our study area, we

273 approached the glacier bedrock by tentatively estimating the ice thickness' spatial  
274 distribution on the two glaciers studied. The "VOLTA" ("Volume and Topography  
275 Automation") ArcGIS toolbox (James and Carrivick, 2016) was applied with the default  
276 parameters. It only requires the glacier outline and its digital elevation model (DEM). In  
277 the first step, the tool "volta\_1\_2\_centrelines" creates the glacier centrelines, and then  
278 the tool "volta\_1\_2\_thickness" estimates ice thickness at points along them, assuming  
279 perfect-plasticity rheology, and interpolates the values using a glaciologically correct  
280 routine. The final result is an ice-free DEM in which we reconstructed the glacier. The  
281 former glacier surface topographies at the different stages/dates were reconstructed  
282 applying the semi-automatic "GLaRe" ArcGIS toolbox designed by Pellitero et al.  
283 (2016), which implements the Benn and Hulton (2010) numerical model and estimates  
284 ice-thickness along glacier flowlines. To simplify the glacier surface modelling, shear-  
285 stress was assumed to be constant along the glacier flowline and over time. Using the  
286 value 110 kPa for the shear-stress resembles best the current longitudinal profile of the  
287 glaciers in the Benn and Hulton (2010) spreadsheet. This value can be considered  
288 appropriate as it falls within the normal shear-stress range of 50-150 kPa observed in  
289 current glaciers and is very close to the standard value of 100 kPa (Paterson, 1994). The  
290 glacier contours were manually adjusted to the ice surface elevation values of the ice-  
291 thickness points estimated by "GLaRe" instead of using an interpolation routine, to  
292 obtain a more realistic surface (concave and convex contours above and below the  
293 ELA).

294 Finally, we calculated the ELAs automatically by using the "ELA calculation" ArcGIS  
295 toolbox (Pellitero et al., 2015). The methods comprised: (i) AABR (Area Altitude  
296 Balance Ratio; Osmaston, 2005) with the ratio  $1.5 \pm 0.4$  proposed for Norwegian glaciers  
297 by Rea (2009) and successfully tested on Tröllaskagi debris-free glaciers in Fernández-

298 [Fernández et al. \(2017\)](#); and (ii) the AAR (Accumulation Area Ratio) with the ratio 0.67  
299 previously used by [Stötter \(1990\)](#) and [Caseldine and Stötter \(1993\)](#) for Tröllaskagi  
300 glaciers. Alternative approaches for ELA calculation in northern Iceland have been  
301 carried out by considering morphometric parameters of glacial cirques (altitude ratio,  
302 cirque floor, minimum point; [Ipsen et al., 2018](#)). However, we preferred the methods  
303 considering the glacier hypsometry as they reflect more evident changes from stage to  
304 stage ([Fernández-Fernández et al., 2017](#); [Fernández-Fernández and Andrés, 2018](#)), if  
305 compared to morphometric parameters of the cirques. In this sense, the cirque floor  
306 elevation is derived from the last erosion period, and it is impossible to know the values  
307 corresponding to previous glacial stages.

### 308 *3.3 Lichenometric dating procedures*

309 Lichenometry was used as a relative dating tool, assuming that the lichens increase in  
310 diameter with respect to age. The results aim to complete the age control (of recent  
311 landforms non suitable for CRE dating) on the periods between aerial photos of known  
312 date as it has been applied successfully to control lichen ([Sancho et al., 2011](#)) and  
313 bryophyte ([Arróniz-Crespo et al., 2014](#)) growth during primary succession in recently  
314 deglaciaded surfaces. First, we surveyed the moraines thoroughly, starting from the  
315 current glacier snouts downwards, looking for large stable boulders (i.e. well embedded  
316 in the moraine, not likely of having been overturned or remobilized by slope processes  
317 which could have affected lichen growth, e.g. snow avalanches, debris-flows, rockfall,  
318 landslides or debris-flows) with surfaces valid for dating (not weathered or resulting  
319 from block break). Lichenometry was applied to date moraine ridge boulders with the  
320 following criteria and assumptions: (i) boulders must clearly belong to the moraine  
321 ridge; (ii) lichen species should be abundant enough to allow measurements of a number  
322 of thalli at each location and hence enable surfaces to be dated under favourable

323 environmental conditions such as basaltic rocks in subpolar mountains; (iii) only the  
324 largest lichen (circular or ellipsoidal thalli) of species *Rhizocarpon geographicum*,  
325 located on smooth horizontal boulder surfaces, was measured; (iv) the lichenometric  
326 procedures should not be applied when the lichen thalli coalesce on the boulder surface  
327 and individual thalli cannot be identified. We preferred the geomorphological criterion  
328 (stability vs. slope processes) to the establishment of lichenometry plots of a fixed area  
329 (e.g. [Bickerton and Matthews, 1992](#)) to ensure that lichens were measured on reliable  
330 boulders. This measurement strategy tries to circumvent or at least to minimize the  
331 specific problems of Tröllaskagi when dating glacial features so that: (i) snow  
332 accumulation should be lower in the moraine crest; (ii) lichen ages will be estimated  
333 only for the boulders located on the crests used to map and reconstruct the glaciers; and  
334 (iii) and lichens subjected to thalli saturation (coalescence) or high competition are not  
335 measured.

336 First, *Rhizocarpon geographicum* lichens were measured with a Bernier calibrator.  
337 Then, digital photographs for high-precision measurements were taken of the most  
338 representative of the largest thallus located in each selected boulder ([Suppl. figure SF1](#)),  
339 using an Icelandic króna coin (21 mm diameter) parallel to the surface of the lichen as a  
340 graphic scale. We preferred the single largest lichen approach as previously has been  
341 done in Tröllaskagi for lichenometric dating of moraines ([Caseldine, 1983, 1985b,](#)  
342 [1987; Kugelmann, 1991](#)). The photos were scaled in ArcGIS to real size and lichen  
343 thalli were outlined manually through visual inspection of the photos and measured  
344 automatically with high accuracy according to the diameter of the smallest circle which  
345 can circumscribe the lichen outline ([Suppl. figure SF1](#)). We preferred the simple  
346 geometrical shape of the circle and its diameter to identify the largest axis to circumvent

347 the problem of complex-shaped lichens. Similar procedures for lichen thalli  
348 measurement from photographs are outlined in [Hooker and Brown \(1977\)](#).

349 Then, we initially applied a  $0.44 \text{ mm yr}^{-1}$  constant growth rate and a 10-year  
350 colonization lag ([Kugelmann, 1991](#)) to the measurement of the largest *Rhizocarpon*  
351 *geographicum* lichen (longest axis). This growth rate is derived from the lichen growth  
352 curve with the highest number of control points so far in Tröllaskagi ([Kugelmann,](#)  
353 [1991](#)), and it is very similar to that reported from the near Hörgárdalur valley ([Häberle,](#)  
354 [1991](#)). However, the authors are aware that using a constant growth rate implies not  
355 taking account the growth rate decline with increasing age. Other longer colonization  
356 lags of 15, 20, 25 and 30 years were added to the age estimate from the growth rate in  
357 order to test the colonization lag originally assumed by [Kugelmann \(1991\)](#), on the  
358 suspicion of longer colonization lags reported elsewhere ([Caseldine, 1983](#); [Evans et al.,](#)  
359 [1999, Table 1](#)). The resulting ages were compared to the dates of historical aerial  
360 photographs where the glacier snout positions constrain the maximum and minimum  
361 ages of the lichen stations.

362 In the case of *Porpidia cf. soredizodes*, since no growth rate value has been described so  
363 far, a value will be tentatively estimated in this study. For this reason, we took  
364 measurements of the two species in the same sampling locations wherever possible. It  
365 should be noted that visual distinction between *Porpidia cf. soredizodes* and *Porpidia*  
366 *tuberculosa* is not always conclusive based on morphological characteristics, but we  
367 feel confident using the measurements of the *Porpidia cf. soredizodes* we identified in  
368 the field.

### 369 3.4 <sup>36</sup>Cl Cosmic-Ray Exposure (CRE) dating

370 Where the thalli either coalesced and prevented identification of the largest thallus or  
371 dating results indicated that a moraine was too old to be dated by this method, rock  
372 samples were collected for CRE dating. The criteria for boulder and surface selection  
373 where the same as for lichenometric purposes: stable boulders with no signs of being  
374 affected by slope processes (landslides, debris-flows) or postglacial overturning, well  
375 embedded in the moraine, and with no sign of surface weathering or previous boulder  
376 break. The cosmogenic nuclide  $^{36}\text{Cl}$  was chosen because of the basalt lithology  
377 ubiquitous in Iceland, which lacks quartz, which is needed for standard  $^{10}\text{Be}$  CRE  
378 methods. Using a hammer and chisel, samples were collected from flat-topped surfaces  
379 of moraine boulders. In order to obtain a maximum time constraint for the deglaciation  
380 of both surveyed valleys, two samples were taken from Elliði (Fig. 1), a glacially  
381 polished ridge downstream from the Tungnahryggsjökull forelands separating  
382 Kolbeinsdalur to the north and Viðinesdalur to the south. The laboratory procedures  
383 applied for  $^{36}\text{Cl}$  extraction from silicate whole rock samples were those described in  
384 Schimmelpfennig et al. (2011). Note that the samples had not enough minerals to  
385 perform the  $^{36}\text{Cl}$  extraction on mineral separates, which is generally the preferred  
386 approach to minimize the uncertainties in age exposure estimates, as in mineral  
387 separates  $^{36}\text{Cl}$  is often produced by less and better known production pathways than in  
388 whole rock samples (Schimmelpfennig et al., 2009). The samples were crushed and  
389 sieved to 0.25-1 mm in the Physical Geography Laboratory in the Complutense  
390 University, Madrid. Chemical processing leading to  $^{36}\text{Cl}$  extraction from the whole rock  
391 was carried out at the Laboratoire National des Nucléides Cosmogéniques (LN<sub>2</sub>C) at the  
392 Centre Européen de Recherche et d'Enseignement des Géosciences de l'Environnement  
393 (CEREGE), Aix-en-Provence (France). Initial weights of about 120 g per sample were  
394 used. A chemically untreated split of each sample was set aside for analyses of the

395 chemical composition of the bulk rocks at CRPG-SARM. First, the samples were rinsed  
396 to remove dust and fines. Then, 25-30% of the mass was dissolved to remove  
397 atmospheric  $^{36}\text{Cl}$  and potentially Cl-rich groundmass by leaching with a mixture of  
398 ultra-pure dilute nitric (10%  $\text{HNO}_3$ ) and concentrated hydrofluoric (HF) acids. In the  
399 next step, 2 g aliquots were taken to determine the major element concentrations; these  
400 were analysed by ICP-OES at CRPG-SARM. Then, before total dissolution,  $\sim 260 \mu\text{L}$  of  
401 a  $^{35}\text{Cl}$  carrier solution (spike) manufactured in-house (concentration:  $6.92 \text{ mg g}^{-1}$ ;  
402  $^{35}\text{Cl}/^{37}\text{Cl}$  ratio: 917) were added to the sample for isotope dilution (Ivy-Ochs et al.,  
403 2004). Total dissolution was achieved with excess quantities of the above mentioned  
404 acid mixture. Following total dissolution, the samples were centrifuged to remove the  
405 undissolved residues and gel (fluoride complexes such as  $\text{CaF}_2$ ). Next, chlorine was  
406 precipitated to silver chloride ( $\text{AgCl}$ ) by adding 2 ml of silver nitrate ( $\text{AgNO}_3$ ) solution  
407 at 10%. After storing the samples for two days in a dark place to allow the  $\text{AgCl}$  to  
408 settle on the bottom, the supernatant acid solution was extracted by a peristaltic pump.  
409 To reduce the isobaric interferences of  $^{36}\text{S}$  during the  $^{36}\text{Cl}$  AMS measurements, the first  
410 precipitate was re-dissolved in 2 ml of ammonia ( $\text{NH}_3 + \text{H}_2\text{O}$  1:1 vol  $\rightarrow$   $\text{NH}_4\text{OH}$ ), and 1  
411 ml of a saturated solution of barium nitrate ( $\text{Ba}(\text{NO}_3)_2$ ) was added to the samples to  
412 precipitate barium sulphate ( $\text{BaSO}_4$ ). It was removed by centrifuging and filtering the  
413 supernatant with a syringe through acrodisc filters.  $\text{AgCl}$  was precipitated again with 3-  
414 4 ml of diluted  $\text{HNO}_3$  (1:1 vol). The precipitate was collected by centrifuging, rinsed,  
415 and dried in an oven at  $80 \text{ }^\circ\text{C}$  for 2 days.

416 The final  $\text{AgCl}$  targets were analysed by accelerator mass spectrometry (AMS) to  
417 measure the  $^{35}\text{Cl}/^{37}\text{Cl}$  and  $^{36}\text{Cl}/^{35}\text{Cl}$  ratios, from which the Cl and  $^{36}\text{Cl}$  concentration  
418 were inferred. The measurements were carried out at the Accélérateur pour les Sciences  
419 de la Terre, Environnement et Risques (ASTER) at CEREGE in March 2017 using

420 inhouse standard SM-CL-12 with an assigned value of  $1.428 (\pm 0.021) \times 10^{-12}$  for the  
421  $^{36}\text{Cl}/^{35}\text{Cl}$  ratio (Merchel et al., 2011) and assuming a natural ratio of 3.127 for the stable  
422 ratio  $^{35}\text{Cl}/^{37}\text{Cl}$ .

423 When calculating exposure ages, the Excel<sup>TM</sup> spreadsheet for in situ  $^{36}\text{Cl}$  exposure age  
424 calculations proposed by Schimmelpfennig et al. (2009) was preferred to other online  
425 calculators (e.g. CRONUS Earth; Marrero et al., 2016) as it allows input of different  
426  $^{36}\text{Cl}$  production rates from spallation, referenced to sea level and high latitude (SLHL).  
427 Thus, three SLHL  $^{36}\text{Cl}$  production rates from Ca spallation, i.e. the most dominant  $^{36}\text{Cl}$   
428 production reaction in our samples, were applied to allow comparisons both with other  
429 Icelandic areas ( $57.3 \pm 5.2$  atoms  $^{36}\text{Cl} (\text{g Ca})^{-1} \text{yr}^{-1}$ ; Licciardi et al., 2008) and other areas  
430 of the world ( $48.8 \pm 3.4$  atoms  $^{36}\text{Cl} (\text{g Ca})^{-1} \text{yr}^{-1}$ , Stone et al., 1996;  $42.2 \pm 4.8$  atoms  $^{36}\text{Cl}$   
431  $(\text{g Ca})^{-1} \text{yr}^{-1}$ , Schimmelpfennig et al., 2011). For  $^{36}\text{Cl}$  production reactions other than Ca  
432 spallation, the following SLHL  $^{36}\text{Cl}$  production parameters were applied:  $148.1 \pm 7.8$   
433 atoms  $^{36}\text{Cl} (\text{g K})^{-1} \text{yr}^{-1}$  for K spallation (Schimmelpfennig et al., 2014b),  $13 \pm 3$  atoms  
434  $^{36}\text{Cl} (\text{g Ti})^{-1} \text{yr}^{-1}$  for Ti spallation (Fink et al., 2000),  $1.9 \pm 0.2$  atoms  $^{36}\text{Cl} (\text{g Fe})^{-1} \text{yr}^{-1}$  for  
435 Fe spallation (Stone et al., 2005) and  $696 \pm 185$  neutrons  $(\text{g air})^{-1} \text{yr}^{-1}$  for the production  
436 rate of epithermal neutrons for fast neutrons in the atmosphere at the land/atmosphere  
437 interface (Marrero et al., 2016). Elevation-latitude scaling factors were based on the  
438 time invariant “St” scheme (Stone et al., 2000). The high-energy neutron attenuation  
439 length value applied was  $160 \text{ g cm}^{-2}$ .

440 All production rates from spallation of Ca mentioned above are based on calibration  
441 samples with a predominant Ca composition. Iceland is permanently affected by a low-  
442 pressure cell, the Icelandic Low (Einarsson, 1984). As the atmospheric pressure  
443 modifies the cosmic-ray particle flux, and thus has an impact on the local cosmogenic  
444 nuclide production rate, the atmospheric pressure anomaly has to be taken into account

445 when scaling the SLHL production rates to the study site. Only [Licciardi et al.'s \(2008\)](#)  
446 production rate already accounts for this anomaly, as the calibration sites of study are  
447 located in south western Iceland (see also [Licciardi et al., 2006](#)). On the other hand,  
448 [Stone et al.'s \(1996\)](#) and [Schimmelfennig et al.'s \(2011\)](#) production rates were  
449 calibrated in Tabernacle Hill (Utah, western U.S.A.) and Etna volcano (Italy),  
450 respectively, hence they need to be corrected for the atmospheric pressure anomaly  
451 when applied in Iceland. [Dunai \(2010\)](#) advises including any long-term atmospheric  
452 pressure anomaly at least for Holocene exposure periods. Therefore, the local  
453 atmospheric pressure at the sample locations was applied in the scaling factor  
454 calculations when using the [Stone et al. \(1996\)](#) and [Schimmelfennig et al. \(2011\)](#)  
455 production rates. Instead of the standard value of 1013.25 hPa at sea level, a sea level  
456 value of 1006.9 hPa (Akureyri meteorological station; [Icelandic Meteorological Office,](#)  
457 [2018](#)) was used. The atmospheric pressure correction assumed a linear variation of  
458 temperature with altitude. The results presented and discussed below are based on the  
459  $^{36}\text{Cl}$  production rate for Ca spallation of [Licciardi et al. \(2008\)](#) as it is calibrated for  
460 Iceland and considers the atmospheric pressure anomaly. The exposure ages presented  
461 throughout the text and figures include analytical and production rate errors unless  
462 stated otherwise. Our <2000 yr CRE ages have also been rounded to the nearest decade,  
463 and then converted to CE dates through their subtraction from the year 2015 (i.e.  
464 fieldwork and sampling campaign). In order to achieve robust comparisons of our  
465 results with those obtained by radiocarbon or tephrochronology, we have calibrated the  
466  $^{14}\text{C}$  ages previously published in the literature through the OxCal 4.3 online calculator  
467 (<https://c14.arch.ox.ac.uk/oxcal/OxCal.html>) implementing the IntCal13 calibration  
468 curve ([Reimer et al., 2013](#)).

#### 469 **4. Results**

#### 470 *4.1 Geomorphological mapping, aerial photos and identified glacial stages*

471 Based on photo-interpretation of aerial photographs and fieldwork, two  
472 geomorphological maps were generated at ~1:7000 scale, in which well preserved  
473 moraine segments, current glacier margins and stream network were also mapped (Figs.  
474 **2 and 3**). In Vesturdalur, over 1000 moraine ridge fragments (including terminal and  
475 lateral moraine segments) were identified and mapped, with increased presence from  
476 1.7 km upwards to the current glacier terminus. In the analysis, we retained only ridge  
477 fragments if they are at least 50 m long, protruding 2 m above the valley bottom and the  
478 alignment of glacial boulders embedded in the moraine crest is preserved, as indicators  
479 of major glacial culminations and well preservation state. Otherwise we considered  
480 either they represented insignificant glacial stages or were most probably affected by  
481 post-glacial slope reworking.

482 Following these criteria, we retained 12 glacial stages based on the geomorphological  
483 mapping of the Vesturdalur foreland (Fig. 2). We were able to verify in the field that the  
484 selected sections had not been affected by postglacial slope processes as none of these  
485 moraines was cut by debris-flows or deformed/covered by landslides. The palaeo-  
486 position of the glacier terminus was clearly defined by pairs of latero-frontal moraines  
487 in stages 1, 4 and 6. In stages 2, 3, 5, 9, 10, 11 and 12, it was poorly defined by short  
488 latero-frontal moraines on one side of the valley, very close to the river, with their  
489 prolongation and intersection with the river assumed to be the former apex, and so a  
490 tentative terminus geometry was drawn. The lateral geometry of the tongue was  
491 accurately reconstructed in stages 6, 8 and 9 based on long and aligned, ridge fragments,  
492 and in the other stages an approximate geometry was drawn from the terminus to the  
493 headwall. The greatest retreat between consecutive stages (1 km) occurred in the

494 transition from the stage 1 to the stage 2. No intermediate frontal moraines were  
495 observed in the transect between the stages 1 and 2.

496 In Austurdalur, over 1600 moraine ridge fragments were identified and mapped.  
497 Following the same criteria as in Vesturdalur, 13 stages were identified based on the  
498 geomorphological evidence (Fig. 3). The furthest moraines marking the maximum  
499 extent of the eastern Tungnahryggsjökull appear at 1.3 km from the current terminus. In  
500 contrast to the other valley, moraines populate the glacier foreland more densely and  
501 regularly on both sides of the valley. Most of them are <50 m long with a few exceeding  
502 100-200 m. The frontal moraine ridge fragments in Austurdalur clearly represent the  
503 geometry of the terminus in all the stages, as they are well-preserved and are only  
504 bisected by the glacier meltwater, with the counterparts easily identifiable. The most  
505 prominent (over 2 m protruding over the bottom of the valley) and well preserved  
506 moraines are those marking the terminus position at stages 1 to 8, with lengths ranging  
507 from 170 to 380 m.

508 Both glaciers were also outlined on aerial photos of 1946, 1985, 1994 (only for western  
509 Tungnahryggsjökull), and 2000, and on a SPOT satellite image (2005), and hence new  
510 recent stages from the past century were studied for the Tungnahryggsjökull, five for the  
511 western glacier (stages 13, 14, 15, 16 and 17) and four for the eastern glacier (stages 11,  
512 15, 16 and 17) (Suppl. figure SF2; Suppl. table ST1). The stages identified on the basis  
513 of the geomorphological mapping and those obtained from glacier outlining over  
514 historical aerial photos sum up to a total of 17 stages for each glacier.

#### 515 *4.2. Glacier length, extent and volume*

516 The reconstructed glacier surfaces corresponding to the different glacial stages is shown  
517 in Suppl. figure SF3. The length of the glaciers during their reconstructed maximum ice

518 extent was unequal, with the western Tungnahryggsjökull being 6.5 km long, and the  
519 eastern glacier being 3.8 km long (Suppl. table ST2). The same occurred with the area,  
520 9.4 and 5.3 km<sup>2</sup>, respectively (Suppl. table ST3). Over the different stages, the western  
521 glacier lost 31% of its area and retreated 51% of its total length (Suppl. tables ST2 and  
522 ST3) while there was less shrinkage of the eastern glacier both in area loss (26%) and  
523 length (34%). Figs. 2B and 3B and Suppl. table ST2 show only one reversal during the  
524 general retreating trend, in the stage 15 of the western and the stage 16 of the eastern  
525 Tungnahryggsjökull. The greatest area losses occurred in the transition to the stages 2,  
526 4, 7, 9 and 14 (>3%) on the western glacier while losses between stages in the eastern  
527 glacier were lower except for the transition between the stages 14 and 17, where a  
528 noticeable reduction of the accumulation area was observed in the aerial photos of 1946  
529 and 1985, and the satellite image of 2005 (Fig. 3B). The volumes calculated from the  
530 reconstructed glacier DEM and the corrected bed DEM show that the glaciers reached  
531 ~1.10 km<sup>3</sup> (western) and ~0.47 km<sup>3</sup> (eastern) at their recorded maximum extent  
532 corresponding to their outmost moraines. From the oldest to the most recent stage they  
533 lost 30% and 23% of their ice volume, respectively. The losses between consecutive  
534 stages of the glaciers were in general lower than 3% with the exception of the stages 2,  
535 4, 7, 9 (western) and stage 14 (eastern), where the values ranged from 3% to 10%  
536 (Suppl. table ST3). Only one slight inversion of the volume trend is seen in the stages  
537 15 of the western glacier and in 16 of the eastern glacier.

#### 538 4.3. Equilibrium-Line Altitudes (ELAs)

539 The application of the AAR (0.67) method showed ELAs ranging from 1021 to 1099 m  
540 a.s.l. (western glacier) and from 1032 to 1065 m a.s.l. (eastern glacier) for the different  
541 reconstructed stages. This means an overall rise of 78 and 33 m respectively (Table 1)  
542 from the maximum to the minimum extent recorded. The results from applying the

543 AABR (1.5) show the same trend and similar ELAs, with differences of up to  $\pm 15$  m  
544 compared with those obtained from the AAR. The AABR-ELAs tend to be higher than  
545 the AAR-ELAs, especially in the second half of the reconstructed stages with the most  
546 remarkable differences occurring in the eastern Tungnahryggsjökull (Table 1).  
547 However, the error derived from the uncertainties associated to the applied balance ratio  
548 (BR,  $\pm 0.4$ ) tends to decrease as the glaciers get smaller. The greatest change in the ELA  
549 between consecutive stages is found between the stages 1 and 2 in the western glacier  
550 (+26 m), fully coincident with the largest retreat measured, about 1 km. An interesting  
551 result is that the ELA rise is attenuated in both glaciers from stage 10 onwards, with  
552 stage-to-stage variations close to zero predominating, and with only one inversion (-3  
553 m) occurring in the western glacier between the stages 14 and 15 (Table 1).

#### 554 4.4. Lichenometric dating

555 Altogether 17 lichenometry stations (8 in Vesturdalur and 9 in Austurdalur) were set up  
556 during fieldwork in the two glacier forelands. Their spatial distribution and  
557 correspondence with the different glacial stages are given in Figs. 2 and 3 and Suppl.  
558 table ST4. The table also shows the measurements of the largest *Rhizocarpon*  
559 *geographicum* thalli found during fieldwork in the moraines (stages) to which the  
560 stations correspond. TUE-0 was the only station where no lichen of either species was  
561 found in 2015. Unlike *Porpidia* cf. *soredizodes* thalli, which are present in all the  
562 remaining lichenometry stations, *Rhizocarpon geographicum* thalli suitable for  
563 measuring (ellipsoidal, not coalescent) were only found in stations TUV-2 to TUV-7 in  
564 Vesturdalur, and in TUE-2 to TUE-7 in Austurdalur.

565 The measurements considered the diameter of the smallest circle bounding the thallus  
566 outline as representative of the longest axis (Suppl. figure SF1). The obtained values  
567 ranged from 19.3 to 71.5 mm in Vesturdalur, and from 19.0 to 47.7 mm in Austurdalur

568 (Suppl. table ST4). Only one size inversion (decreasing size with increasing distance to  
569 the current terminus) was detected in Austurdalur in the station TUE-6 (Fig. 3).  
570 *Rhizocarpon geographicum* thalli were absent in the nearest stations (TUW-1 and TUE-  
571 1) and were coalescent in the most distant stations (TUW-8 and TUE-8) in both glacier  
572 forelands. On the other hand, *Porpidia cf. soredizodes* thalli measurements ranged from  
573 18.3 to 148.4 mm in Vesturdalur, and from 16.8 to 141.8 mm in Austurdalur (Suppl.  
574 table ST4). A size inversion of *Porpidia cf. soredizodes* thalli is also observed in TUE-6  
575 and in TUE-7.

576 When the ages of *Rhizocarpon geographicum* lichens are calculated applying a 0.44  
577 mm yr<sup>-1</sup> growth rate and a 10-year colonization lag following Kugelmann (1991), they  
578 range from 54 to 173 years in Vesturdalur, and from 53 to 119 years in Austurdalur. If  
579 longer colonization lags of 15, 20, 25 and 30 years (see Methods section) are applied  
580 tentatively, the oldest ages obtained are ~170-190 years, and the youngest ~40-70 years  
581 (Table 2). In general, the further away the lichenometry stations are, the older are the  
582 ages (Figs. 2 and 3), with the inversions mentioned above. Apparently the lichenometry-  
583 dated moraines are younger than the CRE-dated distal moraines.

584 The absence of *Rhizocarpon geographicum* lichens in 2015 at lichenometry station  
585 TUW-1 (uncovered by the glacier at some time between 1994 and 2000; Suppl. figure  
586 SF2) suggests a colonization lag of at least 15-21 years. In addition, it is only when the  
587 colonization lag is assumed to be longer than 10 years and shorter than 30 years that the  
588 ages obtained at stations TUW-3 and TUE-2 are in good agreement with the ages  
589 deduced from the aerial photos (Table 2).

590 During the 2015 field campaign, the species *Porpidia cf. soredizodes* was absent in  
591 station TUE-0, located on a glacially polished threshold uncovered by the glacier after  
592 2005 (post-stage 17). However, it was found in stations TUW-1 and TUE-1, dated to

593 1994-2000 and 1946-1985 respectively, based on the position of the snouts in the aerial  
594 photos (Suppl. figure SF2). These observations suggest a colonization lag from 10 to  
595 15-21 years, thus shorter than for *Rhizocarpon geographicum*.

#### 596 4.5. <sup>36</sup>Cl CRE dating

597 The detailed geomorphological analysis carried out on the numerous moraine ridges of  
598 both valleys has greatly limited the number of boulders reliable for successfully  
599 applying <sup>36</sup>Cl CRE and lichenometry dating methods. Due to the great intensity of the  
600 slope processes (especially snow avalanches and debris-flows), only a few boulders are  
601 well-preserved, sometimes only one in each moraine ridge that retains its original  
602 glacier location. Thus, it should be highlighted that this issue prevented performing a  
603 statistically valid sampling for both methods (see e.g. Schaefer et al., 2009; Heymann  
604 et al., 2011).

605 During the fieldwork campaigns in the forelands of the western and eastern  
606 Tungnahryggsjökull glaciers, 12 samples from stable and very protrusive moraine  
607 boulders (Suppl. figure SF4) were collected in areas where lichenometric dating was not  
608 suitable because of lichen thalli coalescence, and also 2 samples from a polished ridge  
609 downwards the confluence of Vesturdalur and Austurdalur (Suppl. figure SF5). The  
610 input data for exposure age calculations, namely sample thickness, topographic  
611 shielding factor, major element concentrations of bulk/target fractions, are summarized  
612 in the Suppl. tables ST5, ST6, ST7 and ST8 includes the <sup>36</sup>Cl CRE ages calculated  
613 according to different Ca spallation production rates and the distance to the most recent  
614 glacier terminus position mapped. Table 3 includes the <sup>36</sup>Cl CRE ages converted to CE  
615 dates format presented throughout the text. The dates presented below are based on the  
616 Licciardi et al. (2008) Ca spallation production rate.

617 Aiming to obtain a maximum (oldest) age for the onset of the deglaciation in the valleys  
618 studied, two samples (ELLID-1 and ELLID-2) were extracted from the western sector  
619 of Elliði, a 660-m-high glacially polished crest separating Viðinesdalur and  
620 Kolbeinsdalur valleys (Suppl. figure SF5), and located at 11 km downstream from the  
621 confluence of Vesturdalur and Austurdalur valleys. Both samples yielded dates of  
622  $14300 \pm 1700$  BCE and  $14200 \pm 1700$  BCE.

623 In Vesturdalur, 8 samples were collected from 5 moraines corresponding to 5 of the  
624 stages identified on the geomorphological map (Fig. 2). Samples TUW-9 and TUW-10  
625 were taken from two boulders in the moraine that correspond to the left latero-frontal  
626 edge of the glacier during the stage 7, ~1 km from the 2005 CE (stage 17) glacier  
627 terminus (measured along the flowline from the reconstructed terminus apex); they  
628 yielded consistent dates of  $1590 \pm 100$  CE and  $1640 \pm 90$  CE. Samples TUW-11 and  
629 TUW-12 were extracted from the moraines corresponding to the glacial stages 6 and 5,  
630 at 185 m and 465 m downstream respectively (~1.2 km and ~1.5 km respectively from  
631 the 2005 CE snout), and gave consistent dates  $1480 \pm 120$  CE and  $1450 \pm 100$  CE. The  
632 next  $^{36}\text{Cl}$  samples (TUW-13 and TUW-14) were taken from two adjacent moraine  
633 boulders on the left latero-frontal moraine ridge corresponding to the stage 3, at 264 m  
634 downstream (1.8 km from the 2005 CE snout); they yielded dates of  $1470 \pm 130$  CE and  
635  $670 \pm 210$  CE, which are significantly different from each other. The most distant  
636 samples (TUW-15 and TUW-16) were extracted from the stage 2 moraine, ~400 m  
637 downstream from the moraine ridge corresponding to stage 3 (2.2 km from the 2005 CE  
638 terminus). They yielded dates of  $1460 \pm 110$  CE and  $1220 \pm 190$  CE, respectively, that are  
639 consistent with each other and in chronological order with sample TUW-13 from the  
640 stage 3. However, these ages are not in agreement with the oldest date of TUW-14  
641 ( $670 \pm 210$  CE) from the stage 3.

642 Four  $^{36}\text{Cl}$  samples were taken from two prominent moraines in the Austurdalur valley  
643 (Fig. 3). Samples TUE-9 and TUE-10 were collected on the frontal moraine  
644 corresponding to stage 4 (1 km from the 2005 CE glacier terminus) and yield  
645 significantly different dates of  $740\pm 170$  CE and  $1460\pm 100$  CE. Samples TUE-11 and  
646 TUE-12 were taken from two moraine boulders located on the ridge of the left lateral  
647 moraine that records the maximum ice extent (Fig. 3). Their calculated  $^{36}\text{Cl}$  dates,  
648  $380\pm 200$  CE and  $400\pm 200$  CE, are consistent with each other and in stratigraphic order  
649 with the ages from stage 4.

650 The dates derived from Stone et al. (1996) Ca spallation production rate are similar to  
651 those presented above, only 4% older. Those derived from the Schimmelpfennig et al.  
652 (2011) production rate yielded dates older by 15% on average (Suppl. table ST8). These  
653 small differences do not represent statistical difference given the calculated age  
654 uncertainties.

## 655 5. Discussion

656

### 657 5.1. $^{36}\text{Cl}$ CRE dating

658 The dates obtained in both valleys range from  $380\pm 200$  CE to  $1640\pm 90$  CE and are  
659 significantly younger than the ages from Elliði polished ridge (Suppl. table ST8). T UW-  
660 14 ( $670\pm 210$  CE) could be the only outlier as it is significantly older than the other  
661 sample obtained from the same moraine of the stage 3 (T UW-13;  $1470\pm 130$  CE) and  
662 also older than the samples T UW-15 ( $1460\pm 110$  CE) and T UW-16 ( $1220\pm 190$  CE),  
663 from the moraine of the previous stage 2 (Fig. 2). This would imply assuming nuclide  
664 inheritance for sample T UW-14 due to either remobilization of an earlier exposed  
665 moraine boulder (see Matthews et al., 2017) or to previous exposure periods, but the

666 high geomorphological dynamism of the slopes limits this possibility (Andres et al.,  
667 2019). Another possible interpretation is that the samples T UW-15 and T UW-16 (stage  
668 2) would be the outliers since they may have experienced incomplete exposure due to  
669 post-depositional shielding (Heymann, 2011). The possibility of both samples being  
670 affected by proglacial processes can be ruled out given the distance to the meltwaters  
671 channel or the absence of glacial burst features (see Caseldine, 1985a) in the  
672 surroundings of the sampled boulders. Thus, the ages of samples T UW-14 and T UW-13  
673 would indicate that the moraine of stage 3 was built during two overlapped glacial  
674 advances at  $670\pm 210$  CE and  $1470\pm 130$  CE. In Austurdalur, the interpretation of the  
675 ages is also complex. Samples T UE-9 ( $740\pm 170$  CE) and T UE-10 ( $1460\pm 100$  CE) from  
676 the same moraine are significantly different, but it is difficult to decide whether or not  
677 one of these two samples is an outlier. It is also possible that the younger age indicates  
678 the timing of a further readvance with the snout reaching the same moraine. It would be  
679 necessary to take more samples, but it will be difficult to find other sectors of these  
680 moraines that are not affected by slope processes, especially debris-flows. The  
681 hypothesis of supraglacial debris dumping can be rejected due to the lack of supraglacial  
682 debris or other features indicative of a palaeo debris-covered glacier. Other possibility  
683 to be consider is that older boulders may be incorporated in the formation of push  
684 moraines as has been shown in maritime Scandinavia, and identified to give  
685 overestimated ages for LIA-moraines (Matthews et al., 2017). The asynchronicity of  
686 glacial advances and retreat in both valleys should not be surprising as glaciers can  
687 retreat or advance differently in adjacent valleys due to a number of factors such as  
688 hypsometry, aspect, gradient, etc. Caseldine (1985b) suggested a high climate  
689 sensitivity of the glacier in Vesturdalur due to its steeper wally floor and thinness”,  
690 which could explain a different behaviour of the glacier compared to the eastern glacier.

691 *5.1.1. Pre-LIA glacial advances*

692  $^{36}\text{Cl}$  CRE dating results from glacially polished surfaces on the Elliði crest show an age  
693 of  $14250 \pm 1700$  yr (mean) for the Kolbeinsdalur deglaciation ([Suppl. figure SF5](#)).  
694 However, this should be considered as a minimum age since this probably indicates  
695 when the retreating and thinning glacier uncovered the ridge, and thus the start of the  
696 final deglaciation of the main valley. From this point to the outmost frontal moraines  
697 surveyed in this paper, no glacially polished outcrops or erratic boulders suitable for  
698  $^{36}\text{Cl}$  sampling were found, impeding us to provide further chronological constraints for  
699 the deglaciation pattern of these valleys.

700 Our  $^{36}\text{Cl}$  CRE dating results suggest late Holocene glacial advances prior to the LIA, at  
701 around  $\sim 400$  and  $\sim 700$  CE, in Vesturdalur and Austurdalur, respectively, coinciding  
702 with the Dark Ages Cold Period (DACP) (between 400 and 765 CE) in central Europe,  
703 according to [Helama et al. \(2017\)](#). In fact, recent synthesis about Icelandic lake records  
704 indicate a strong decline in temperature at 500 CE ([Geirsdóttir et al., 2018](#)).

705 The presence of Late Holocene moraines outside the outermost LIA moraines in other  
706 valleys of Tröllaskagi has been suggested through radiocarbon dating and  
707 tephrochronology in the Vatnsdalur (first, between  $4880 \pm 325$  cal. BCE (tephra Hekla 5)  
708 and  $3430 \pm 510$  cal. BCE, and another after  $1850 \pm 425$  cal. BCE; [Stötter, 1991](#)),  
709 Lambárdalur (before  $3915 \pm 135$  cal. BCE; [Wastl and Stötter, 2005](#)), Þverárdalur (before  
710  $3500 \pm 130$  cal. BCE; [Wastl and Stötter, 2005](#)), Kóngsstaðadalur (after  $1945 \pm 170$  cal.  
711 BCE; [Wastl and Stötter, 2005](#)), Barkárdalur (between  $375 \pm 375$  cal. BCE and  $190 \pm 340$   
712 cal. CE and before  $460 \pm 200$  cal. CE; [Häberle, 1991](#)) and Bægisárdalur ( $2280 \pm 205$  cal.  
713 BCE and  $1050 \pm 160$  cal. CE; [Häberle, 1991](#)) valleys. Specifically, our oldest  $^{36}\text{Cl}$  dates  
714 ( $\sim 400$  and  $\sim 700$  CE) coincide with glacial advances that are radiocarbon dated from

715 intra-morainic peat bogs in other valleys in Tröllaskagi and southern Iceland, e.g. the  
716 Barkárdalur II stage (ca. 460 CE) in Subatlantic times (Häberle, 1991, 1994), and given  
717 the uncertainties of our dates (200 yr), also with Drangajökull (NW Iceland) advancing  
718 at the same time (~300 CE; Harning et al., 2018). On the other hand, Meyer and Venzke  
719 (1985) had already suggested the presence of pre-LIA moraines at Klængshóll (eastern  
720 cirque, tributary of Skíðadalur). Caseldine (1987, 1991) proposed a date of 5310±345  
721 cal. BCE as the youngest for a moraine in that cirque, based on tephrochronology  
722 (tephra layer Hekla 5 dated in a similar ground in Gljúfurárdalur) and rock weathering  
723 measurements using the Schmidt hammer technique. Based on the big size of some  
724 moraines in Skíðadalur and Holárdalur, Caseldine (1987, 1991) also supports the  
725 hypothesis of pre-LIA moraines formed during several advances. All this information is  
726 not in agreement with the hypothesis that all the glaciers in Tröllaskagi reached their  
727 maximum ice extent since the Early Holocene during the LIA (Hjort et al., 1985;  
728 Caseldine, 1987, 1991; Caseldine and Hatton, 1994).

729 In south and central and northwest Iceland, the ice caps reached their Late Holocene  
730 maximum advance during the LIA (Brynjólfsson, et al. 2015a; Larsen et al. 2015;  
731 Harning et al., 2016a; Anderson et al., 2018; Geirsdóttir et al., 2018). But also pre-LIA  
732 advances have been identified and dated through radiocarbon and tephrochronology in a  
733 moraine sequence of Kvíárjökull (south-east Vatnajökull), the first of which occurred at  
734 Subatlantic times (before 110±240 cal. BCE) and the second at 720±395 CE (Black,  
735 1990; cited in Guðmundsson, 1997). Considering the uncertainty of our ~400 and ~700  
736 CE dates, these advances likely were coetaneous with other advances reported from  
737 southern Iceland in Kötlujökull (after 450±100 cal. CE, radiocarbon dated and  
738 supported by tephrochronology; Schomaker et al., 2003) and Sólheimajökull (southern  
739 Mýrkdalsjökull, “Ystagil stage”; Dugmore, 1989). In fact, the 669±211 CE advance of

740 western Tungnahryggsjökull (stage 3) also overlaps with the Drangajökull and  
741 Langjökull advances at ~560 CE and 550 CE, respectively (Larsen et al., 2011; Harning  
742 et al., 2016a) during DACP, in response to the summer cooling between ~250 CE and  
743 ~750 CE (Harning et al., 2016a). These advances would correspond to the general  
744 atmospheric cooling in the North Atlantic reflected by widespread glacier advances  
745 (Solomina et al., 2016).

746 The timing of the stage 2 in Vesturdalur is difficult to define because the sample TUW-  
747 16 (1220±190 CE) has almost 200-year uncertainty, and thus overlaps with both the  
748 LIA and the higher temperatures of the Medieval Warm Period (MWP, Lamb, 1965; 950-  
749 1250 CE, see Solomina et al., 2016) not conducive to glacier development as it has been  
750 observed in northwest and central Iceland (Larsen et al., 2011; Harning et al., 2016a).  
751 On the other hand, moraines in Greenland Arctic environments date within the MWP,  
752 based on cosmogenic nuclide dating (Young et al., 2015; Jomelli et al., 2016),  
753 suggesting a cooling in the western North Atlantic while the eastern sector remained  
754 warm. Iceland is located in the middle of this dipole “see-saw” pattern (Rogers and van  
755 Loon, 1979). Thus, the correlations with the glacier fluctuations Greenland or Norway,  
756 are complicated as the climate anomalies in both regions show opposing signs in the  
757 different see-saw modes. To increase the difficulty of interpretation, glaciers of  
758 Tröllaskagi are known to surge occasionally (Brynjólfsson et al., 2012; Ingólfsson et al.,  
759 2016), which could explain additional complexity in the glacial advances pattern, as it  
760 would not be driven by climatic variability. Brynjólfsson et al. (2012) pointed out that  
761 only four surges from three glaciers (Teigarjökull, Búrfellsjökull, Bægisárjökull) have  
762 been reported in the Tröllaskagi peninsula, where over 160 cirque glaciers exist.

763 *5.1.2. LIA glacial advances (15<sup>th</sup>-17<sup>th</sup> centuries)*

764 The remaining  $^{36}\text{Cl}$  ages obtained from Vesturdalur and Austurdalur are within the  
765 1450-1640 CE range ([Suppl. table ST8; Table 3](#)) and so correspond to different glacial  
766 advances or standstills during the second third of the LIA during the 15<sup>th</sup>, 16<sup>th</sup> and 17<sup>th</sup>  
767 centuries. According to our results, one of the largest glacier extents of the LIA  
768 culminated in both valleys at the latest around the mid-15<sup>th</sup> century (samples: TUW-12:  
769 1450±100 CE / stage 6; TUE-10: 1460±100 CE / stage 4). This is a very early date  
770 compared to the LIA advances previously dated in Tröllaskagi. Earlier lichenometric  
771 research carried out in nearby valleys report more recent dates for the LIA maximum:  
772 mid-18<sup>th</sup> century in Barkárdalur ([Häberle, 1991](#)); early 19<sup>th</sup> century in Bægisárjökull and  
773 Skríðudalur ([Häberle, 1991](#)), and in Búrfellsdalur and Vatnsdalur ([Kugelmann, 1991](#),  
774 [Fig. 7](#)); mid-19<sup>th</sup> century (1845-1875 CE) in Myrkárjökull, Vindheimajökull ([Häberle](#),  
775 [1991](#)), Þverárdalur, Teigardalur, Grýtudalur, Vesturárdalur ([Kugelmann, 1991, Fig. 7](#)),  
776 Heiðinnamannadalur and Kvarnárdalur ([Caseldine, 1991](#)); and late 19<sup>th</sup> century (1880s-  
777 1890s CE) in Gljúfurárdalur ([Caseldine, 1985b, 1991](#)). [Caseldine \(1991\)](#) proposed  
778 1810-1820 CE as the date of the “outer” moraine of Vesturdalur based on a minimum  
779 lichenometric age. According to our  $^{36}\text{Cl}$  moraine ages, the LIA maximum of  
780 Tungnahryggsjökull glaciers occurred ~400 years earlier than these dates. This should  
781 not be surprising as [Kirkbride and Dugmore \(2001\)](#) reported lichenometric ages >100  
782 years younger than those derived from tephrochronology in the same landforms. Our  
783 results also give the earliest LIA dates based on moraine dating obtained so far in  
784 Iceland, compared to the previously published dates all obtained through lichenometric  
785 dating: 1740-1760 CE in south-east Iceland ([Chenet et al., 2010](#)). In northwestern  
786 Iceland, glaciolacustrine sediments recorded a contemporary expansion of Drangajökull  
787 at ~1400 CE ([Harning et al., 2016a](#)). Likewise a first major advance of Langjökull  
788 (western central Iceland; [Fig. 1A](#)) between 1450 and 1550 CE has been reported ([Larsen](#)

789 [et al., 2011](#)), as well as advances in central Iceland between 1690 and 1740 CE  
790 ([Kirkbride and Dugmore, 2006](#)), based on varve thickness variance together with annual  
791 layer counting and C:N mass ratio, and tephrochronology (geochemical analysis),  
792 respectively.

793 The dates of samples TUV-13, TUV-12 and TUV-11 in Vesturdalur (average date  
794  $1470 \pm 120$  CE; stages 3, 5 and 6) cannot be distinguished statistically if their internal  
795 uncertainty is considered ([Fig. 4](#); [Suppl. table ST8](#)). The spatial scatter of these  
796 sampling sites ([Fig. 2](#)) may indicate frequent and intense terminus fluctuations in a short  
797 time interval. Different ages obtained from the moraines of the stages 3 and 4 in  
798 Vesturdalur and Austurdalur, respectively, may indicate that in the 15<sup>th</sup> century the  
799 glacier termini reached the moraines deposited at  $\sim 700$  CE ([Figs. 2 and 3](#)) and rebuilt  
800 them, which may explain the large size of these moraines. [Caseldine \(1987\)](#) argued that  
801 other moraines in Skíðadalur were formed during more than one advance. Based on the  
802 size of the largest moraines, he also pointed out that many glaciers must have advanced  
803 to positions similar to those of the late 19<sup>th</sup> century earlier in the Neoglacial.

804 The glacier advances in the 15<sup>th</sup> century in Vesturdalur and Austurdalur may have been  
805 the result of different climate forcings during that century: negative radiative forcing  
806 and summer cooling were linked to intense volcanic activity ([Miller et al., 2012](#)), the  
807 low solar activity of the Spörer Minimum (1460-1550 CE; [Eddy, 1976](#)), the sea-  
808 ice/ocean feedback with increased sea ice ([Miller et al., 2012](#)) and the weakening of the  
809 Atlantic Meridional Overturning Circulation (AMOC) ([Zhong et al., 2011](#)). Solar  
810 activity may have played a major role in these glacial advances if we consider that the  
811 climate in the North Atlantic is highly influenced by solar activity variability ([Jiang et al.,](#)  
812 [2015](#)). On the contrary, historical records, although not determinant, suggest a mild  
813 climate for 1430-1550 CE ([Ogilvie and Jonsdóttir, 2000](#)), and especially for 1412-1470

814 CE (Ogilvie, 1984). This would also be compatible with increased precipitation and  
815 hence more winter snow in warm periods (Caseldine and Stötter, 1993; Stötter et al.,  
816 1999; Fernández-Fernández et al., 2017), and also with potential surge activity with  
817 glacial advances not directly linked to specific climate periods (e.g. Brynjólfsson et al.,  
818 2012; Ingólfsson et al., 2016).

819 In Vesturdalur, the dates of samples TUW-9 (1590±100 CE) and TUW-10 (1640±90  
820 CE) are compatible with a cold period from the late 1500s to 1630 CE (Ogilvie and  
821 Jónsson, 2001). Nevertheless, considering the uncertainties of these samples, their dates  
822 also overlap with the Maunder Minimum (1645-1715 CE) (Eddy, 1976), when the LIA  
823 maximum glacial advance occurred in the Alps (Holzhauser et al., 2005).

## 824 5.2. Lichenometric dating.

### 825 5.2.1. $^{36}\text{Cl}$ CRE dating vs. lichenometric dating. Multiple lichen species dating 826 approach.

827 The contrast between our CRE dating results and earlier lichenometry-based results  
828 published elsewhere evidences the clear underestimation of the latter. This could be  
829 explained either by lichen growth inhibition due to saturation of the rock surface and  
830 competition of other thalli (Wiles et al., 2010; Le Roy et al., 2017) or a colonization lag  
831 longer than assumed up to now, from 10 to 15 years in Tröllaskagi (Kugelmann, 1991;  
832 Caseldine, 1985b, respectively). However, other factors affect the reliability of the  
833 lichen-derived ages, and may explain the differences with CRE dates. One of them is  
834 the reliability of the growth rates and lichenometric calibration curves that are  
835 commonly assumed to be linear (constant) growth in northern Iceland (e.g. Caseldine,  
836 1983, 1985b; Häberle, 1991; Kugelmann, 1991), although it has been demonstrated that  
837 the lichen diameter growth declines with age (see e.g. Winkler, 2003, Fig. 4). This

838 might lead to significant age underestimations for the oldest dates, putting potentially  
839 earlier dates in the 19<sup>th</sup> century. Most of the fixed control points from which lichen  
840 growth rates have been derived in northern Iceland comprise abandoned gravestones,  
841 memorial stones, old bridges and mostly abandoned farmsteads (Caseldine, 1983;  
842 Kugelmann, 1991). Time of death is commonly assumed for gravestones, and  
843 abandonment date for farmsteads. Although the latter is well known on the basis of  
844 historical documentation, the colonization lag sometimes relies on the “the likely  
845 duration” of the deterioration of the buildings after abandonment that depends on the  
846 quality and stability of the constructions (see Kugelmann, 1991), and hence affect the  
847 results. However, it should be highlighted that our approach circumvents this last issue  
848 by combining field observations with historical aerial photographs. In addition, given  
849 that lichen growth of *Rhizocarpon* subgenus depends mostly on available humidity, the  
850 location of the measured lichens has also a potential effect on the results, i.e. to micro-  
851 climatic changes (see Innes, 1985; Hamilton and Whalley, 1995) between the location  
852 of the fixed points and the location on the moraine (crest: dryer and more exposed;  
853 green zone on the proximal slope, etc.). In the literature cited above about lichenometry-  
854 dated LIA advances no detailed information is provided about the location of the lichen  
855 measured for dating purposes, so potential error derived from this issue can not be  
856 assessed. Nevertheless, given that we measured lichens on horizontal flat surfaces  
857 where there is no restriction to the moisture receipt of the lichens, we can consider our  
858 results presented throughout the next sections valid. In any case, such a great difference  
859 of our CRE dates and the previous lichen-derived is more likely to be explained by the  
860 technical limitations of the technique rather than environmental factors.

861 Our field observations and historical aerial photos of known age restricted the dates of  
862 the moraines colonized by *Rhizocarpon geographicum* lichens. This approach would

863 support the dates obtained from the 0.44 mm yr<sup>-1</sup> growth rate of Kugelmann (1991) and  
864 the 20-year colonization lag. This rate is slightly higher than those reported from the  
865 Antarctic Peninsula (0.31 mm yr<sup>-1</sup>; Sancho et al., 2017), but lower than in Tierra del  
866 Fuego (0.63 mm yr<sup>-1</sup>; Sancho et al., 2011). The correlation between the sizes of largest  
867 *Rhizocarpon geographicum* and *Porpidia* cf. *soredizodes* thalli at the same stations  
868 showed a proportionality between the largest thalli of both species: thalli of *Porpidia* cf.  
869 *soredizodes* species grow faster than those of *Rhizocarpon geographicum*. The sizes of  
870 the largest *Rhizocarpon geographicum* thalli were plotted against the sizes of the largest  
871 *Rhizocarpon geographicum* lichens (Fig. 5). The slope of the best-fit linear curve  
872 obtained was around 1.675 (r<sup>2</sup>=0.82) that suggests that *Porpidia* cf. *soredizodes* lichens  
873 grow 1.675 times faster than those of *Rhizocarpon geographicum*. So if we assume 0.44  
874 mm yr<sup>-1</sup> growth rate for *Rhizocarpon geographicum* lichens, a tentative growth rate of  
875 *Porpidia* cf. *soredizodes* would be 0.737 mm yr<sup>-1</sup>. However, this approach should be  
876 taken with caution due to the limited number of lichens (n=7) used of each species.  
877 Aiming to obtain a tentative date (Table 2), this growth rate was applied to the largest  
878 *Porpidia* cf. *soredizodes* lichens found in those stations where no *Rhizocarpon*  
879 *geographicum* lichens could be measured (TUW-1, TUW-8, TUE-1 and TUE-8).

880 Assuming colonization lags of 20 and 15 years for *Rhizocarpon geographicum* and  
881 *Porpidia* cf. *soredizodes* lichens, respectively, and the above-mentioned growth rates,  
882 several glacial advances or standstills are tentatively placed in the 19<sup>th</sup> and 20<sup>th</sup>  
883 centuries, in the context of a general retreat from the most advanced LIA positions, as  
884 discussed in the next section.

#### 885 5.2.2. LIA glacial advances/standstills: 19<sup>th</sup> century

886 Despite the low number of lichenometry stations surveyed and the limitations of this  
887 dating approach discussed in the previous sections, our results are in accordance with

888 the geomorphological logic and with the chronological frame obtained from historical  
889 aerial photos. The ages derived from *Rhizocarpon geographicum* thalli measurements at  
890 lichenometry stations pre-dating 1946 suggest that the western and eastern  
891 Tungnahryggsjökull culminated successive advances/standstills around the 1830s,  
892 1840s, 1860s and 1890s CE (Figs. 2 and 3, Table 2). Ages tentatively estimated from  
893 *Porpidia* cf. *soredizodes* thalli considering its apparently higher growth rate suggest  
894 glacial advances/standstills around the 1800s (Figs. 2 and 3, Table 2). No inconsistency  
895 (age inversions) is detected in the lichenometry-dated moraine sequence, but we  
896 recognise that some age underestimation may occur since: (i) we assume linear growth  
897 when applying a growth rate; and (ii) our 19<sup>th</sup> dates were derived from >40-45 mm-  
898 diameter lichens (Table 2 and Suppl. table ST4), which exceed the size of the biggest  
899 control point from which Kugelmann's growth rate was estimated (Kugelmann, 1991,  
900 Fig. 3). This problem reinforces the need of taking lichen-derived ages as relative. The  
901 interpretation of the chronology in Austurdalur is more complicated: the lichen sizes  
902 measured at the stations TUE-6 (1890s CE, stage 9) and TUE-7 (1880s CE; stage 7)  
903 yield more recent dates than at station TUE-5 (1860s CE; stage 10) despite being  
904 representative of earlier stages (Fig. 3). Given that this anomaly occurs in both lichen  
905 species, it is reasonable to conclude that an environmental factor could have affected the  
906 lichen populations at both stations. It could even indicate a date when the boulders may  
907 have been remobilized by postglacial processes.

908 Our chronology of the 19<sup>th</sup> century glacial advances in both valleys (Table 2) does not  
909 coincide exactly with the phases identified by Kugelmann (1991) in Svarfaðardalur-  
910 Skíðadalur (1810, 1850, 1870-1880, 1890-1900 CE). It also differs appreciably from the  
911 chronology proposed by Caseldine (1985b) in Vesturdalur (moraines of 1868, 1878,  
912 1887, 1898 CE). Nevertheless, it should be borne in mind that we are considering only

913 two glaciers with their own glaciological properties. Moreover, we have estimated the  
914 ages from the growth rate (instead of a specific calibration growth curve), longer  
915 colonization lag based on field observations, and applied to the longest axis  
916 measurements ([Kugelmann, 1991](#)). On the other hand, micro-climatic differences  
917 between the location of fixed points and our lichen measured may occur. However, we  
918 recognise that the comparisons with [Caseldine's \(1985b\)](#) results are quite difficult since:  
919 (i) the moraines dated by Caseldine are poorly located in his mapping (and hard to  
920 identify over aerial photos and our moraine mapping); (ii) we are not able to apply the  
921 same parameters to his measurements, as he used the mean longest axis of the five  
922 largest lichen is not provided (only the average value); and (iii) he recognised the lichen  
923 growth slowdown when dating the outermost moraine, which probably is one of those  
924 dated with  $^{36}\text{Cl}$  in this work.

925 Our results, despite the limitations of the applied method, largely due to the low number  
926 of moraine boulders suitable for its application can be considered compatible and in  
927 good agreement with glacial advances and cold periods during the first third of the 19<sup>th</sup>  
928 century as we show below. [Martin et al. \(1991\)](#) pointed out the existence of a moraine  
929 dated to ca. 1810-1820 CE in “Western Tröllaskagi Tungnahryggsjökull” (ambiguously,  
930 without providing any detail of its location), as well as others of this period in  
931 Svarfaðardalur, Búrfellsdalur and Vatnsdalur. Other dates obtained from more  
932 sophisticated statistical techniques applied to lichenometry dating procedures also  
933 evidenced a glacial advance phase 1810-1820 CE ([Chenet et al., 2010](#)). These advance  
934 phases were coetaneous with significant sea ice persistence in the early 1800s ([Ogilvie  
935 and Jónsson, 2001](#)), decreased solar activity, and strong volcanic eruptions (Dalton  
936 Minimum, 1790-1830 CE; [Wagner et al., 2005](#)). The moraines dated in Vesturdalur to  
937 around 1830 CE (TUW-7: 1830s CE, stage 10) and the early 1890s CE (TUW-5: 1890s

938 CE, stage 12) are in good agreement with the glacial advances in Svarfaðardalur-  
939 Skíðadalur during the 1830s and early 1890s CE (Kugelmann, 1991, Fig. 8), as well as  
940 with the low temperatures and presence of sea ice at these dates (Koch, 1945; Ogilvie,  
941 1996; Ogilvie and Jonsdóttir, 2000; Ogilvie and Jónsson, 2001; Kirkbride, 2002).

### 942 5.2.3. Post-LIA glacial advances/standstills.

943 Lichen-derived ages from *Rhizocarpon geographicum* thalli suggest the occurrence of  
944 glacial advances or standstills at the first half of the 20<sup>th</sup> century, culminating in 1910s,  
945 1930s, 1940s and 1950s CE, although the 1930s CE date (TUE-3; stage 12) disagrees  
946 with the date inferred from the aerial photos, at some point between 1946 and 1985 CE  
947 (Suppl. figure SF2; Table 2). However, the 1910s CE date in both valleys is in good  
948 agreement with the moraine abandonment during the first two decades of the 20<sup>th</sup>  
949 century; it would be the result of the accumulated effect of the temperature rise since the  
950 latter half of the 19<sup>th</sup> century (Caseldine, 1987; Wanner et al., 2008). Thus, the  
951 subsequent advances would be the response to specific relative thermal minima within a  
952 warmer climate (Stötter et al., 1999). The date of TUW-3 (stage 13) representing the  
953 moraine abandonment in ~1940 CE is in agreement with the overall context of general  
954 glacier retreat as a result of the warmest decades of the 1930s and 1940s CE, which  
955 triggered an intense retreat of the glaciers (Einarsson, 1991; Martin et al., 1991;  
956 Kirkbride, 2002). The advances/standstills dated to the early 1950s CE in both  
957 Tungnahryggsjökull glaciers are likely to be synchronous given the similarity of the  
958 dates obtained (Table 2). They could represent glacial advances in consonance with the  
959 late 1940s – early/mid-1950s CE cooling (Einarsson, 1991; Fernández-Fernández et al.,  
960 2017), recorded both in Akureyri and many other weather stations throughout Iceland.  
961 Caseldine (1983) found a similar chronology in Gljúfurárdalur (Skíðadalur headwater,

962 10 km to the east), with moraine deposition between mid-1910s and 1930, around mid-  
963 1930s and late 1940s-1950 CE.

964 The subsequent trend of the Tungnahryggsjökull glaciers, inferred from aerial  
965 photographs, a satellite image, geomorphological mapping, and glacier reconstruction,  
966 was characterized by continuous retreat and volume loss, in line with the increasing  
967 temperature trend since the end of the LIA. This trend was only reversed between the  
968 mid-1960s and mid-1980s CE by a major cooling event (Einarsson, 1991; Sigurðsson,  
969 2005; Fernández-Fernández et al., 2017). Two moraines have been dated after the 1950s  
970 CE. The date obtained in station TUE-1 (1970s CE; stage 14) agrees with the date  
971 deduced from the 1946 and 1985 aerial photographs (Suppl. figure SF2). However, the  
972 date estimated in station TUW-1 (1970s CE; between stages 15 and 16) is prior to that  
973 obtained from the 1994 and 2000 aerial photographs. The reason for this mismatch may  
974 be a non-linear growth phase of the *Porpidia* cf. *soredizodes* thalli measured (i.e. its real  
975 growth rate may have been lower than the estimated). Nevertheless, more research on  
976 this species is required to use it successfully in lichenometric dating.

977 The aerial photographs from 1994 (stage 15 western Tungnahryggsjökull) and 2000  
978 (stage 16) show a reversal in the trend of both Tungnahryggsjökull glaciers (Suppl.  
979 figure SF2), as the positions of their termini are more advanced than in 1985 (stages 14  
980 and 15; see Fernández-Fernández et al., 2017). These advances in Vesturdalur and  
981 Austurdalur, culminating after 1985 in a period non-conducive to glacier expansion,  
982 may have been linked to above average precipitation for 1988-1995, which prevented a  
983 negative mass balance of the glaciers (Sigurðsson, 2005). The 2000 aerial photo (stage  
984 16) and 2005 SPOT satellite image (stage 17) display the retreat of both glaciers. This  
985 trend was reinforced by the sudden warming initiated in 1995, which triggered  
986 decreased snowfall, negative mass balances for 1996-2000, and retreat of the non-

987 surging glaciers after 2000 (Sigurðsson, 2005). In spite of these glacial fluctuations in  
988 response to the intense climatic fluctuations of the last century, the ELAs estimated in  
989 this paper only show a general rise of 5-10 m (Table 1). This small ELA increase may  
990 be derived from some artifacts of the glacier reconstruction or the attenuating effect of  
991 the increase in winter precipitation suggested by glacier-climate models (Caseldine and  
992 Stötter, 1993; Fernández-Fernández et al., 2017).

993 *5.3. Final remarks: Can the occurrence of pre-LIA glacial advances be confirmed? Was*  
994 *the LIA in northern Iceland the Holocene glacial maximum? Was it a single maximum*  
995 *advance?*

996 Our results demonstrate that Tungnahryggsjökull advanced during Late Holocene glacial  
997 stages prior to the LIA and reached considerably more advanced positions, even though  
998 the Iceland large ice caps reached generally their Late Holocene maximum advance  
999 during the LIA (Larsen et al. 2015, Harning et al., 2016a; Anderson et al., 2018,  
1000 Geirsdóttir et al., 2018). The chronological data presented in the previous sections  
1001 suggests that during the LIA the glaciers overlapped moraines deposited in pre-LIA  
1002 glacial stages. Our results also show LIA advances since the 15<sup>th</sup> century and are thus  
1003 contrary to the traditional proposal of a single maximum LIA advance occurring during  
1004 either mid-18<sup>th</sup> or late-19<sup>th</sup> centuries in Tröllaskagi peninsula, followed by subsequent  
1005 minor readvances in an overall retreating trend (see Caseldine, 1983, 1985b, 1987;  
1006 Kugelmann, 1991; Martin et al., 1991). The use of the <sup>36</sup>Cl production rates from Ca  
1007 spallation reported by Stone et al. (1996) does not lead to major changes in the  
1008 interpretation and conclusions as the changes in the nominal dates (up to 90 yr earlier;  
1009 Table 3) are within the external uncertainty and also overlap with the results presented  
1010 above based on the Licciardi et al. (2008) production rate. Similarly, if we consider the  
1011 results derived by the Schimmelpfennig et al. (2011) production rate, we obtain even

1012 earlier ages, which still overlap with the results derived by the other production rates  
1013 due to a higher external uncertainty (see [Table 3](#)). Although the snow cover duration is  
1014 known to be high in northern Iceland (see [Dietz et al., 2012](#)), quantifying the effect of  
1015 snow cover on sub-surface  $^{36}\text{Cl}$  production is a complex issue: on the one side, snow  
1016 lowers the isotopic production rates related to spallation reactions due to the shielding  
1017 effect on high-energy neutrons ([Benson et al., 2004](#); [Schildgen et al., 2005](#)), and on the  
1018 other side it increases the  $^{36}\text{Cl}$  production rate from thermal neutrons below the rock  
1019 surface, due to the enhancing effect of hydrogen on these low-energy neutrons ([Dunai et](#)  
1020 [al., 2014](#)). Both effects might cancel out depending on the composition of the samples,  
1021 and their quantification is still debated and affected by high uncertainties ([Zweck et al.,](#)  
1022 [2013](#); [Dunai et al., 2014](#); [Delunel et al., 2014](#)). Given this complexity, snow shielding  
1023 was not applied. In any case its effect is unlikely to be higher than the uncertainty  
1024 derived from extracting  $^{36}\text{Cl}$  from whole rock instead of minerals.

1025 Our results are in concordance with several valleys in northern Iceland, but also with the  
1026 results that are being obtained in other sectors of Arctic and North Atlantic region in the  
1027 last years, such as: in Baffin Island (northern Canada), where glaciers reached Late  
1028 Holocene maximum positions prior to the LIA ([Young et al., 2015](#);  $^{10}\text{Be}$  dating), or  
1029 West Greenland, with several advances or stabilizations at  $1450\pm 90$  CE and  $1720\pm 60$   
1030 CE ([Jomelli et al., 2016](#);  $^{36}\text{Cl}$  dating). However, it is striking that the early LIA  
1031 advances of northern Iceland reported in the present paper do not agree with maritime  
1032 Norway with later maximum culminations (see [Nesje et al., 2008](#)) despite being the  
1033 glaciated region most comparable with Iceland in terms of climate and glaciology. Our  
1034 results also agree with farther and southern areas such as the Alps, with maximum  
1035 advances at around 1430 CE ([Schimmelpfennig et al., 2012, 2014a](#));  $^{10}\text{Be}$  dates; and  
1036 Sierra Nevada (Iberian Peninsula), where LIA advances have been reported between the

1037 14<sup>th</sup> and 17<sup>th</sup> centuries (Palacios et al., 2019; <sup>10</sup>Be dates). Our detailed moraine  
1038 mapping, combined with CRE dating in the surveyed valleys, clearly shows a number of  
1039 advances throughout the LIA, in response to the great climatic variability of the region  
1040 with alternating cold and mild/warm periods (Ogilvie, 1984, 1996; Ogilvie and  
1041 Jónsdóttir, 2000; Ogilvie and Jónsson, 2001; Geirsdóttir et al., 2009) as occurred in the  
1042 Alps (e.g. Schimmelpfennig et al., 2014a) or the Iberian mountains (e.g. Oliva et al.,  
1043 2018). The ELA calculations show that the major long-lasting rise of the glacier ELA  
1044 (24-50 m depending on the calculation method) took place prior to 1900s/1910s.

1045 According to the results, the evolution pattern described by Fernández-Fernández et al.  
1046 (2017) for the Tungnahryggsjökull glaciers should be revised as the <sup>36</sup>Cl CRE dates  
1047 from the 15<sup>th</sup> and 17<sup>th</sup> centuries indicate that LIA maximum was reached earlier than  
1048 previously thought. Thus, if we consider the ELA of the earliest LIA dates obtained  
1049 with <sup>36</sup>Cl CRE (i.e. stages 5 and 4 of western and eastern Tungnahryggsjökull), these  
1050 imply ELA depressions (with reference to the 2005 date) of 24-50 m (depending on the  
1051 ELA calculation method), occurring for at least 560 years (Table 1) and not 150 years as  
1052 had been previously assumed (Caseldine and Stötter, 1993; Fernández-Fernández et al.,  
1053 2017).

## 1054 **Conclusions**

1055 (i) This paper highlights the detailed geomorphological analysis of the glacial landforms  
1056 as an essential pre-requisite prior to the application of dating methods on them.  
1057 Nevertheless, this has greatly limited the number of valid moraine boulders to be dated,  
1058 since the vast majority of those were affected by post-glacial processes. This issue which  
1059 has prevented a statistically acceptable sampling and the validation or invalidation of  
1060 the “inconsistent” ages yielded by several boulders, so a conclusive explanation cannot  
1061 be given.

1062 (ii) Applying  $^{36}\text{Cl}$  CRE dating for the first time in the Tröllaskagi peninsula enabled us  
1063 to identify pre-LIA glacial advances in Vesturdalur and Austurdalur. Thus, the western  
1064 and eastern Tungnahryggsjökull glaciers did not reach their Late Holocene maximum  
1065 extent during the LIA. The maximum extent for the eastern glacier was dated to ~400  
1066 CE. For the western glacier a latest date of ~700 CE and an earliest of 16300 years ago  
1067 (when the Elliði crest was deglaciated) have been obtained.

1068 (iii) The LIA maximum in Vesturdalur and Austurdalur was reached by the 15<sup>th</sup> century  
1069 at the latest. A combination of detailed moraine mapping and  $^{36}\text{Cl}$  CRE dating confirm a  
1070 number of glacial advances between the 15<sup>th</sup> and 17<sup>th</sup> centuries, the earliest LIA  
1071 advances dated in Tröllaskagi at present.

1072 (iv) For the recent dates, the complementary use of aerial photographs, a satellite image  
1073 and fieldwork has aided to obtain lichenometry-derived ages tentatively in good  
1074 agreement with the morpho-stratigraphic order of the glacial landforms. It has also  
1075 compensated some of the limitations and error sources of lichenometric dating. Thus, it  
1076 has proved to be a useful tool to assess the colonization lags and the validity of the  
1077 lichenometry-derived ages.

1078 (v) Fieldwork on recently deglaciated surfaces and historical aerial photographs have  
1079 shown clearly that the colonization lag of *Rhizocarpon geographicum* lichen species is  
1080 from 15-21 to 30 years, considerably longer than previously assumed in Tröllaskagi.  
1081 Colonization of the *Porpidia* cf. *soredizodes* species is shorter, between 10 and 21  
1082 years.

1083 (vi) From the measurements carried out in different lichenometry stations, growth of  
1084 *Porpidia* cf. *soredizodes* lichen appeared to be higher than in the case of *Rhizocarpon*  
1085 *geographicum*, and also proportional to that. Its growth rate has been tentatively

1086 estimated for the first time, at around 0.737 mm yr<sup>-1</sup>. However, further research on the  
1087 growth rates of this species is required for its potential use in lichenometric dating as a  
1088 complementary species, since it also shows a shorter colonisation lag than *Rhizocarpon*  
1089 *geographicum*.

## 1090 **Acknowledgements**

1091 This paper was supported by the project CGL2015-65813-R (Spanish Ministry of  
1092 Economy and Competitiveness) and Nils Mobility Program (EEA GRANTS), and with  
1093 the help of the High Mountain Physical Geography Research Group (Complutense  
1094 University Madrid). We thank the Icelandic Association for Search and Rescue, the  
1095 Icelandic Institute of Natural History, the Hólar University College, and David Palacios  
1096 Jr. and María Palacios for their support in the field. José M. Fernández-Fernández  
1097 received a PhD fellowship from the FPU programme (Spanish Ministry of Education,  
1098 Culture and Sport; reference FPU14/06150). The <sup>36</sup>Cl measurements were performed at  
1099 the ASTER AMS national facility (CEREGE, Aix en Provence), which is supported by  
1100 the INSU/CNRS and the ANR through the "Projets thématiques d'excellence" program  
1101 for the "Equipements d'excellence" ASTER-CEREGE action and IRD.

## 1102 **References**

- 1103 Anderson, L.S., Flowers, G.E., Jarosch, A.H., Aðalgeirsdóttir, G.T., Geirsdóttir, Á.,  
1104 Miller, G.H., Harning, D.J., Thorsteinsson, T., Magnússon, E., Pálsson, F., 2018.  
1105 Holocene glacier and climate variations in Vestfirðir, Iceland, from the modeling of  
1106 Drangajökull ice cap. *Quat. Sci. Rev.* 190, 39–56.  
1107 doi:10.1016/j.quascirev.2018.04.024
- 1108 Andrews, J.T., Giraudeau, J., 2003. Multi-proxy records showing significant Holocene  
1109 environmental variability: the inner N. Iceland shelf (Húnaflói). *Quat. Sci. Rev.* 22,  
1110 175–193. doi: 10.1016/S0277-3791(02)00035-5
- 1111 Andrés, N., Palacios, D., Sæmundsson, Þ., Brynjólfsson, S., Fernández-Fernández, J.M.,  
1112 2018. The rapid deglaciation of the Skagafjörður fjord, northern Iceland. *Boreas*.  
1113 doi:10.1111/bor.12341

- 1114 Andrés, N., Tanarro, L.M., Fernández, J.M., Palacios, D., 2016. The origin of glacial  
1115 alpine landscape in Tröllaskagi Peninsula (North Iceland). *Cuad. Investig.*  
1116 *Geográfica* 42, 341–368. doi:10.18172/cig.2935
- 1117 Arróniz-Crespo, M., Pérez-Ortega, S., De Los Ríos, A., Green, T.G.A., Ochoa-Hueso,  
1118 R., Casermeiro, M.Á., De La Cruz, M.T., Pintado, A., Palacios, D., Rozzi, R.,  
1119 Tysklind, N., Sancho, L.G., 2014. Bryophyte-cyanobacteria associations during  
1120 primary succession in recently deglaciated areas of Tierra del Fuego (Chile). *PLoS*  
1121 *One* 9, 15–17. doi:10.1371/journal.pone.0096081
- 1122 Barker, S., Knorr, G., Vautravers, M.J., Diz, P., Skinner, L.C., 2010. Extreme  
1123 deepening of the Atlantic overturning circulation during deglaciation. *Nat. Geosci.*  
1124 3, 567–571. doi:10.1038/ngeo921
- 1125 Benn, D.I., Hulton, N.R.J., 2010. An Excel™ spreadsheet program for reconstructing  
1126 the surface profile of former mountain glaciers and ice caps. *Comput. Geosci.* 36,  
1127 605–610. doi:10.1016/j.cageo.2009.09.016
- 1128 Benson, L., Madole, R., Phillips, W., Landis, G., Thomas, T., Kubik, P., 2004. The  
1129 probable importance of snow and sediment shielding on cosmogenic ages of north-  
1130 central Colorado Pinedale and pre-Pinedale moraines. *Quat. Sci. Rev.* 23, 193–206.  
1131 doi:10.1016/j.quascirev.2003.07.002
- 1132 Bergþórsson, P., 1969. An Estimate of Drift Ice and Temperature in Iceland in 1000  
1133 Years. *Jökull* 19, 94-101.
- 1134 Bickerton, R.W., Matthews, J.A., 1992. On the accuracy of lichenometric dates: an  
1135 assessment based on the “Little Ice Age” moraine sequence of Nigardsbreen,  
1136 southern Norway.” *Holocene* 2, 227–237. doi:10.1177/095968369200200304
- 1137 Björnsson, H., 1978. Surface area of glaciers in Iceland. *Jökull* 28, 31.
- 1138 Black, T.A., 1990. The Holocene fluctuation of the Kvíárjökull glacier, southeastern  
1139 Iceland. Unpublished MA thesis. University of Colorado.
- 1140 Bradwell, T., 2004a. Lichenometric dating in southeast Iceland: The size- frequency  
1141 approach. *Geogr. Ann. Ser. A Phys. Geogr.* 86, 31–41. doi:10.1111/j.0435-  
1142 3676.2004.00211.x
- 1143 Bradwell, T., 2004b. Annual Moraines and Summer Temperatures at  
1144 Lambatungnajökull, Iceland. *Arctic, Antarct. Alp. Res.* 36, 502–508.  
1145 [https://doi.org/10.1657/1523-0430\(2004\)036\[0502:AMASTA\]2.0.CO;2](https://doi.org/10.1657/1523-0430(2004)036[0502:AMASTA]2.0.CO;2)
- 1146 Bradwell, T., 2001. A new lichenometric dating curve for Southeast Iceland. *Geogr.*  
1147 *Ann. Ser. A Phys. Geogr.* 83, 91–101. doi:10.1111/j.0435-3676.2001.00146.x
- 1148 Bradwell, T., Armstrong, R.A., 2006. Growth rates of *Rhizocarpon geographicum*  
1149 lichens: a review with new data from Iceland. *J. Quat. Sci.* 22, 311–320.  
1150 doi:10.1002/jqs.1058

- 1151 Brugger, K.A., 2006. Late Pleistocene climate inferred from the reconstruction of the  
1152 Taylor River glacier complex, southern Sawatch Range, Colorado. *Geomorphology*  
1153 75, 318–329. doi:10.1016/j.geomorph.2005.07.020
- 1154 Brynjólfsson, S., Ingólfsson, Ó., Schomacker, A., 2012. Surge fingerprintings of cirque  
1155 glaciers at Tröllaskagi peninsula, North Iceland. *Jökull* 62, 153–168.
- 1156 Brynjólfsson, S., Schomacker, A., Guðmundsdóttir, E.R., Ingólfsson, Ó., 2015a. A 300-  
1157 year surge history of the Drangajökull ice cap, northwest Iceland, and its maximum  
1158 during the Little Ice Age. *The Holocene* 25(7), 1076-1092. doi:  
1159 10.1177/0959683615576232
- 1160 Brynjólfsson, S., Schomacker, A., Ingólfsson, Ó., Keiding, J.K., 2015b. Cosmogenic  
1161 <sup>36</sup>Cl exposure ages reveal a 9.3 ka BP glacier advance and the Late Weichselian-  
1162 Early Holocene glacial history of the Drangajökull region, northwest Iceland. *Quat.*  
1163 *Sci. Rev.* 126, 140–157. doi:10.1016/j.quascirev.2015.09.001
- 1164 Caseldine, C., 1987. Neoglacial glacier variations in northern Iceland: Examples from  
1165 the Eyjafjörður area. *Arct. Alp. Res.* 19, 296–304.
- 1166 Caseldine, C., 1983. Resurvey of the margins of Gljúfurárjökull and the chronology of  
1167 recent deglaciation. *Jökull* 33, 111–118.
- 1168 Caseldine, C., Hatton, J., 1994. Environmental change in Iceland. *Münchener Geogr.*  
1169 *Abhandlungen. R. B Bd. B* 12 41–62.
- 1170 Caseldine, C., Stotter, J., 1993. “Little Ice Age” glaciation of Tröllaskagi peninsula,  
1171 northern Iceland: climatic implications for reconstructed equilibrium line altitudes  
1172 (ELAs).” *Holocene* 3, 357–366. doi:10.1177/095968369300300408
- 1173 Caseldine, C.J., 1991. Lichenometric dating, lichen population studies and Holocene  
1174 glacial history in Tröllaskagi, Northern Iceland, in: Maizels, J.K., Caseldine, C.  
1175 (Eds.), *Environmental Change in Iceland: Past and Present. Glaciology and*  
1176 *Quaternary Geology, Vol 7.* Springer, Dordrecht, pp. 219–233. doi:10.1007/978-  
1177 94-011-3150-6\_15
- 1178 Caseldine, C.J., 1990. A review of dating methods and their application in the  
1179 development of a Holocene glacial chronology for Northern Iceland, in: *Gletscher-*  
1180 *Und Landschaftsgeschichtliche Untersuchungen in Nordisland.* pp. 59–82.
- 1181 Caseldine, C.J., 1985a. Survey of Gljúfurárjökull and features associated with a glacier  
1182 burst in Gljúfurárdalur, Northern Iceland. *Jökull* 35, 61-68.
- 1183 Caseldine, C.J., 1985b. The Extent of Some Glaciers in Northern Iceland during the  
1184 Little Ice Age and the Nature of Recent Deglaciation. *Geogr. J.* 151, 215–227.  
1185 doi:10.2307/633535
- 1186 Chen, T., Robinson, L.F., Burke, A., Southon, J., Spooner, P., Morris, P.J., Ng, H.C.,  
1187 2015. Synchronous centennial abrupt events in the ocean and atmosphere during the  
1188 last deglaciation. *Science* 349, 1537–1541. doi:10.1126/science.aac6159

- 1189 Chenet, M., Roussel, E., Jomelli, V., Grancher, D., 2010. Asynchronous Little Ice Age  
1190 glacial maximum extent in southeast Iceland. *Geomorphology* 114, 253–260.  
1191 doi:10.1016/j.geomorph.2009.07.012
- 1192 Coquin, J., Mercier, D., Bourgeois, O., Cossart, E., Decaulne, A., 2015. Gravitational  
1193 spreading of mountain ridges coeval with Late Weichselian deglaciation: Impact on  
1194 glacial landscapes in Tröllaskagi, northern Iceland. *Quat. Sci. Rev.* 107, 197–213.  
1195 doi:10.1016/j.quascirev.2014.10.023
- 1196 Cossart, E., Mercier, D., Decaulne, A., Feuillet, T., Jónsson, H.P., Sæmundsson, Þ.,  
1197 2014. Impacts of post-glacial rebound on landslide spatial distribution at a regional  
1198 scale in northern Iceland (Skagafjörður). *Earth Surf. Process. Landforms* 39, 336–  
1199 350. doi:10.1002/esp.3450
- 1200 Crochet, P., Jóhannesson, T., Jónsson, T., Sigurðsson, O., Björnsson, H., Pálsson, F.,  
1201 Barstad, I., 2007. Estimating the Spatial Distribution of Precipitation in Iceland  
1202 Using a Linear Model of Orographic Precipitation. *J. Hydrometeorol.* 8, 1285–  
1203 1306. doi:10.1175/2007JHM795.1
- 1204 Dahl, S.O., Nesje, A., 1992. Paleoclimatic implications based on equilibrium-line  
1205 altitude depressions of reconstructed Younger Dryas and Holocene cirque glaciers  
1206 in inner Nordfjord, western Norway. *Palaeogeogr. Palaeoclimatol. Palaeoecol.* 94,  
1207 87–97. doi:10.1016/0031-0182(92)90114-K
- 1208 Decaulne, A., 2016. Lichenometry in Iceland, results and application. *Géomorphologie*  
1209 *Reli. Process. Environ.* 22, 77–91. doi:10.4000/geomorphologie.11291
- 1210 Decaulne, A., Saemundsson, T., 2006. Geomorphic evidence for present-day snow-  
1211 avalanche and debris-flow impact in the Icelandic Westfjords. *Geomorphology* 80,  
1212 80–93. doi:10.1016/J.GEOMORPH.2005.09.007
- 1213 Delunel, R., Boulès, D.L., van der Beek, P.A., Schlunegger, F., Leya, I., Masarik, J.,  
1214 Paquet, E., 2014. Snow shielding factors for cosmogenic nuclide dating inferred  
1215 from long-term neutron detector monitoring. *Quat. Geochronol.* 24, 16–26. doi:  
1216 10.1016/J.QUAGEO.2014.07.003
- 1217 Dietz, A.J., Wohner, C., Kuenzer, C., 2012. European Snow Cover Characteristics  
1218 between 2000 and 2011 Derived from Improved MODIS Daily Snow Cover  
1219 Products. *Remote Sens.* 4, 2432–2454. doi:10.3390/rs4082432
- 1220 Dong, G., Zhou, W., Yi, C., Zhang, L., Li, M., Fu, Y., Zhang, Q., 2017. Cosmogenic  
1221 <sup>10</sup>Be surface exposure dating of ‘Little Ice Age’ glacial events in the Mount  
1222 Jaggang area, central Tibet. *The Holocene* 27(10), 1516-1525.  
1223 doi:10.1177/0959683617693895
- 1224 Dugmore, A.J., 1989. Tephrochronological studies of Holocene glacial fluctuations in  
1225 South Iceland, in: *Glacier Fluctuations and Climatic Change*. pp. 37–55.  
1226 doi:10.1007/978-94-015-7823-3\_3

- 1227 Dunai, T.J., 2010. *Cosmogenic Nuclides*. Cambridge University Press, Cambridge.  
1228 doi:10.1017/CBO9780511804519
- 1229 Dunai, T.J., Binnie, S.A., Hein, A.S., Paling, S.M., 2014. The effects of a hydrogen-rich  
1230 ground cover on cosmogenic thermal neutrons: Implications for exposure dating.  
1231 *Quat. Geochronol.* 22, 183–191. doi:10.1016/J.QUAGEO.2013.01.001
- 1232 Eddy, J.A., 1976. The Maunder Minimum. *Science* 192 (4245), 1189–1202.  
1233 doi:10.1126/science.192.4245.1189
- 1234 Einarsson, M.Á., 1984. Climate of Iceland. In van Loon, H. (Eds.), *World Survey of*  
1235 *Climatology: 15: Climates of the Oceans*. Elsevier, Amsterdam, pp. 673-697.
- 1236 Einarsson, M.A., 1991. Temperature conditions in Iceland 1901-1990. *Jökull* 41, 1–20.
- 1237 Etzelmüller, B., Farbrót, H., Guðmundsson, Á., Humlum, O., Tveito, O.E., Björnsson,  
1238 H., 2007. The regional distribution of mountain permafrost in Iceland. *Permafr.*  
1239 *Periglac. Process.* 18, 185–199. doi:10.1002/ppp.583
- 1240 Evans, D.J.A., Archer, S., Wilson, D.J.H., 1999. A comparison of the lichenometric and  
1241 Schmidt hammer dating techniques based on data from the proglacial areas of some  
1242 Icelandic glaciers. *Quat. Sci. Rev.* 18, 13–41. doi:10.1016/S0277-3791(98)00098-5
- 1243 Fernández-Fernández, J.M., Andrés, N., 2018. Methodological Proposal for the  
1244 Analysis of the Evolution of Glaciers Since the Little Ice Age and Its Application in  
1245 the Tröllaskagi Peninsula (Northern Iceland). *Cuad. Investig. Geográfica Geogr.*  
1246 *Res. Lett.* No 44, 69–97. doi:10.18172/cig.3392
- 1247 Fernández-Fernández, J.M., Andrés, N., Sæmundsson, Þ., Brynjólfsson, S., Palacios, D.,  
1248 2017. High sensitivity of North Iceland (Tröllaskagi) debris-free glaciers to climatic  
1249 change from the ‘Little Ice Age’ to the present. *The Holocene* 27, 1187–1200.  
1250 doi:10.1177/0959683616683262
- 1251 Feuillet, T., Coquin, J., Mercier, D., Cossart, E., Decaulne, A., Jónsson, H.P.,  
1252 Sæmundsson, Þ., 2014. Focusing on the spatial non-stationarity of landslide  
1253 predisposing factors in northern Iceland. *Prog. Phys. Geogr.* 38, 354–377.  
1254 doi:10.1177/0309133314528944
- 1255 Fink, D., Vogt, S., Hotchkis, M., 2000. Cross-sections for  $^{36}\text{Cl}$  from Ti at  $E_p=35\text{--}150$   
1256 MeV: Applications to in-situ exposure dating. *Nucl. Instruments Methods Phys.*  
1257 *Res. Sect. B Beam Interact. with Mater. Atoms* 172, 861–866. doi:10.1016/S0168-  
1258 583X(00)00200-7
- 1259 Flowers, G.E., Björnsson, H., Geirsdóttir, Á., Miller, G.H., Black, J.L., Clarke, G.K.C.,  
1260 2008. Holocene climate conditions and glacier variation in central Iceland from  
1261 physical modelling and empirical evidence. *Quat. Sci. Rev.* 27, 797–813.  
1262 doi:10.1016/J.QUASCIREV.2007.12.004
- 1263 Gardner, A.S., Moholdt, G., Cogley, J.G., Wouters, B., Arendt, A.A., Wahr, J., Berthier,  
1264 E., Hock, R., Pfeffer, W.T., Kaser, G., Ligtenberg, S.R.M., Bolch, T., Sharp, M.J.,

- 1265 Hagen, J.O., Van Den Broeke, M.R., Paul, F., 2013. A reconciled estimate of  
1266 glacier contributions to sea level rise: 2003 to 2009. *Science* 340, 852–857.  
1267 doi:10.1126/science.1234532
- 1268 Geirsdóttir, Á., Miller, G.H., Axford, Y., Sædis Ólafsdóttir, 2009. Holocene and latest  
1269 Pleistocene climate and glacier fluctuations in Iceland. *Quat. Sci. Rev.* 28, 2107–  
1270 2118. doi:10.1016/j.quascirev.2009.03.013
- 1271 Geirsdóttir, Á., Miller, G. H., Andrews, J. T., Harning, D. J., Anderson, L. S.,  
1272 Thordarson, T., 2018. The onset of Neoglaciation in Iceland and the 4.2 ka event.  
1273 *Clim. Past Discuss.*, doi:10.5194/cp-2018-130. Manuscript under review
- 1274 Gordon, J.E., Sharp, M., 1983. Lichenometry in dating recent glacial landforms and  
1275 deposits, southeast Iceland. *Boreas* 12, 191–200. doi:10.1111/j.1502-  
1276 3885.1983.tb00312.x
- 1277 Grove, J.M., 1988. *The Little Ice Age*. Routledge, London.
- 1278 Guðmundsson, H.J., 1997. A review of the Holocene environmental history of Iceland.  
1279 *Quat. Sci. Rev.* 16, 81–92. doi:10.1016/S0277-3791(96)00043-1
- 1280 Häberle, T., 1994. Glacial, Late Glacial and Holocene History of the Hörgárdalur Area,  
1281 Tröllaskagi, Northern Iceland, in: Stöttter, J., Wilhelm, F. (Eds.), *Environmental*  
1282 *Change in Iceland*. Münchener Geographische Abhandlungen, Reihe B, pp. 133–  
1283 145.
- 1284 Häberle, T., 1991. Holocene Glacial History of the Hörgárdalur Area, Tröllaskagi,  
1285 Northern Iceland, in: Maizels, J.K., Caseldine, C. (Eds.), *Environmental Change in*  
1286 *Iceland: Past and Present*. Glaciology and Quaternary Geology, Vol 7. Springer,  
1287 Dordrecht, pp. 193–202. doi:10.1007/978-94-011-3150-6\_13
- 1288 Hamilton, S.J., Whalley, W.B., 1995. Rock glacier nomenclature: A re-assessment.  
1289 *Geomorphology* 14, 73–80. doi:10.1016/0169-555X(95)00036-5
- 1290 Harning, D.J., Geirsdóttir, Á., Miller, G.H., 2018. Punctuated Holocene climate of  
1291 Vestfirðir, Iceland, linked to internal/external variables and oceanographic  
1292 conditions. *Quat. Sci. Rev.* 189, 31–42. doi:10.1016/j.quascirev.2018.04.009
- 1293 Harning, D.J., Geirsdóttir, Á., Miller, G.H., Anderson, L., 2016a. Episodic expansion of  
1294 Drangajökull, Vestfirðir, Iceland, over the last 3 ka culminating in its maximum  
1295 dimension during the Little Ice Age. *Quat. Sci. Rev.* 152, 118–131.  
1296 <https://doi.org/10.1016/j.quascirev.2016.10.001>
- 1297 Harning, D.J., Geirsdóttir, Á., Miller, G.H., Zalzal, K., 2016b. Early Holocene  
1298 deglaciation of Drangajökull, Vestfirðir, Iceland. *Quat. Sci. Rev.* 153, 192–198.  
1299 doi:10.1016/j.quascirev.2016.09.030
- 1300 Harris, T., Tweed, F.S., Knudsen, Ó., 2004. A polygenetic landform at Stígá,  
1301 Öräfajökull, southern Iceland. *Geogr. Ann. Ser. A Phys. Geogr.* 86, 143–154.  
1302 doi:10.1111/j.0435-3676.2004.00220.x

- 1303 Helama, S., Jones, P.D., Briffa, K.R., 2017. Dark Ages Cold Period: A literature review  
1304 and directions for future research. *The Holocene* 27, 1600–1606.  
1305 doi:10.1177/0959683617693898
- 1306 Heyman, J., Stroeven, A.P., Harbor, J.M., Caffee, M.W., 2011. Too young or too old:  
1307 Evaluating cosmogenic exposure dating based on an analysis of compiled boulder  
1308 exposure ages. *Earth Planet. Sci. Lett.* 302, 71–80. doi:10.1016/j.epsl.2010.11.040
- 1309 Hjort, C., Ingólfsson, Ó., Norðdahl, H., 1985. Late Quaternary geology and glacial  
1310 history of Hornstrandir, Northwest Iceland: a reconnaissance study. *Jökull* 35, 9–  
1311 29.
- 1312 Holzhauser, H., Magny, M., Zumbuühl, H.J., 2005. Glacier and lake-level variations in  
1313 west-central Europe over the last 3500 years. *The Holocene* 15, 789–801.  
1314 doi:10.1191/0959683605hl853ra
- 1315 Hooker, T.N., Brown, D.H., 1977. A photographic method for accurately measuring the  
1316 growth of crustose and foliose saxicolous lichens. *Lichenol.* 9, 65–75.  
1317 doi:10.1017/S0024282977000073
- 1318 Hughes, P.D., Woodward, J.C., van Calsteren, P.C., Thomas, L.E., Adamson, K.R.,  
1319 2010. Pleistocene ice caps on the coastal mountains of the Adriatic Sea. *Quat. Sci.*  
1320 *Rev.* 29, 3690–3708. doi:10.1016/j.quascirev.2010.06.032
- 1321 Icelandic Meteorological Office, 2018. Climatological data. Available  
1322 <http://en.vedur.is/climatology/data/> (accessed 13 April 2018).
- 1323 Ingólfsson, Ó., Benediktsson, Í.Ö., Schomacker, A., Kjær, K., Brynjólfsson, S., Jónsson,  
1324 S.A., Korsgaard, N.J., Johnson, M., 2016. Glacial geological studies of surge type  
1325 glaciers in Iceland – Research status and future challenges. *Earth Science Reviews*  
1326 152, 37–69.
- 1327 Innes, J.L., 1985. Lichenometry, *Progress in Physical Geography*.  
1328 doi:10.1177/030913338500900202
- 1329 Ivy-Ochs, S., Synal, H.-A., Roth, C., Schaller, M., 2004. Initial results from isotope  
1330 dilution for Cl and <sup>36</sup>Cl measurements at the PSI/ETH Zurich AMS facility. *Nucl.*  
1331 *Instruments Methods Phys. Res. Sect. B Beam Interact. with Mater. Atoms* 223–  
1332 224, 623–627. doi:10.1016/j.nimb.2004.04.115
- 1333 Ipsen, H.A., Principato, S.M., Grube, R.E., Lee, J.F., 2018. Spatial analysis of cirques  
1334 from three regions of Iceland: implications for cirque formation and palaeoclimate.  
1335 *Boreas* 47, 565–576. doi:10.1111/bor.12295
- 1336 Jacob, T., Wahr, J., Pfeffer, W.T., Swenson, S., 2012. Recent contributions of glaciers  
1337 and ice caps to sea level rise. *Nature* 482, 514–518. doi:10.1038/nature10847
- 1338 Jaksch, K., 1984. Das Gletshervorfeld des Vatnajökull am Oberflauf des Djúpá,  
1339 Südisland. *Jökull* 34, 97–103.

- 1340 Jaksch, K., 1975. Das Gletschervorfeld des Sólheimajökull. *Jökull* 25, 34–38.
- 1341 Jaksch, K., 1970. Beobachtungen in den Gletschervorfeldern des Sólheima und  
1342 Siðujökull im Sommer 1970. *Jökull* 20.
- 1343 James, W.H.M., Carrivick, J.L., 2016. Automated modelling of spatially-distributed  
1344 glacier ice thickness and volume. *Comput. Geosci.* 92, 90–103.  
1345 doi:10.1016/j.cageo.2016.04.007
- 1346 Janke, J.R., Bellisario, A.C., Ferrando, F.A., 2015. Classification of debris-covered  
1347 glaciers and rock glaciers in the Andes of central Chile. *Geomorphology* 241, 98–  
1348 121. doi:10.1016/j.geomorph.2015.03.034
- 1349 Jiang, H., Muscheler, R., Björck, S., Seidenkrantz, M.S., Olsen, J., Sha, L., Sjolte, J.,  
1350 Eiríksson, J., Ran, L., Knudsen, K.L., Knudsen, M.F., 2015. Solar forcing of  
1351 Holocene summer sea-surface temperatures in the northern North Atlantic. *Geology*  
1352 43, 203–206. doi:10.1130/G36377.1
- 1353 Jóhannesson, T., Sigurðsson, O., 1998. Interpretation of glacier variations in Iceland  
1354 1930-1995. *Jökull* 45, 27–33.
- 1355 Jóhannesson, H., Sæmundsson, K., 1989. Geological map of Iceland. 1:500.000.  
1356 Bedrock. Icelandic Institute of Natural History, Reykjavik.
- 1357 Jomelli, V., Lane, T., Favier, V., Masson-Delmotte, V., Swingedouw, D., Rinterknecht,  
1358 V., Schimmelpfennig, I., Brunstein, D., Verfaillie, D., Adamson, K., Leanni, L.,  
1359 Mokadem, F., Aumaître, G., Bourlès, D.L., Keddadouche, K., 2016. Paradoxical  
1360 cold conditions during the medieval climate anomaly in the Western Arctic. *Sci.*  
1361 *Rep.* 6, 32984. <https://doi.org/10.1038/srep32984>
- 1362 Jónsson, O., 1976. Berghlaup. Ræktunarfélag Norðurlands, Akureyri.
- 1363 Kirkbride, M.P., 2002. Icelandic climate and glacier fluctuations through the  
1364 termination of the “Little Ice Age”. *Polar Geogr.* 26, 116–133.  
1365 doi:10.1080/789610134
- 1366 Kirkbride, M.P., 2011. Debris-covered glaciers. In: Singh, V.P., Singh, P., Haritashya,  
1367 U.K. (Eds.), *Encyclopedia of Snow, Ice and Glaciers: Encyclopedia of Earth Series*.  
1368 Springer, Netherlands, pp. 180–182. doi:10.1007/978-90-481-2642-2\_622
- 1369 Kirkbride, M.P., Dugmore, A.J., 2006. Responses of mountain ice caps in central  
1370 Iceland to Holocene climate change. *Quat. Sci. Rev.* 25, 1692–1707.  
1371 doi:10.1016/j.quascirev.2005.12.004
- 1372 Kirkbride, M.P., Dugmore, A.J., 2001. Can lichenometry be used to date the “Little Ice  
1373 Age” glacial maximum in Iceland? *Clim. Change* 48, 151–167.  
1374 doi:10.1023/A:1005654503481

- 1375 Knight, J., Harrison, S., Jones, D.B., 2018. Rock glaciers and the geomorphological  
1376 evolution of deglaciating mountains. *Geomorphology* 311, 127–142.  
1377 doi:10.1016/j.geomorph.2018.09.020
- 1378 Koblet, T., Gärtner-Roer, I., Zemp, M., Jansson, P., Thee, P., Haeberli, W., Holmlund,  
1379 P., 2010. Reanalysis of multi-temporal aerial images of Storglaciären, Sweden  
1380 (1959-99); Part 1: Determination of length, area, and volume changes. *Cryosph.* 4,  
1381 333–343. doi:10.5194/tc-4-333-2010
- 1382 Koch, L., 1945. The East Greenland Ice. *Medd. Grøn.* 130, 1–374.
- 1383 Kugelmann, O., 1991. Dating Recent Glacier Advances in the Svarfaðardalur-  
1384 Skíðadalur Area of Northern Iceland by Means of a New Lichen Curve, in:  
1385 Maizels, J.K., Caseldine, C. (Eds.), *Environmental Change in Iceland: Past and*  
1386 *Present. Glaciology and Quaternary Geology, Vol 7.* Springer, Dordrecht, pp. 203–  
1387 217. doi:10.1007/978-94-011-3150-6\_14
- 1388 Lamb, H.H., 1965. The early medieval warm epoch and its sequel. *Palaeogeogr.*  
1389 *Palaeoclimatol. Palaeoecol.* 1, 13–37. doi:10.1016/0031-0182(65)90004-0
- 1390 Larsen, D.J., Miller, G.H., Geirsdóttir, Á., Thordarson, T., 2011. A 3000-year varved  
1391 record of glacier activity and climate change from the proglacial lake Hvítárvatn,  
1392 Iceland. *Quat. Sci. Rev.* 30, 2715–2731. doi:10.1016/j.quascirev.2011.05.026
- 1393 Larsen, D.J., Geirsdóttir, Á., Miller, G.H., 2015. Precise chronology of Little Ice Age  
1394 expansion and repetitive surges of Langjökull, central Iceland. *Geology* 43, 167–  
1395 170. <https://doi.org/10.1130/G36185.1>
- 1396 Le Roy, M., Deline, P., Carcaillet, J., Schimmelpfennig, I., Ermini, M., 2017. <sup>10</sup>Be  
1397 exposure dating of the timing of Neoglacial glacier advances in the Ecrins-Pelvoux  
1398 massif, southern French Alps. *Quat. Sci. Rev.* 178, 118–138.  
1399 doi:10.1016/j.quascirev.2017.10.010
- 1400 Li, Y., Li, Y., Harbor, J., Liu, G., Yi, C., Caffee, M.W., 2016. Cosmogenic<sup>10</sup>Be  
1401 constraints on Little Ice Age glacial advances in the eastern Tian Shan, China.  
1402 *Quat. Sci. Rev.* 138, 105–118. doi:10.1016/j.quascirev.2016.02.023
- 1403 Licciardi, J.M., Denoncourt, C.L., Finkel, R.C., 2008. Cosmogenic<sup>36</sup>Cl production  
1404 rates from Ca spallation in Iceland. *Earth Planet. Sci. Lett.* 267, 365–377.  
1405 doi:10.1016/j.epsl.2007.11.036
- 1406 Licciardi, J.M., Kurz, M.D., Curtice, J.M., 2007. Glacial and volcanic history of  
1407 Icelandic table mountains from cosmogenic<sup>3</sup>He exposure ages. *Quat. Sci. Rev.* 26,  
1408 1529–1546. doi:10.1016/j.quascirev.2007.02.016
- 1409 Licciardi, J.M., Kurz, M.D., Curtice, J.M., 2006. Cosmogenic<sup>3</sup>He production rates from  
1410 Holocene lava flows in Iceland. *Earth Planet. Sci. Lett.* 246, 251–264.  
1411 doi:10.1016/j.epsl.2006.03.016

- 1412 Maizels, J.K., Dugmore, A.J., 1985. Lichenometric dating and tephrochronology of  
1413 sandur deposits, Sólheimajökull area, southern Iceland. *Jökull* 35, 69–77.
- 1414 Marrero, S.M., Phillips, F.M., Caffee, M.W., Gosse, J.C., 2016. CRONUS-Earth  
1415 cosmogenic  $^{36}\text{Cl}$  calibration. *Quat. Geochronol.* 31, 199–219.  
1416 doi:10.1016/j.quageo.2015.10.002
- 1417 Martin, H.E., Whalley, W.B., Caseldine, C., 1991. Glacier Fluctuations and Rock  
1418 Glaciers in Tröllaskagi, Northern Iceland, with Special Reference to 1946–1986, in:  
1419 Maizels, J.K., Caseldine, C. (Eds.), *Environmental Change in Iceland: Past and*  
1420 *Present*. Springer Netherlands, Dordrecht, pp. 255–265. doi:10.1007/978-94-011-  
1421 3150-6\_17
- 1422 Marzeion, B., Cogley, J.G., Richter, K., Parkes, D., 2014. Attribution of global glacier  
1423 mass loss to anthropogenic and natural causes. *Science* 345, 919–921.  
1424 doi:10.1126/science.1254702
- 1425 Matthews, J.A., Shakesby, R.A., Fabel, D., 2017. Very low inheritance in cosmogenic  
1426 surface exposure ages of glacial deposits: A field experiment from two Norwegian  
1427 glacier forelands. *Holocene* 27, 1406–1414. doi:10.1177/0959683616687387
- 1428 Merchel, S., Bremser, W., Alfimov, V., Arnold, M., Aumaître, G., Benedetti, L.,  
1429 Bournès, D.L., Caffee, M., Fifield, L.K., Finkel, R.C., Freeman, S.P.H.T.,  
1430 Martschini, M., Matsushi, Y., Rood, D.H., Sasa, K., Steier, P., Takahashi, T.,  
1431 Tamari, M., Tims, S.G., Tosaki, Y., Wilcken, K.M., Xu, S., 2011. Ultra-trace  
1432 analysis of  $^{36}\text{Cl}$  by accelerator mass spectrometry: an interlaboratory study. *Anal.*  
1433 *Bio- anal. Chem.* doi:10.1007/s00216-011-4979-2.
- 1434 Meyer, H.H., Venzke, J.F., 1985. Der Klængshóll-Kargletscher in Nordisland. *Natur*  
1435 *and Museum* 115, 29–46.
- 1436 Miller, G.H., Geirsdóttir, Á., Zhong, Y., Larsen, D.J., Otto-Bliesner, B.L., Holland,  
1437 M.M., Bailey, D.A., Refsnider, K.A., Lehman, S.J., Southon, J.R., Anderson, C.,  
1438 Björnsson, H., Thordarson, T., 2012. Abrupt onset of the Little Ice Age triggered  
1439 by volcanism and sustained by sea-ice/ocean feedbacks. *Geophys. Res. Lett.* 39, 1–  
1440 5. doi:10.1029/2011GL050168
- 1441 National Land Survey of Iceland, 2018. Aerial photo collection. Available  
1442 <https://www.lmi.is/landupplýsingar/loftmyndasafn-2-2/> (accessed 5 July 2018).
- 1443 Nesje, A., Bakke, J., Dahl, S.O., Lie, Ø., Matthews, J.A., 2008. Norwegian mountain  
1444 glaciers in the past, present and future. *Glob. Planet. Change* 60, 10–27.  
1445 doi:10.1016/j.gloplacha.2006.08.004
- 1446 Ogilvie, A., 1996. Sea-ice conditions off the coasts of Iceland A. D. 1601-1850 with  
1447 special reference to part of the Maunder Minimum period (1675-1715). *AmS-Varia*  
1448 25, 9–12.

- 1449 Ogilvie, A.E.J., 1984. The past climate and sea-ice record from Iceland, Part 1: Data to  
1450 A.D. 1780. *Clim. Change* 6, 131–152. doi:10.1007/BF00144609
- 1451 Ogilvie, A.E.J., Jónsdóttir, I., 2000. Sea ice, climate, and Icelandic fisheries in the  
1452 eighteenth and nineteenth centuries. *Arctic* 53, 383–394. doi:10.14430/arctic869
- 1453 Ogilvie, A.E.J., Jónsson, T., 2001. “Little Ice Age” Research: a perspective from  
1454 Iceland. *Clim. Change* 48, 9–52.
- 1455 Oliva, M., Ruiz-Fernández, J., Barriendos, M., Benito, G., Cuadrat, J.M., Domínguez-  
1456 Castro, F., García-Ruiz, J.M., Giralt, S., Gómez-Ortiz, A., Hernández, A., López-  
1457 Costas, O., López-Moreno, J.I., López-Sáez, J.A., Martínez-Cortizas, A., Moreno,  
1458 A., Prohom, M., Saz, M.A., Serrano, E., Tejedor, E., Trigo, R., Valero-Garcés, B.,  
1459 Vicente-Serrano, S.M., 2018. The Little Ice Age in Iberian mountains. *Earth-  
1460 Science Rev.* 177, 175–208. doi:10.1016/j.earscirev.2017.11.010
- 1461 Orwin, J.F., Mckinzey, K.M., Stephens, M.A., Dugmore, A.J., 2008. Identifying  
1462 moraine surfaces with similar histories using lichen size distributions and the U2  
1463 statistic, Southeast Iceland. *Geogr. Ann. Ser. A Phys. Geogr.* 90 A, 151–164.  
1464 doi:10.1111/j.1468-0459.2008.00168.x
- 1465 Osborn, G., McCarthy, D., LaBrie, A., Burke, R., 2015. Lichenometric dating: Science  
1466 or pseudo-science? *Quat. Res. (United States)* 83, 1–12.  
1467 doi:10.1016/j.yqres.2014.09.006
- 1468 Osmaston, H., 2005. Estimates of glacier equilibrium line altitudes by the Area ×  
1469 Altitude, the Area × Altitude Balance Ratio and the Area × Altitude Balance Index  
1470 methods and their validation. *Quat. Int.* 138–139, 22–31.  
1471 doi:10.1016/j.quaint.2005.02.004
- 1472 Palacios, D., Gómez-Ortiz, A., Alcalá-Reygosa, J., Andrés, N., Oliva, M., Tanarro,  
1473 L.M., Salvador-Franch, F., Schimmelpfennig, I., Fernández-Fernández, J.M.,  
1474 Léanni, L., 2019. The challenging application of cosmogenic dating methods in  
1475 residual glacial landforms: The case of Sierra Nevada (Spain). *Geomorphology*  
1476 325, 103–118. doi:10.1016/j.geomorph.2018.10.006
- 1477 Paterson, W.S.B., 1994. *The Physics of Glaciers*, 3<sup>rd</sup> Edition. Pergamon/Elsevier,  
1478 London.
- 1479 Pellitero, R., Rea, B.R., Spagnolo, M., Bakke, J., Hughes, P., Ivy-Ochs, S., Lukas, S.,  
1480 Ribolini, A., 2015. A GIS tool for automatic calculation of glacier equilibrium-line  
1481 altitudes. *Comput. Geosci.* 82, 55–62. doi:10.1016/j.cageo.2015.05.005
- 1482 Pellitero, R., Rea, B.R., Spagnolo, M., Bakke, J., Ivy-Ochs, S., Frew, C.R., Hughes, P.,  
1483 Ribolini, A., Lukas, S., Renssen, H., 2016. GlaRe, a GIS tool to reconstruct the 3D  
1484 surface of palaeoglaciers. *Comput. Geosci.* 94, 77–85.  
1485 doi:10.1016/j.cageo.2016.06.008

- 1486 Principato, S.M., Geirsdóttir, Á., Jóhannsdóttir, G.E., Andrews, J.T., 2006. Late  
1487 Quaternary glacial and deglacial history of eastern Vestfirðir, Iceland using  
1488 cosmogenic isotope ( $^{36}\text{Cl}$ ) exposure ages and marine cores. *J. Quat. Sci.* 21, 271–  
1489 285. doi:10.1002/jqs.978
- 1490 Rea, B.R., 2009. Defining modern day Area-Altitude Balance Ratios (AABRs) and their  
1491 use in glacier-climate reconstructions. *Quat. Sci. Rev.* 28, 237–248.  
1492 doi:10.1016/j.quascirev.2008.10.011
- 1493 Reimer PJ, Bard E, Bayliss A, Beck JW, Blackwell PG, Bronk Ramsey C, Buck CE,  
1494 Cheng H, Edwards RL, Friedrich M, Grootes PM, Guilderson TP, Hafliðason H,  
1495 Hajdas I, Hatté C, Heaton TJ, Hoffmann DL, Hogg AG, Hughen KA, Kaiser KF,  
1496 Kromer B, Manning SW, Niu M, Reimer RW, Richards DA, Scott EM, Southon  
1497 JR, Staff RA, Turney CSM, van der Plicht J. 2013. IntCal13 and Marine13  
1498 radiocarbon age calibration curves 0–50,000 years cal BP. *Radiocarbon*  
1499 55(4):1869–1887.
- 1500 Roca-Valiente, B., Hawksworth, D.L., Pérez-Ortega, S., Sancho, L.G., Crespo, A.,  
1501 2016. Type studies in the *Rhizocarpon geographicum* group (Rhizocarpaceae,  
1502 lichenized Ascomycota). *Lichenologist* 48, 97–110.  
1503 doi:10.1017/S002428291500050X
- 1504 Rogers, J.C., Van Loon, H., 1979. The Seesaw in Winter Temperatures between  
1505 Greenland and Northern Europe. Part II: Some Oceanic and Atmospheric Effects in  
1506 Middle and High Latitudes. *Mon. Weather Rev.* 107, 509–519. doi:10.1175/1520-  
1507 0493(1979)107<0509:TSIWTB>2.0.CO;2
- 1508 Russell, A.J., Knight, P.G., Van Dijk, T.A.G.P., 2001. Glacier surging as a control on  
1509 the development of proglacial, fluvial landforms and deposits, Skeiðarársandur,  
1510 Iceland. *Glob. Planet. Change* 28, 163–174. doi:10.1016/S0921-8181(00)00071-0
- 1511 Sancho, L.G., Pintado, A., Navarro, F., Ramos, M., De Pablo, M.A., Blanquer, J.M.,  
1512 Raggio, J., Valladares, F., Green, T.G.A., 2017. Recent Warming and Cooling in  
1513 the Antarctic Peninsula Region has Rapid and Large Effects on Lichen Vegetation.  
1514 *Sci. Rep.* 7, 5689. <https://doi.org/10.1038/s41598-017-05989-4>
- 1515 Sancho, L.G., Palacios, D., Green, T.G.A., Vivas, M., Pintado, A., 2011. Extreme high  
1516 lichen growth rates detected in recently deglaciaded areas in Tierra del Fuego. *Polar*  
1517 *Biol.* 34, 813–822. <https://doi.org/10.1007/s00300-010-0935-4>
- 1518 Sæmundsson, K., Kristjánsson, L., McDougall, I., Watkins, N.D., 1980. K-Ar dating,  
1519 geological and paleomagnetic study of a 5-km lava succession in northern Iceland.  
1520 *J. Geophys. Res. Solid Earth* 85, 3628–3646. doi:10.1029/JB085iB07p03628
- 1521 Sæmundsson, Þ., Morino, C., Helgason, J.K., Conway, S.J., Pétursson, H.G., 2018. The  
1522 triggering factors of the Móafellshyrna debris slide in northern Iceland: Intense  
1523 precipitation, earthquake activity and thawing of mountain permafrost. *Sci. Total*  
1524 *Environ.* 621, 1163–1175. doi:10.1016/J.SCITOTENV.2017.10.111

- 1525 Schaefer, J.M., Denton, G.H., Kaplan, M., Putnam, A., Finkel, R.C., Barrell, D.J.A.,  
 1526 Andersen, B.G., Schwartz, R., Mackintosh, A., Chinn, T., Schlüchter, C., 2009.  
 1527 High-frequency Holocene glacier fluctuations in New Zealand differ from the  
 1528 northern signature. *Science* 324, 622–625. doi:10.1126/science.1169312
- 1529 Schildgen, T.F., Phillips, W.M., Purves, R.S., 2005. Simulation of snow shielding  
 1530 corrections for cosmogenic nuclide surface exposure studies. *Geomorphology* 64,  
 1531 67–85. doi:10.1016/j.geomorph.2004.05.003
- 1532 Schimmelpfennig, I., 2009. Cosmogenic <sup>36</sup>Cl in Ca and K rich minerals: analytical  
 1533 developments, production rate calibrations and cross calibration with <sup>3</sup>He and  
 1534 <sup>21</sup>Ne. Ph. D. Thesis, Université Aix-Marseille III, France. <http://tel.archives-ouvertes.fr/tel-00468337/fr>  
 1535
- 1536 Schimmelpfennig, I., Benedetti, L., Finkel, R., Pik, R., Blard, P.H., Bourlès, D.,  
 1537 Burnard, P., Williams, A., 2009. Sources of in-situ <sup>36</sup>Cl in basaltic rocks.  
 1538 Implications for calibration of production rates. *Quat. Geochronol.* 4, 441–461.  
 1539 doi:10.1016/j.quageo.2009.06.003
- 1540 Schimmelpfennig, I., Benedetti, L., Garreta, V., Pik, R., Blard, P.H., Burnard, P.,  
 1541 Bourlès, D., Finkel, R., Ammon, K., Dunai, T., 2011. Calibration of cosmogenic  
 1542 <sup>36</sup>Cl production rates from Ca and K spallation in lava flows from Mt. Etna (38°N,  
 1543 Italy) and Payun Matru (36°S, Argentina). *Geochim. Cosmochim. Acta* 75, 2611–  
 1544 2632. doi:10.1016/j.gca.2011.02.013
- 1545 Schimmelpfennig, I., Schaefer, J.M., Akçar, N., Ivy-Ochs, S., Finkel, R.C., Schlüchter,  
 1546 C., 2012. Holocene glacier culminations in the Western Alps and their hemispheric  
 1547 relevance. *Geology* 40, 891–894. doi:10.1130/G33169.1
- 1548 Schimmelpfennig, I., Schaefer, J.M., Akçar, N., Koffman, T., Ivy-Ochs, S., Schwartz,  
 1549 R., Finkel, R.C., Zimmerman, S., Schlüchter, C., 2014a. A chronology of Holocene  
 1550 and Little Ice Age glacier culminations of the Steingletscher, Central Alps,  
 1551 Switzerland, based on high-sensitivity beryllium-10 moraine dating. *Earth Planet.  
 1552 Sci. Lett.* 393, 220–230. doi:10.1016/j.epsl.2014.02.046
- 1553 Schimmelpfennig, I., Schaefer, J.M., Putnam, A.E., Koffman, T., Benedetti, L., Ivy-  
 1554 Ochs, S., Team, A., Schlüchter, C., 2014b. <sup>36</sup>Cl production rate from K-spallation  
 1555 in the European Alps (Chironico landslide, Switzerland). *J. Quat. Sci.* 29, 407–413.  
 1556 doi:10.1002/jqs.2720
- 1557 Schomacker, A., Krüger, J., Larsen, G., 2003. An extensive late Holocene glacier  
 1558 advance of Kötlujökull, central south Iceland. *Quat. Sci. Rev.* 22, 1427–1434.  
 1559 doi:10.1016/S0277-3791(03)00090-8
- 1560 Schomacker, A., Brynjólfsson, S., Andreassen, J.M., Gudmundsdóttir, E.R., Olsen, J.,  
 1561 Odgaard, B.V., Håkansson, L., Ingólfsson, O., Larsen, N.K., 2016. The Drangajökull  
 1562 ice cap, northwest Iceland, persisted into the early-mid Holocene. *Quat. Sci. Rev.*  
 1563 148, 66–84.

- 1564 Sigurðsson, O., 1998. Glacier variations in Iceland 1930-1995. *Jökull* 45, 27–33.
- 1565 Sigurðsson, O., 2005. 10. Variations of termini of glaciers in Iceland in recent centuries  
1566 and their connection with climate, in: *Developments in Quaternary Science*. pp.  
1567 241–255. doi:10.1016/S1571-0866(05)80012-0
- 1568 Sigurðsson, O., Jónsson, T., Jóhannesson, T., 2007. Relation between glacier-termini  
1569 variations and summer temperature in Iceland since 1930. *Ann. Glaciol.* 46, 170–  
1570 176. doi:10.3189/172756407782871611
- 1571 Sissons, J.B., 1974. A Late-Glacial Ice Cap in the Central Grampians, Scotland. *Trans.*  
1572 *Inst. Br. Geogr.* 95. doi:10.2307/621517
- 1573 Solomina, O.N., Bradley, R.S., Jomelli, V., Geirsdottir, A., Kaufman, D.S., Koch, J.,  
1574 McKay, N.P., Masiokas, M., Miller, G., Nesje, A., Nicolussi, K., Owen, L.A.,  
1575 Putnam, A.E., Wanner, H., Wiles, G., Yang, B., 2016. Glacier fluctuations during  
1576 the past 2000 years. *Quat. Sci. Rev.* 149, 61–90.  
1577 doi:10.1016/j.quascirev.2016.04.008
- 1578 Stone, J.O., 2000. Air pressure and cosmogenic isotope production. *J. Geophys. Res.*  
1579 *Solid Earth* 105, 23753–23759. doi:10.1029/2000JB900181
- 1580 Stone, J.O., Allan, G.L., Fifield, L.K., Cresswell, R.G., 1996. Cosmogenic chlorine-36  
1581 from calcium spallation. *Geochim. Cosmochim. Acta* 60, 679–692.  
1582 doi:10.1016/0016-7037(95)00429-7
- 1583 Stone, J.O., Fifield, K., Vasconcelos, P., 2005. Terrestrial chlorine-36 production from  
1584 spallation of iron, in: *Abstract of 10th International Conference on Accelerator*  
1585 *Mass Spectrometry*. Berkeley, CA.
- 1586 Stötter, J., 1991. New Observations on the Postglacial Glacial History of Tröllaskagi,  
1587 Northern Iceland, in: Maizels, J.K., Caseldine, C. (Eds.), *Environmental Change in*  
1588 *Iceland: Past and Present. Glaciology and Quaternary Geology, Vol 7*. Springer,  
1589 Dordrecht, pp. 181–192. doi:10.1007/978-94-011-3150-6\_12
- 1590 Stötter, J., 1990. Geomorphologische und landschaftsgeschichtliche Untersuchungen im  
1591 Svarfaðardalur-Skiðadalur, Tröllaskagi, N-Island. *Münchener Geogr.*  
1592 *Abhandlungen* 9.
- 1593 Stötter, J., Wastl, M., Caseldine, C., Häberle, T., 1999. Holocene palaeoclimatic  
1594 reconstruction in northern Iceland: Approaches and results. *Quat. Sci. Rev.* 18,  
1595 457–474. doi:10.1016/S0277-3791(98)00029-8
- 1596 Tanarro, L.M., Palacios, D., Andrés, N., Fernández-Fernández, J.M., Zamorano, J.J.,  
1597 Sæmundsson, Þ., Brynjólfsson, S., 2019. Unchanged surface morphology in debris-  
1598 covered glaciers and rock glaciers in Tröllaskagi peninsula (northern Iceland). *Sci.*  
1599 *Total Environ.* 648, 218–235. <https://doi.org/10.1016/j.scitotenv.2018.07.460>

- 1600 Thompson, A., Jones, A., 1986. Rates and causes of proglacial river terrace formation in  
1601 southeast Iceland: an application of lichenometric dating techniques. *Boreas* 15,  
1602 231–246. doi:10.1111/j.1502-3885.1986.tb00928.x
- 1603 Van der Veen, C.J., 1999. *Fundamentals of glacier dynamics*. Balkema, Rotterdam.
- 1604 Wagner, S., Zorita, E., 2005. The influence of volcanic, solar and CO<sub>2</sub> forcing on the  
1605 temperatures in the Dalton Minimum (1790-1830): A model study. *Clim. Dyn.* 25,  
1606 205–218. doi:10.1007/s00382-005-0029-0
- 1607 Wanner, H., Beer, J., Bütikofer, J., Crowley, T.J., Cubasch, U., Flückiger, J., Goosse,  
1608 H., Grosjean, M., Joos, F., Kaplan, J.O., Küttel, M., Müller, S.A., Prentice, I.C.,  
1609 Solomina, O., Stocker, T.F., Tarasov, P., Wagner, M., Widmann, M., 2008. Mid- to  
1610 Late Holocene climate change: an overview. *Quat. Sci. Rev.* 27, 1791–1828.  
1611 doi:10.1016/j.quascirev.2008.06.013
- 1612 Wastl, M., Stötter, J., 2005. 9. Holocene glacier history, in: *Developments in*  
1613 *Quaternary Science*. pp. 221–240. doi:10.1016/S1571-0866(05)80011-9
- 1614 Wiles, G.C., Barclay, D.J., Young, N.E., 2010. A review of lichenometric dating of  
1615 glacial moraines in Alaska. *Geogr. Ann. Ser. A Phys. Geogr.* 92, 101–109.  
1616 doi:10.1111/j.1468-0459.2010.00380.x
- 1617 Winkler, S., 2003. A new interpretation of the date of the “Little Ice Age” glacier  
1618 maximum at Svartisen and Okstindan, northern Norway. *Holocene* 13, 83–95.  
1619 doi:10.1191/0959683603hl573rp
- 1620 Xiao, X., Zhao, M., Knudsen, K.L., Sha, L., Eiríksson, J., Gudmundsdóttir, E., Jiang,  
1621 H., Guo, Z., 2017. Deglacial and Holocene sea–ice variability north of Iceland and  
1622 response to ocean circulation changes. *Earth Planet. Sci. Lett.* 472, 14–24.  
1623 doi:10.1016/J.EPSL.2017.05.006
- 1624 Young, N.E., Schweinsberg, A.D., Briner, J.P., Schaefer, J.M., 2015. Glacier maxima in  
1625 Baffin Bay during the Medieval Warm Period coeval with Norse settlement. *Sci.*  
1626 *Adv.* 1. doi:10.1126/sciadv.1500806
- 1627 Zhong, Y., Miller, G.H., Otto-Bliesner, B.L., Holland, M.M., Bailey, D.A., Schneider,  
1628 D.P., Geirsdóttir, A., 2011. Centennial-scale climate change from decadal-paced  
1629 explosive volcanism: a coupled sea ice-ocean mechanism. *Clim. Dyn.* 37, 2373–  
1630 2387. doi:10.1007/s00382-010-0967-z
- 1631 Zweck, C., Zreda, M., Desilets, D., 2013. Snow shielding factors for cosmogenic  
1632 nuclide dating inferred from Monte Carlo neutron transport simulations. *Earth*  
1633 *Planet. Sci. Lett.* 379, 64–71. doi:10.1016/J.EPSL.2013.07.023
- 1634

1635 **Figure captions.**

1636 Figure 1. Location of the Tungnahryggsjökull glaciers and their forelands (C)  
1637 (Vesturdalur and Austurdalur) in the context of Iceland (A) and the Tröllaskagi  
1638 peninsula (B). The red boxes in panels A and B are panels B and C, respectively. The  
1639 figure also includes the location of the place names mentioned throughout the paper.  
1640 This figure is available in colour in the online version.

1641 Figure 2. Geomorphological map of the Vesturdalur foreland. (A) General view of the  
1642 Western Tungnahryggsjökull foreland. (B) Detailed moraine mapping and glacier  
1643 margin geometry reconstructed throughout the different glacial stages identified, and  
1644  $^{36}\text{Cl}$  CRE and lichenometric dating results (both are expressed in ages and calendar  
1645 years). Note that stages 13, 14, 15 and 16 correspond to the years 1946, 1985, 1994 and  
1646 2000. The surface-contoured glacier (white) corresponds to the year 2005 (stage 17).  
1647 The abbreviations “Rg” and “Ps” in lichenometry stations indicate that the estimated  
1648 dates are derived from the *Rhizocarpon geographicum* and *Porpidia soredizodes*  
1649 lichens, respectively, and the number correspond to the longest axis of the largest lichen  
1650 measured. This figure is available in colour in the online version.

1651 Figure 3. Geomorphological map of the Austurdalur foreland. (A) General view of the  
1652 Eastern Tungnahryggsjökull foreland. (B) Detailed moraine mapping and glacier margin  
1653 geometry reconstructed throughout the different glacial stages identified, and  $^{36}\text{Cl}$  CRE  
1654 and lichenometric dating results (both are expressed in ages and calendar years). Note  
1655 that stages 11, 15 and 16 correspond to the years 1946, 1985 and 2000. The surface-  
1656 contoured glacier (white) corresponds to the year 2005 (stage 17). The abbreviations  
1657 “Rg” and “Ps” in lichenometry stations indicate that the estimated dates are derived  
1658 from the *Rhizocarpon geographicum* and *Porpidia soredizodes* lichens, respectively,

1659 and the number correspond to the longest axis of the largest lichen measured. This  
1660 figure is available in colour in the online version.

1661 Figure 4.  $^{36}\text{Cl}$  CRE ages and internal (analytical) uncertainty at  $1\sigma$  level of the samples  
1662 from Vesturdalur and Austurdalur. Note that the samples clustering around 500 yr (15<sup>th</sup>  
1663 century) in Austurdalur are indistinguishable. Distance to the terminus (year 2005) is  
1664 measured along the flowline from the reconstructed snout apex of the phase where the  
1665 samples were collected. This figure is available in colour in the online version.

1666 Figure 5. Correlation between largest thalli (longest axis) of species *Rhizocarpon*  
1667 *geographicum* and *Porpidia* cf. *soredizodes* in several lichenometry stations. With the  
1668 aim of avoiding those lichens potentially affected for any environmental factor  
1669 disturbing their normal growth, the largest lichens used come from those lichenometry  
1670 stations where no lichen size decrease with increasing distance to the terminus was  
1671 observed (i.e., TUV-2, TUV-4, TUV-5, TUV-6, TUV-2, TUE-4 and TUE-5). From  
1672 the measurements, it appears that *Porpidia* cf. *soredizodes* lichens grow faster than  
1673 those of *Rhizocarpon geographicum*.

1674

1675 **Table captions**

1676 Table 1. Glacial Equilibrium-Line Altitudes (ELAs) calculated over  
1677 Tungnahryggsjökull glaciers through the application of the AAR and AABR methods  
1678 over the 3D glacier reconstructions.

1679 Table 2. Surface ages estimated from *Kugelmann's (1991)*  $0.44 \text{ mm yr}^{-1}$  growth rate for  
1680 different colonization lags. The ages obtained from *Rhizocarpon geographicum* lichens  
1681 discussed throughout the text are those derived from a 20-yr colonization lag. The  
1682 figures in italics correspond to ages tentatively inferred from the largest *Porpidia*  
1683 *soredizodes* lichen, assuming a  $0.737 \text{ mm yr}^{-1}$  growth rate and a 15-year colonization  
1684 lag (see section 5.2.1).

1685 Table 3.  $^{36}\text{Cl}$  CRE ages converted to CE/BCE dates according to the different  $^{36}\text{Cl}$   
1686 production rates from Ca spallation. Uncertainties include the analytical and production  
1687 rate error.

1688 **Supplementary figures captions**

1689 **SF1.** Examples of *Rhizocarpon geographicum* group and *Porpidia soredizodes* thalli  
1690 measured over scaled field photos from the lichenometric station TUW-3. The lines  
1691 refer to the minimum circle (white) bounding the thalli outlines (yellow) and the  
1692 diameter of the circle (black). Note the contrasted size of the largest thalli in the  
1693 different species.

1694 **SF2.** Location of the lichenometry stations in relation to the glacier snout position  
1695 shown in the different aerial photographs and the satellite image. The lines refer to the  
1696 glacier margin outlined over the aerial photo at a specific date (red) and at the previous  
1697 date with aerial photo available (green dashed line). The points display the location of  
1698 the lichenometry stations. The aerial photos provide the dating control for the validation  
1699 of the lichenometric dates.

1700 **SF3.** Glacier surface reconstruction for the CRE- and lichenometry-dated glacial stages.

1701 **SF4.** Examples of moraine boulders sampled for  $^{36}\text{Cl}$  CRE dating in Vesturdalur  
1702 (“TUW” samples) and Austurdalur (“TUE” samples) and their dates derived from the  
1703 [Licciardi et al. \(2008\)](#)  $^{36}\text{Cl}$  production rate from Ca spallation.

1704 **SF5.** Location and BCE dates of the  $^{36}\text{Cl}$  samples from the Elliði crest.

1705 **Supplementary tables captions.**

1706 ST1. Correspondence between glacial stages mapped over historical aerial photos and  
1707 the dates.

1708 ST2. Glacier length and snout position variations measured along the flowline.

1709 ST3. Glacier extent and volume variations calculated from 2D and 3D glacier  
1710 reconstructions.

1711 ST4. Size of the largest lichen at the lichenometry stations in the forelands of the  
1712 western and eastern Tungnahryggsjökull glaciers.

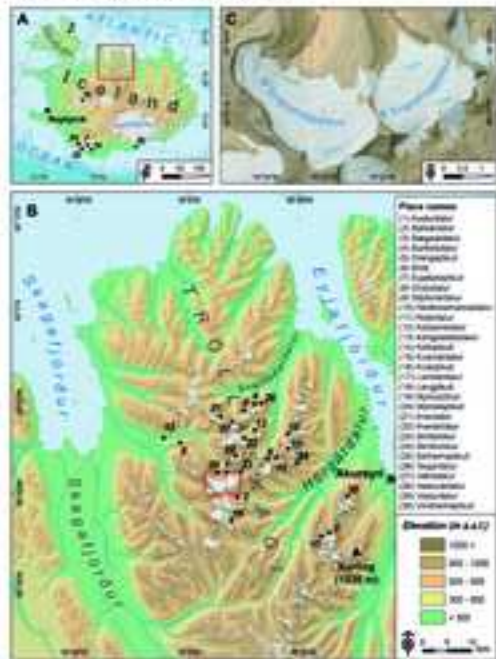
1713 ST5. Geographic sample locations, topographic shielding factor, sample thickness and  
1714 distance from terminus.

1715 ST6. Chemical composition of the bulk rock samples before chemical treatment. The  
1716 figures in italic correspond to the average values of the bulk samples analysed and were  
1717 those used for the age-exposure calculations of the samples without bulk chemical  
1718 composition analysis.

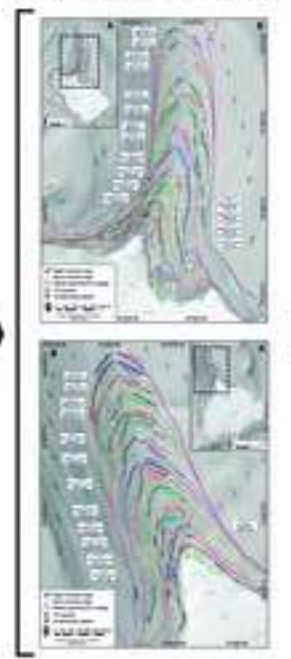
1719 ST7. Concentrations of the  $^{36}\text{Cl}$  target elements Ca, K, Ti and Fe, determined in splits  
1720 taken after the chemical pre-treatment (acid etching).

1721 ST8.  $^{36}\text{Cl}$  analytical data and CRE dating results according to different  $^{36}\text{Cl}$  production  
1722 rates from Ca spallation.  $^{36}\text{Cl}/^{35}\text{Cl}$  and  $^{35}\text{Cl}/^{37}\text{Cl}$  ratios were inferred from measurements  
1723 at the ASTER AMS facility. The numbers in italic correspond to the internal  
1724 (analytical) uncertainty at  $1\sigma$  level.

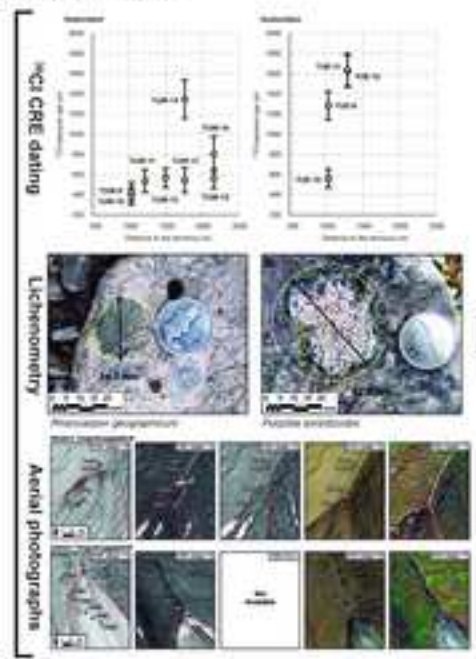
Tröllaskagi Peninsula (Northern Iceland) and the Tungnahryggsjökull glaciers



Glacial landforms and geomorphological mapping



Dating of glacial stages and study of the recent evolution



Reconstruction of the Late Holocene glacier fluctuations



### Highlights

- A multi-disciplinary approach reconstructs Late Holocene glacial evolution.
- High-detail moraine mapping was done for two glacier forelands.
- Late Holocene glacial maximum occurred prior to the Little Ice Age.
- Maximum Little Ice Age glacial culminations were prior to the 19<sup>th</sup> century.
- *Porpidia soledizodes* species is tested for lichenometric dating.

## 1 **Abstract**

2 The Tröllaskagi Peninsula in northern Iceland hosts more than a hundred small glaciers  
3 that have left a rich terrestrial record of Holocene climatic fluctuations in their  
4 forelands. Traditionally, it has been assumed that most of the Tröllaskagi glaciers  
5 reached their Late Holocene maximum extent during the Little Ice Age (LIA). However,  
6 there is evidence of slightly more advanced pre-LIA positions. LIA moraines from  
7 Iceland have been primary dated mostly through lichenometric dating, but the limitations  
8 of this technique do not allow dating of glacial advances prior to the 18<sup>th</sup> or 19<sup>th</sup>  
9 centuries. The application of <sup>36</sup>Cl Cosmic-Ray Exposure (CRE) dating to  
10 Tungnahryggsjökull moraine sequences in Vesturdalur and Austurdalur (central  
11 Tröllaskagi) has revealed a number of pre-LIA glacial advances at ~400 and ~700 CE,  
12 and a number of LIA advances in the 15<sup>th</sup> and 17<sup>th</sup> centuries, the earliest LIA advances  
13 dated so far in Tröllaskagi. This technique hence shows that the LIA chronology in  
14 Tröllaskagi agrees with that of other European areas such as the Alps or the  
15 Mediterranean mountains. The combined use of lichenometric dating, aerial  
16 photographs, satellite images and fieldwork shows that the regional colonization lag of  
17 the commonly used lichen species *Rhizocarpon geographicum* is longer than previously  
18 assumed. For exploratory purposes, an alternative lichen species (*Porpidia soredizodes*)  
19 has been tested for lichenometric dating, estimating a tentative growth rate of 0.737 mm  
20 yr<sup>-1</sup>.

## 21 **1. Introduction**

22 The Tröllaskagi Peninsula (northern Iceland) hosts over 160 small alpine cirque glaciers  
23 ([Björnsson, 1978](#); see synthesis in [Andrés et al., 2016](#)). Only a few of these small  
24 glaciers do not have supraglacial debris cover that allows them to react quickly to small  
25 climatic fluctuations ([Caseldine, 1985b](#); [Häberle, 1991](#); [Kugelmann, 1991](#)), compared to

26 the reduced dynamism of the predominant rock glaciers and debris-covered glaciers  
27 ([Martin et al., 1991](#); [Andrés et al., 2016](#); [Tanarro et al., 2019](#)). As a result of their high  
28 sensitivity to climatic changes, the few debris-free glaciers in Tröllaskagi fluctuated  
29 repeatedly in the past, forming a large number of moraines in front of their termini (see  
30 [Caseldine, 1983, 1985b, 1987](#); [Kugelmann, 1991](#) amongst others). However, the  
31 relation between glacier fluctuations and the climate is complicated due to: (i) the well-  
32 known surging potential activity in Tröllaskagi ([Brynjólfsson et al., 2012](#); [Ingólfsson et](#)  
33 [al., 2016](#)); (ii) the possibility of glaciers being debris-covered in the past, with the  
34 subsequent change of their climate sensitivity over time; (iii) the intense and dynamic  
35 slope geomorphological activity, paraglacial to a great extent ([Jónsson, 1976](#); [Whalley](#)  
36 [et al., 1983](#); [Mercier et al., 2013](#); [Cossart et al., 2014](#); [Feuillet et al., 2014](#); [Decaulne and](#)  
37 [Sæmundsson, 2006](#); [Sæmundsson et al., 2018](#)) that hides and erases the previous glacial  
38 features.

39 In Iceland, a great part of the research on glacial fluctuations during the late Holocene,  
40 LIA ([Grove, 1988](#); 1250-1850 CE, see [Solomina et al., 2016](#)) and later stages has been  
41 approached through application of radiocarbon dating of organic material, analyzing  
42 lake sediment varves ([Larsen et al., 2011](#); [Striberger et al., 2012](#)), dead vegetation  
43 remnants ([Harning et al., 2018](#)) and threshold lake sediment records ([Harning et al.,](#)  
44 [2016b](#); [Schomacker et al., 2016](#)). These provide high-resolution records of glacier  
45 variability. In Tröllaskagi, very few reliable dates exist at present, obtained from  
46 radiocarbon and tephrochronology ([Häberle, 1991, 1994](#); [Stötter, 1991](#); [Stötter et al.,](#)  
47 [1999](#); [Wastl and Stötter, 2005](#)). They suggest that late Holocene glaciers were slightly  
48 more advanced than during the LIA maximum in Tröllaskagi. However, these  
49 techniques only provide minimum or maximum ages for Holocene glacier history in  
50 northern Iceland ([Wastl and Stötter, 2005](#)). In addition, at Tröllaskagi most of the

51 moraines are at 600-1000 m a.s.l., where the applicability of tephrochronology is very  
52 limited (Caseldine, 1990) due to the great intensity of slope geomorphological  
53 processes.

54 In any case, most of the moraine datings of Tröllaskagi –especially those of the last  
55 millenium– comes from lichenometry (see synthesis in Decaulne, 2016). However, the  
56 ages derived from this technique tend to be younger if they are compared to those  
57 estimated from tephra layers (Kirkbride and Dugmore, 2001). Generally, there is  
58 disagreement about the validity of the results provided by lichenometry, due to the  
59 difficulty of the lichen species identification in the field, the complexity and reliability  
60 of the sampling and measurement strategies, the uncertainty estimates, the nature of the  
61 ages provided as relative, as well as the relative reliability at producing lichen growth  
62 curves of the different species, with an extreme dependence on local environmental  
63 factors (see Osborn et al., 2015).

64 In fact, these problems had already been detected in northern Iceland, where in spite of  
65 the time elapsed since the first applications of this technique (Jaksch, 1970, 1975, 1984;  
66 Gordon and Sharp, 1983; Maizels and Dugmore, 1985) and contrasting with its  
67 widespread use in the south and southeast of the island (Thompson and Jones, 1986;  
68 Evans et al., 1999; Russell et al., 2001; Kirkbride and Dugmore, 2001; Bradwell, 2001,  
69 2004a; Harris et al., 2004; Bradwell and Armstrong, 2006; Orwin et al., 2008; Chenet et  
70 al., 2010 and others), there are still very few established growth rates for the lichen  
71 group *Rhizocarpon geographicum* (Roca-Valiente et al., 2016) from Tröllaskagi  
72 (Caseldine, 1983; Häberle, 1991; Kugelmann, 1991; Caseldine and Stötter, 1993; see  
73 synthesis in Decaulne, 2016). In general, the growth curves from Tröllaskagi suffer  
74 from a few control points (i.e. surfaces of known age) for calibration. This leads to  
75 considerable underestimation when lichen thalli sizes are beyond the calibration growth

76 curve (Caseldine, 1990; see e.g. Caseldine, 1985b; Caseldine and Stötter, 1993;  
77 Kugelmann, 1991). That is to say, the extrapolation does not account for the decreasing  
78 growth rate with increasing age (i.e. non-linear growth). Kugelmann's (1991) growth  
79 curve has the highest number of control points to date (19 in total). In addition, the  
80 colonization lag in Tröllaskagi is poorly defined, although 10-15 years have been  
81 assumed for the *Rhizocarpon geographicum* (Caseldine, 1983; Kugelmann, 1991).  
82 Other issues, such as the absence of large thalli (Maizels and Dugmore, 1985), lichen  
83 saturation (e.g. Wiles et al., 2010), and other environmental factors (Innes, 1985 and  
84 references included; Hamilton and Whalley, 1995) contribute to appreciable age  
85 underestimations when dating surfaces using this approach. Snow is also a major  
86 environmental factor for lichenometry in Iceland due to its long residence time on the  
87 ground (Dietz et al., 2012) and the avalanching frequency –especially in Tröllaskagi–,  
88 whose effect restricts the growth rate of lichens, and even destroys them (Sancho et al.,  
89 2017). These problems considerably limit the quality (reliability) of the lichenometric  
90 dating range of utility for applying lichenometric dating in Iceland, where the oldest  
91 ages estimated so far are between 160 and 220 years (Maizels and Dugmore, 1985;  
92 Thompson and Jones, 1986; Evans et al., 1999), thus preventing the dating of glacial  
93 advances prior to the 18<sup>th</sup> century.

94 In spite of the high uncertainty of the lichenometric dating, many authors working in  
95 Tröllaskagi have treated their lichenometric results as absolute ages (see Caseldine,  
96 1983, 1985b, 1987; Kugelmann, 1991; Häberle, 1991; Caseldine and Stötter, 1993,  
97 amongst others). In fact, previously considered dates of LIA maximum glacier  
98 culmination are restricted to the very late 18<sup>th</sup> and early 19<sup>th</sup> centuries (Caseldine, 1983,  
99 1985b, 1987; Kugelmann, 1991; Caseldine and Stötter, 1993; Caseldine, 1991; Martin  
100 et al., 1991), very close to the applicability threshold of this method. Consequently, no

101 evidence of previous advances during phases of the LIA that were more conducive to  
102 glacier expansion (probably colder; see e.g. [Ogilvie, 1984, 1996](#); [Ogilvie and Jónsdóttir,](#)  
103 [2000](#); [Ogilvie and Jónsson, 2001](#)) has been found ([Kirkbride and Dugmore, 2001](#)).

104 In the recent years, dating methods based on the Exposure to the Cosmic-Rays (CRE)  
105 have been introduced successfully to date moraines of the last millennium, and even  
106 formed during the LIA ([Schimmelpfennig et al., 2012, 2014](#); [Le Roy et al., 2017](#);  
107 [Young et al., 2015](#); [Jomelli et al., 2016](#); [Li et al., 2016](#); [Dong et al., 2017](#); [Palacios et](#)  
108 [al., 2018](#)). The cosmogenic nuclides  $^{36}\text{Cl}$  and  $^3\text{He}$  have been applied previously in  
109 northern Iceland to date the Pleistocene deglaciation. [Principato et al. \(2006\)](#) studied the  
110 deglaciation of Vestfirðir combining  $^{36}\text{Cl}$  CRE dating of moraine boulders and bedrock  
111 surfaces with marine records and tephra marker beds. [Andrés et al. \(2018\)](#) reconstructed  
112 the deglaciation at the Late Pleistocene to Holocene transition at Skagafjörður through  
113  $^{36}\text{Cl}$  CRE dating applied to polished surfaces along a transect from the highlands to the  
114 mouth of the fjord. [Brynjólfsson et al. \(2015b\)](#) applied the same isotope to samples  
115 coming from the highlands and the fjords to reconstruct the glacial history of the  
116 Drangajökull region. The other cosmogenic isotope used is  $^3\text{He}$ , applied to helium-  
117 retentive olivine phenocrysts by [Licciardi et al. \(2007\)](#) to determine eruption ages of  
118 Icelandic table mountains and to reconstruct the volcanic history and the thickness  
119 evolution of the Icelandic Ice Sheet during the last glacial cycle. However, CRE dating  
120 has not yet been applied to the late Holocene glacial landforms both in Iceland as a  
121 whole and the Tröllaskagi Peninsula. CRE dating is an alternative to the use of high-  
122 resolution continuous lacustrine records in northern Iceland, given the rarity of lakes in  
123 this peninsula, which limits the application of radiocarbon to date the deglaciation  
124 processes ([Striberger et al., 2012](#); [Harning et al., 2016b](#)).

125 Nevertheless, CRE dating methods approach the nuclides' detection limit when applied  
126 to very recent moraines (Marrero et al., 2016; Jomelli et al., 2016). This issue precludes  
127 the application of CRE dating to the abundant post-LIA moraines existing in some of  
128 the Tröllaskagi valleys whose headwalls are occupied by climate-sensitive debris-free  
129 glaciers (Caseldine and Cullingford, 1981; Caseldine, 1983,1985b; Kugelmann, 1991;  
130 Fernández-Fernández et al., 2017). Dating these post-LIA moraines allows to  
131 reconstruct recent climate evolution, and even to match and assess the climate  
132 reconstructions with the instrumental climate records (see Dahl and Nesje, 1992;  
133 Caseldine and Stötter, 1993; Fernández-Fernández et al., 2017). Furthermore, improving  
134 the knowledge of the recent evolution of alpine mountain glaciers, such as those of  
135 Tröllaskagi, is fundamental in the assessment of present global warming (Marzeion et  
136 al., 2014)

137 The use of aerial photographs from different dates is a reliable approach to the glacier  
138 evolution during the last decades (Fernández-Fernández et al., 2017; Tanarro et al.,  
139 2019). The main advantage of this technique is the possibility of studying the evolution  
140 of glacier snouts in recent dates with high accuracy. In fact, there is no dependence on  
141 the glacial features (i.e. moraines), which circumvents moraine deterioration issues  
142 derived by the geomorphological activity of the slopes. However, the main shortcoming  
143 of the aerial photo imagery is the availability only on few dates, at least in Tröllaskagi.  
144 This circumstance makes it impossible to obtain the glacier fluctuations with a high  
145 time resolution (i.e. only the periods between the available aerial photos; Fernández-  
146 Fernández et al., 2017; Tanarro et al., 2019), and hence to match them to short-term  
147 (decadal scale) climate fluctuations that are known to exert a major control especially  
148 on small mountain glaciers with short time responses (see Caseldine, 1985b;  
149 Sigurðsson, 1998; Sigurðsson et al., 2007; Fernández-Fernández et al., 2017). The only

150 way to fill the gap between two dates with available aerial photos is through applying  
151 lichenometric dating (Sancho et al., 2011), as there is no tree species suitable to apply  
152 dendrochronology. In addition, the information provided by the aerial photo imagery  
153 (i.e. glacier snout position) constrains the period when the lichens appear and begin to  
154 grow, which circumvents many of the criticisms made on lichenometry (see Osborn et  
155 al., 2015).

156 Moreover, a detailed geomorphological mapping allows for identification of stable  
157 moraines, not remobilized or destroyed by glacier advances or slope processes  
158 (avalanches, slope deformations, debris-flows, etc.) and also to reconstruct the glacier  
159 snout geometry throughout different phases (see Caseldine, 1981; Bradwel, 2004b;  
160 Principato et al., 2006 amongst others). The analysis of the moraine morphology and the  
161 glacial features on the forelands is a key tool to confirm whether the glaciers were  
162 debris-free or debris-covered in the past (Kirkbride, 2011; Janke et al., 2015; Knight, et  
163 al., 2018, amongst others) as this issue determines their climate sensitivity (see  
164 Fernández-Fernández et al., 2017; Tanarro et al., 2019).

165 The western and eastern Tungnahryggsjökull glaciers, in the Vesturdalur and  
166 Austurdalur Valleys (central Tröllaskagi), respectively (Fig. 1), are two of the few  
167 debris-free glaciers –or almost debris-free in the case of the western glacier– of the  
168 peninsula that are both small and highly sensitive to climatic fluctuations (Fernández-  
169 Fernández et al., 2017). This makes them ideal for studying glacial and climatic  
170 evolution during last last millennia.

171 The aim of our work was to apply the best methodology possible to analyze the glacial  
172 evolution of western and eastern Tungnahryggsjökull glaciers during the last millennia  
173 to the present. Applying for the first time a number of dating techniques to study the  
174 Late Holocene evolution of the two glaciers, the objectives of this paper are:

175 (i) To carry out a detailed geomorphological survey of the glacier forelands in order to  
176 map accurately well-preserved glacial features. This mapping is used both to devise the  
177 sampling strategy for dating, and also to reconstruct the palaeoglaciers in 3D in order to  
178 obtain glaciologic climate indicators such as the Equilibrium-Line Altitudes (ELAs).  
179 These can be used as a proxy to infer palaeoclimatic information (see [Dahl and Nesje,](#)  
180 [1992](#); [Caseldine and Stötter, 1993](#); [Brugger, 2006](#); [Hughes et al., 2010](#); [Fernández-](#)  
181 [Fernández et al., 2017](#) amongst others).

182 (ii) To use aerial photographs / satellite imagery post-dating 1946 to map the glacier  
183 extent in each available date in order to improve the information of ELA evolution in  
184 the recent decades. Aerial photographs will be used to constrain the possible periods of  
185 lichen colonization and growth over stable boulders, and will be useful to identify  
186 phases of advance, stagnation or retreat of the glacier snouts. By this way we will  
187 complete the glacier evolution from pre-instrumental glacial stages (identified from  
188 geomorphological evidence, i.e. moraines) to their current situation.

189 (iii) To apply CRE dating when possible depending on the preservation degree of the  
190 glacial features, and when moraines were too old to be dated by lichenometry.

191 (iv) To apply lichenometric relative dating to recent moraines or those where CRE  
192 dating might not be suitable (i.e. limit of applicability) and provided that: 1) the  
193 geomorphological criteria evidence a good preservation of glacial features; and 2) aerial  
194 photographs constrain the earliest and oldest possible lichen ages. This approach will  
195 also allow to check the growth rates and colonization lags of the lichen species usually  
196 used in Iceland for lichenometric dating purposes.

197 The experimentation and validation of this methodological purpose will help to improve  
198 the knowledge of the recent climate evolution of northern Iceland. This is of maximum

199 interest if we consider its location within the current atmospheric and oceanic setting,  
200 strongly linked to the evolution of the Meridional Overturning Circulation ([Andrews](#)  
201 [and Giraudeau, 2003](#); [Xiao et al., 2017](#)), a key factor in the studies for the assessment of  
202 the global climate change effects ([Barker et al., 2010](#); [Chen et al., 2015](#) amongst others).  
203 Moreover, if this proposal is valid, it could be applied to the research on the recent  
204 evolution of other mountain glaciers similar to those of Tröllaskagi. This aspect is a  
205 main research objective at present, as these glaciers represent the greatest contribution  
206 to the current sea-level rise ([Jacob et al., 2012](#); [Gardner et al., 2013](#) amongst others).

## 207 **2. Regional setting**

208 The Tröllaskagi Peninsula extends into the Atlantic Ocean at 66°12' N from the central  
209 highland plateau (65°23' N) of Iceland ([Fig. 1](#)). The fjords of Skagafjörður (19°30' W)  
210 and Eyjafjörður (18°10' W) separate it from the Skagi and Flateyjarskagi peninsulas,  
211 respectively. Tröllaskagi is an accumulation of successive Miocene basalt flows,  
212 interspersed with reddish sedimentary strata ([Sæmundsson et al., 1980](#); [Jóhannesson](#)  
213 [and Sæmundsson, 1989](#)). The plateau culminates at altitudes of 1000-1500 m a.s.l. (with  
214 the highest peak Kerling at 1536 m a.s.l.) and is dissected by deep valleys with steep  
215 slopes whose headwaters are currently glacial cirques. These cirques host more than 160  
216 small glaciers, mostly north-facing, resulting from the leeward accumulation of snow  
217 from the plateau ([Caseldine and Stötter, 1993](#)) and reduced exposure to solar radiation.  
218 In fact, deposits caused by rock-slope failure are common in Tröllaskagi valley slopes  
219 and have been considered a result of the final deglaciation during the early Holocene  
220 ([Jónsson, 1976](#); [Feuillet et al., 2014](#); [Cossart et al., 2014](#); [Coquin et al., 2015](#)). Most of  
221 the glaciers are rock or debris-covered glaciers, due to the intense paraglacial activity  
222 affecting the walls that minimizes cosmogenic nuclide concentrations from earlier  
223 exposure periods on the cirque headwalls ([Andrés et al, 2018](#)).

224 The climate in Tröllaskagi is characterized by a mean annual air temperature (MAAT;  
225 1901-1990 series) of 2 to 4 °C at sea level, dropping to between -2 and -4 °C at the  
226 summits (Etzelmüller et al., 2007). At the town of Akureyri, located in the east of the  
227 peninsula at the mouth of Eyjafjarðardalur (Fig. 1), the MAAT is 3.4 °C and the average  
228 temperature in the three summer months is about 9 to 10 °C (Einarsson, 1991). Annual  
229 precipitation (1971-2000) ranges from 400 mm at lower altitudes to 2500 mm at the  
230 summits (Crochet et al., 2007).

231 The frontier location of Icelandic glaciers in relation to atmosphere and ocean systems  
232 (warm/moist Subtropical and cold/dry Arctic air masses; and the warm Irminger and  
233 cold East Greenland sea currents) makes them exceptionally sensitive to climate  
234 oscillations (Bergþórsson, 1969; Flowers et al., 2008; Geirsdóttir et al., 2009), and these  
235 debris-free glaciers are thus reliable indicators of climatic evolution and the impact of  
236 climate change on the cryosphere (see Jóhannesson and Sigurðsson, 1998; Bradwell,  
237 2004b; Sigurðsson, 2005; Geirsdóttir et al., 2009; Fernández-Fernández et al., 2017).

238 The glaciers studied here are the western (6.5 km<sup>2</sup>) and eastern (3.9 km<sup>2</sup>)  
239 Tungnahryggsjökull, located in the Vesturdalur and Austurdalur valleys respectively,  
240 separated from each other by the crest of Tungnaryggur, and tributaries of the  
241 Kolbeinsdalur Valley (Fig. 1).

### 242 **3. Methodology**

#### 243 *3.1 Geomorphological mapping and glacier geometry mapping*

244 Four summer field campaigns (2012, 2013, 2014 and 2015) were conducted in  
245 Vesturdalur and Austurdalur, with the objective of identifying moraines that clearly  
246 provided evidence of various glacial culminations of the western and eastern  
247 Tungnahryggsjökull glaciers. We identified the palaeo-positions of the glacier snouts,

248 the glacier geometry and extent through photo interpretation of stereoscopic pairs and  
249 previous fieldwork. Mapping of glacial and non-glacial landforms was conducted on  
250 two enlarged 50-cm-resolution aerial orthophotos ([National Land Survey of Iceland,](#)  
251 [2015](#)) plotted at scale  $\approx 1:7000$ . These maps were imported into an ArcGIS 1.4.1  
252 database after geo-referencing. Finally, all the glacial linear landforms were digitized,  
253 and where the moraines were prominent, continuous, or well-preserved, they were  
254 assumed to represent major culminations, and hence, glacial stages. In addition to the  
255 geomorphological evidence, glacier variations in recent years were mapped, based on  
256 the photo interpretation of four historical aerial photographs from 1946, 1985, 1994 and  
257 2000 ([National Land Survey of Iceland, 2015](#)), and also one SPOT satellite image  
258 (2005), previously geo-referenced in ArcGIS. For more details of the aerial photograph  
259 processing, see [Fernández-Fernández and Andrés \(2018\)](#). As the glacier headwalls are  
260 ice diffluences in both cases, it was assumed that: (i) the ice divides are the upper  
261 boundaries of the glaciers for the different stages, and (ii) the ice divide is invariant for  
262 the different stages/dates, following [Koblet et al. \(2010\)](#) as changes in the extent of the  
263 accumulation zone are smaller than the outlining differences derived from the operator  
264 mapping. Likewise, in the case of the upper glacier edge constrained by the cirque wall,  
265 the glacier geometry was also assumed to be invariant from stage to stage unless the  
266 aerial photographs showed otherwise.

### 267 *3.2 Glacier reconstruction and equilibrium-line altitude (ELA) calculation*

268 [Benn and Hulton's \(2010\)](#) glacier reconstruction approach using a physical-based model  
269 describing ice rheology and glacier flow ([Van der Veen, 1999](#)) was preferred to  
270 arbitrary hand-drawn contouring (e.g. [Sissons, 1974](#)) in order to achieve more robust  
271 reconstructions ([Fernández-Fernández and Andrés, 2018](#)). This model operates on  
272 deglaciated areas with non-extant glaciers. As this is not the case in our study area, we

273 approached the glacier bedrock by tentatively estimating the ice thickness' spatial  
274 distribution on the two glaciers studied. The "VOLTA" ("Volume and Topography  
275 Automation") ArcGIS toolbox (James and Carrivick, 2016) was applied with the default  
276 parameters. It only requires the glacier outline and its digital elevation model (DEM). In  
277 the first step, the tool "volta\_1\_2\_centrelines" creates the glacier centrelines, and then  
278 the tool "volta\_1\_2\_thickness" estimates ice thickness at points along them, assuming  
279 perfect-plasticity rheology, and interpolates the values using a glaciologically correct  
280 routine. The final result is an ice-free DEM in which we reconstructed the glacier. The  
281 former glacier surface topographies at the different stages/dates were reconstructed  
282 applying the semi-automatic "GLaRe" ArcGIS toolbox designed by Pellitero et al.  
283 (2016), which implements the Benn and Hulton (2010) numerical model and estimates  
284 ice-thickness along glacier flowlines. To simplify the glacier surface modelling, shear-  
285 stress was assumed to be constant along the glacier flowline and over time. Using the  
286 value 110 kPa for the shear-stress resembles best the current longitudinal profile of the  
287 glaciers in the Benn and Hulton (2010) spreadsheet. This value can be considered  
288 appropriate as it falls within the normal shear-stress range of 50-150 kPa observed in  
289 current glaciers and is very close to the standard value of 100 kPa (Paterson, 1994). The  
290 glacier contours were manually adjusted to the ice surface elevation values of the ice-  
291 thickness points estimated by "GLaRe" instead of using an interpolation routine, to  
292 obtain a more realistic surface (concave and convex contours above and below the  
293 ELA).

294 Finally, we calculated the ELAs automatically by using the "ELA calculation" ArcGIS  
295 toolbox (Pellitero et al., 2015). The methods comprised: (i) AABR (Area Altitude  
296 Balance Ratio; Osmaston, 2005) with the ratio  $1.5 \pm 0.4$  proposed for Norwegian glaciers  
297 by Rea (2009) and successfully tested on Tröllaskagi debris-free glaciers in Fernández-

298 [Fernández et al. \(2017\)](#); and (ii) the AAR (Accumulation Area Ratio) with the ratio 0.67  
299 previously used by [Stötter \(1990\)](#) and [Caseldine and Stötter \(1993\)](#) for Tröllaskagi  
300 glaciers. Alternative approaches for ELA calculation in northern Iceland have been  
301 carried out by considering morphometric parameters of glacial cirques (altitude ratio,  
302 cirque floor, minimum point; [Ipsen et al., 2018](#)). However, we preferred the methods  
303 considering the glacier hypsometry as they reflect more evident changes from stage to  
304 stage ([Fernández-Fernández et al., 2017](#); [Fernández-Fernández and Andrés, 2018](#)), if  
305 compared to morphometric parameters of the cirques. In this sense, the cirque floor  
306 elevation is derived from the last erosion period, and it is impossible to know the values  
307 corresponding to previous glacial stages.

### 308 *3.3 Lichenometric dating procedures*

309 Lichenometry was used as a relative dating tool, assuming that the lichens increase in  
310 diameter with respect to age. The results aim to complete the age control (of recent  
311 landforms non suitable for CRE dating) on the periods between aerial photos of known  
312 date as it has been applied successfully to control lichen ([Sancho et al., 2011](#)) and  
313 bryophyte ([Arróniz-Crespo et al., 2014](#)) growth during primary succession in recently  
314 deglaciaded surfaces. First, we surveyed the moraines thoroughly, starting from the  
315 current glacier snouts downwards, looking for large stable boulders (i.e. well embedded  
316 in the moraine, not likely of having been overturned or remobilized by slope processes  
317 which could have affected lichen growth, e.g. snow avalanches, debris-flows, rockfall,  
318 landslides or debris-flows) with surfaces valid for dating (not weathered or resulting  
319 from block break). Lichenometry was applied to date moraine ridge boulders with the  
320 following criteria and assumptions: (i) boulders must clearly belong to the moraine  
321 ridge; (ii) lichen species should be abundant enough to allow measurements of a number  
322 of thalli at each location and hence enable surfaces to be dated under favourable

323 environmental conditions such as basaltic rocks in subpolar mountains; (iii) only the  
324 largest lichen (circular or ellipsoidal thalli) of species *Rhizocarpon geographicum*,  
325 located on smooth horizontal boulder surfaces, was measured; (iv) the lichenometric  
326 procedures should not be applied when the lichen thalli coalesce on the boulder surface  
327 and individual thalli cannot be identified. We preferred the geomorphological criterion  
328 (stability vs. slope processes) to the establishment of lichenometry plots of a fixed area  
329 (e.g. [Bickerton and Matthews, 1992](#)) to ensure that lichens were measured on reliable  
330 boulders. This measurement strategy tries to circumvent or at least to minimize the  
331 specific problems of Tröllaskagi when dating glacial features so that: (i) snow  
332 accumulation should be lower in the moraine crest; (ii) lichen ages will be estimated  
333 only for the boulders located on the crests used to map and reconstruct the glaciers; and  
334 (iii) and lichens subjected to thalli saturation (coalescence) or high competition are not  
335 measured.

336 First, *Rhizocarpon geographicum* lichens were measured with a Bernier calibrator.  
337 Then, digital photographs for high-precision measurements were taken of the most  
338 representative of the largest thallus located in each selected boulder ([Suppl. figure SF1](#)),  
339 using an Icelandic króna coin (21 mm diameter) parallel to the surface of the lichen as a  
340 graphic scale. We preferred the single largest lichen approach as previously has been  
341 done in Tröllaskagi for lichenometric dating of moraines ([Caseldine, 1983, 1985b,](#)  
342 [1987; Kugelmann, 1991](#)). The photos were scaled in ArcGIS to real size and lichen  
343 thalli were outlined manually through visual inspection of the photos and measured  
344 automatically with high accuracy according to the diameter of the smallest circle which  
345 can circumscribe the lichen outline ([Suppl. figure SF1](#)). We preferred the simple  
346 geometrical shape of the circle and its diameter to identify the largest axis to circumvent

347 the problem of complex-shaped lichens. Similar procedures for lichen thalli  
348 measurement from photographs are outlined in [Hooker and Brown \(1977\)](#).

349 Then, we initially applied a  $0.44 \text{ mm yr}^{-1}$  constant growth rate and a 10-year  
350 colonization lag ([Kugelmann, 1991](#)) to the measurement of the largest *Rhizocarpon*  
351 *geographicum* lichen (longest axis). This growth rate is derived from the lichen growth  
352 curve with the highest number of control points so far in Tröllaskagi ([Kugelmann,](#)  
353 [1991](#)), and it is very similar to that reported from the near Hörgárdalur valley ([Häberle,](#)  
354 [1991](#)). However, the authors are aware that using a constant growth rate implies not  
355 taking account the growth rate decline with increasing age. Other longer colonization  
356 lags of 15, 20, 25 and 30 years were added to the age estimate from the growth rate in  
357 order to test the colonization lag originally assumed by [Kugelmann \(1991\)](#), on the  
358 suspicion of longer colonization lags reported elsewhere ([Caseldine, 1983](#); [Evans et al.,](#)  
359 [1999, Table 1](#)). The resulting ages were compared to the dates of historical aerial  
360 photographs where the glacier snout positions constrain the maximum and minimum  
361 ages of the lichen stations.

362 In the case of *Porpidia cf. soredizodes*, since no growth rate value has been described so  
363 far, a value will be tentatively estimated in this study. For this reason, we took  
364 measurements of the two species in the same sampling locations wherever possible. It  
365 should be noted that visual distinction between *Porpidia cf. soredizodes* and *Porpidia*  
366 *tuberculosa* is not always conclusive based on morphological characteristics, but we  
367 feel confident using the measurements of the *Porpidia cf. soredizodes* we identified in  
368 the field.

369 *3.4 <sup>36</sup>Cl Cosmic-Ray Exposure (CRE) dating*

370 Where the thalli either coalesced and prevented identification of the largest thallus or  
371 dating results indicated that a moraine was too old to be dated by this method, rock  
372 samples were collected for CRE dating. The criteria for boulder and surface selection  
373 where the same as for lichenometric purposes: stable boulders with no signs of being  
374 affected by slope processes (landslides, debris-flows) or postglacial overturning, well  
375 embedded in the moraine, and with no sign of surface weathering or previous boulder  
376 break. The cosmogenic nuclide  $^{36}\text{Cl}$  was chosen because of the basalt lithology  
377 ubiquitous in Iceland, which lacks quartz, which is needed for standard  $^{10}\text{Be}$  CRE  
378 methods. Using a hammer and chisel, samples were collected from flat-topped surfaces  
379 of moraine boulders. In order to obtain a maximum time constraint for the deglaciation  
380 of both surveyed valleys, two samples were taken from Elliði (Fig. 1), a glacially  
381 polished ridge downstream from the Tungnahryggsjökull forelands separating  
382 Kolbeinsdalur to the north and Viðinesdalur to the south. The laboratory procedures  
383 applied for  $^{36}\text{Cl}$  extraction from silicate whole rock samples were those described in  
384 Schimmelpfennig et al. (2011). Note that the samples had not enough minerals to  
385 perform the  $^{36}\text{Cl}$  extraction on mineral separates, which is generally the preferred  
386 approach to minimize the uncertainties in age exposure estimates, as in mineral  
387 separates  $^{36}\text{Cl}$  is often produced by less and better known production pathways than in  
388 whole rock samples (Schimmelpfennig et al., 2009). The samples were crushed and  
389 sieved to 0.25-1 mm in the Physical Geography Laboratory in the Complutense  
390 University, Madrid. Chemical processing leading to  $^{36}\text{Cl}$  extraction from the whole rock  
391 was carried out at the Laboratoire National des Nucléides Cosmogéniques (LN<sub>2</sub>C) at the  
392 Centre Européen de Recherche et d'Enseignement des Géosciences de l'Environnement  
393 (CEREGE), Aix-en-Provence (France). Initial weights of about 120 g per sample were  
394 used. A chemically untreated split of each sample was set aside for analyses of the

395 chemical composition of the bulk rocks at CRPG-SARM. First, the samples were rinsed  
396 to remove dust and fines. Then, 25-30% of the mass was dissolved to remove  
397 atmospheric  $^{36}\text{Cl}$  and potentially Cl-rich groundmass by leaching with a mixture of  
398 ultra-pure dilute nitric (10%  $\text{HNO}_3$ ) and concentrated hydrofluoric (HF) acids. In the  
399 next step, 2 g aliquots were taken to determine the major element concentrations; these  
400 were analysed by ICP-OES at CRPG-SARM. Then, before total dissolution,  $\sim 260 \mu\text{L}$  of  
401 a  $^{35}\text{Cl}$  carrier solution (spike) manufactured in-house (concentration:  $6.92 \text{ mg g}^{-1}$ ;  
402  $^{35}\text{Cl}/^{37}\text{Cl}$  ratio: 917) were added to the sample for isotope dilution (Ivy-Ochs et al.,  
403 2004). Total dissolution was achieved with excess quantities of the above mentioned  
404 acid mixture. Following total dissolution, the samples were centrifuged to remove the  
405 undissolved residues and gel (fluoride complexes such as  $\text{CaF}_2$ ). Next, chlorine was  
406 precipitated to silver chloride ( $\text{AgCl}$ ) by adding 2 ml of silver nitrate ( $\text{AgNO}_3$ ) solution  
407 at 10%. After storing the samples for two days in a dark place to allow the  $\text{AgCl}$  to  
408 settle on the bottom, the supernatant acid solution was extracted by a peristaltic pump.  
409 To reduce the isobaric interferences of  $^{36}\text{S}$  during the  $^{36}\text{Cl}$  AMS measurements, the first  
410 precipitate was re-dissolved in 2 ml of ammonia ( $\text{NH}_3+\text{H}_2\text{O}$  1:1 vol  $\rightarrow$   $\text{NH}_4\text{OH}$ ), and 1  
411 ml of a saturated solution of barium nitrate ( $\text{Ba}(\text{NO}_3)_2$ ) was added to the samples to  
412 precipitate barium sulphate ( $\text{BaSO}_4$ ). It was removed by centrifuging and filtering the  
413 supernatant with a syringe through acrodisc filters.  $\text{AgCl}$  was precipitated again with 3-  
414 4 ml of diluted  $\text{HNO}_3$  (1:1 vol). The precipitate was collected by centrifuging, rinsed,  
415 and dried in an oven at  $80 \text{ }^\circ\text{C}$  for 2 days.

416 The final  $\text{AgCl}$  targets were analysed by accelerator mass spectrometry (AMS) to  
417 measure the  $^{35}\text{Cl}/^{37}\text{Cl}$  and  $^{36}\text{Cl}/^{35}\text{Cl}$  ratios, from which the Cl and  $^{36}\text{Cl}$  concentration  
418 were inferred. The measurements were carried out at the Accélérateur pour les Sciences  
419 de la Terre, Environnement et Risques (ASTER) at CEREGE in March 2017 using

420 inhouse standard SM-CL-12 with an assigned value of  $1.428 (\pm 0.021) \times 10^{-12}$  for the  
421  $^{36}\text{Cl}/^{35}\text{Cl}$  ratio (Merchel et al., 2011) and assuming a natural ratio of 3.127 for the stable  
422 ratio  $^{35}\text{Cl}/^{37}\text{Cl}$ .

423 When calculating exposure ages, the Excel<sup>TM</sup> spreadsheet for in situ  $^{36}\text{Cl}$  exposure age  
424 calculations proposed by Schimmelpfennig et al. (2009) was preferred to other online  
425 calculators (e.g. CRONUS Earth; Marrero et al., 2016) as it allows input of different  
426  $^{36}\text{Cl}$  production rates from spallation, referenced to sea level and high latitude (SLHL).  
427 Thus, three SLHL  $^{36}\text{Cl}$  production rates from Ca spallation, i.e. the most dominant  $^{36}\text{Cl}$   
428 production reaction in our samples, were applied to allow comparisons both with other  
429 Icelandic areas ( $57.3 \pm 5.2$  atoms  $^{36}\text{Cl}$  (g Ca) $^{-1}$  yr $^{-1}$ ; Licciardi et al., 2008) and other areas  
430 of the world ( $48.8 \pm 3.4$  atoms  $^{36}\text{Cl}$  (g Ca) $^{-1}$  yr $^{-1}$ , Stone et al., 1996;  $42.2 \pm 4.8$  atoms  $^{36}\text{Cl}$   
431 (g Ca) $^{-1}$  yr $^{-1}$ , Schimmelpfennig et al., 2011). For  $^{36}\text{Cl}$  production reactions other than Ca  
432 spallation, the following SLHL  $^{36}\text{Cl}$  production parameters were applied:  $148.1 \pm 7.8$   
433 atoms  $^{36}\text{Cl}$  (g K) $^{-1}$  yr $^{-1}$  for K spallation (Schimmelpfennig et al., 2014b),  $13 \pm 3$  atoms  
434  $^{36}\text{Cl}$  (g Ti) $^{-1}$  yr $^{-1}$  for Ti spallation (Fink et al., 2000),  $1.9 \pm 0.2$  atoms  $^{36}\text{Cl}$  (g Fe) $^{-1}$  yr $^{-1}$  for  
435 Fe spallation (Stone et al., 2005) and  $696 \pm 185$  neutrons (g air) $^{-1}$  yr $^{-1}$  for the production  
436 rate of epithermal neutrons for fast neutrons in the atmosphere at the land/atmosphere  
437 interface (Marrero et al., 2016). Elevation-latitude scaling factors were based on the  
438 time invariant “St” scheme (Stone et al., 2000). The high-energy neutron attenuation  
439 length value applied was  $160 \text{ g cm}^{-2}$ .

440 All production rates from spallation of Ca mentioned above are based on calibration  
441 samples with a predominant Ca composition. Iceland is permanently affected by a low-  
442 pressure cell, the Icelandic Low (Einarsson, 1984). As the atmospheric pressure  
443 modifies the cosmic-ray particle flux, and thus has an impact on the local cosmogenic  
444 nuclide production rate, the atmospheric pressure anomaly has to be taken into account

445 when scaling the SLHL production rates to the study site. Only [Licciardi et al.'s \(2008\)](#)  
446 production rate already accounts for this anomaly, as the calibration sites of study are  
447 located in south western Iceland (see also [Licciardi et al., 2006](#)). On the other hand,  
448 [Stone et al.'s \(1996\)](#) and [Schimmelfennig et al.'s \(2011\)](#) production rates were  
449 calibrated in Tabernacle Hill (Utah, western U.S.A.) and Etna volcano (Italy),  
450 respectively, hence they need to be corrected for the atmospheric pressure anomaly  
451 when applied in Iceland. [Dunai \(2010\)](#) advises including any long-term atmospheric  
452 pressure anomaly at least for Holocene exposure periods. Therefore, the local  
453 atmospheric pressure at the sample locations was applied in the scaling factor  
454 calculations when using the [Stone et al. \(1996\)](#) and [Schimmelfennig et al. \(2011\)](#)  
455 production rates. Instead of the standard value of 1013.25 hPa at sea level, a sea level  
456 value of 1006.9 hPa (Akureyri meteorological station; [Icelandic Meteorological Office,](#)  
457 [2018](#)) was used. The atmospheric pressure correction assumed a linear variation of  
458 temperature with altitude. The results presented and discussed below are based on the  
459  $^{36}\text{Cl}$  production rate for Ca spallation of [Licciardi et al. \(2008\)](#) as it is calibrated for  
460 Iceland and considers the atmospheric pressure anomaly. The exposure ages presented  
461 throughout the text and figures include analytical and production rate errors unless  
462 stated otherwise. Our <2000 yr CRE ages have also been rounded to the nearest decade,  
463 and then converted to CE dates through their subtraction from the year 2015 (i.e.  
464 fieldwork and sampling campaign). In order to achieve robust comparisons of our  
465 results with those obtained by radiocarbon or tephrochronology, we have calibrated the  
466  $^{14}\text{C}$  ages previously published in the literature through the OxCal 4.3 online calculator  
467 (<https://c14.arch.ox.ac.uk/oxcal/OxCal.html>) implementing the IntCal13 calibration  
468 curve ([Reimer et al., 2013](#)).

#### 469 **4. Results**

#### 470 *4.1 Geomorphological mapping, aerial photos and identified glacial stages*

471 Based on photo-interpretation of aerial photographs and fieldwork, two  
472 geomorphological maps were generated at ~1:7000 scale, in which well preserved  
473 moraine segments, current glacier margins and stream network were also mapped (Figs.  
474 **2 and 3**). In Vesturdalur, over 1000 moraine ridge fragments (including terminal and  
475 lateral moraine segments) were identified and mapped, with increased presence from  
476 1.7 km upwards to the current glacier terminus. In the analysis, we retained only ridge  
477 fragments if they are at least 50 m long, protruding 2 m above the valley bottom and the  
478 alignment of glacial boulders embedded in the moraine crest is preserved, as indicators  
479 of major glacial culminations and well preservation state. Otherwise we considered  
480 either they represented insignificant glacial stages or were most probably affected by  
481 post-glacial slope reworking.

482 Following these criteria, we retained 12 glacial stages based on the geomorphological  
483 mapping of the Vesturdalur foreland (Fig. 2). We were able to verify in the field that the  
484 selected sections had not been affected by postglacial slope processes as none of these  
485 moraines was cut by debris-flows or deformed/covered by landslides. The palaeo-  
486 position of the glacier terminus was clearly defined by pairs of latero-frontal moraines  
487 in stages 1, 4 and 6. In stages 2, 3, 5, 9, 10, 11 and 12, it was poorly defined by short  
488 latero-frontal moraines on one side of the valley, very close to the river, with their  
489 prolongation and intersection with the river assumed to be the former apex, and so a  
490 tentative terminus geometry was drawn. The lateral geometry of the tongue was  
491 accurately reconstructed in stages 6, 8 and 9 based on long and aligned, ridge fragments,  
492 and in the other stages an approximate geometry was drawn from the terminus to the  
493 headwall. The greatest retreat between consecutive stages (1 km) occurred in the

494 transition from the stage 1 to the stage 2. No intermediate frontal moraines were  
495 observed in the transect between the stages 1 and 2.

496 In Austurdalur, over 1600 moraine ridge fragments were identified and mapped.  
497 Following the same criteria as in Vesturdalur, 13 stages were identified based on the  
498 geomorphological evidence (Fig. 3). The furthest moraines marking the maximum  
499 extent of the eastern Tungnahryggsjökull appear at 1.3 km from the current terminus. In  
500 contrast to the other valley, moraines populate the glacier foreland more densely and  
501 regularly on both sides of the valley. Most of them are <50 m long with a few exceeding  
502 100-200 m. The frontal moraine ridge fragments in Austurdalur clearly represent the  
503 geometry of the terminus in all the stages, as they are well-preserved and are only  
504 bisected by the glacier meltwater, with the counterparts easily identifiable. The most  
505 prominent (over 2 m protruding over the bottom of the valley) and well preserved  
506 moraines are those marking the terminus position at stages 1 to 8, with lengths ranging  
507 from 170 to 380 m.

508 Both glaciers were also outlined on aerial photos of 1946, 1985, 1994 (only for western  
509 Tungnahryggsjökull), and 2000, and on a SPOT satellite image (2005), and hence new  
510 recent stages from the past century were studied for the Tungnahryggsjökull, five for the  
511 western glacier (stages 13, 14, 15, 16 and 17) and four for the eastern glacier (stages 11,  
512 15, 16 and 17) (Suppl. figure SF2; Suppl. table ST1). The stages identified on the basis  
513 of the geomorphological mapping and those obtained from glacier outlining over  
514 historical aerial photos sum up to a total of 17 stages for each glacier.

#### 515 *4.2. Glacier length, extent and volume*

516 The reconstructed glacier surfaces corresponding to the different glacial stages is shown  
517 in Suppl. figure SF3. The length of the glaciers during their reconstructed maximum ice

518 extent was unequal, with the western Tungnahryggsjökull being 6.5 km long, and the  
519 eastern glacier being 3.8 km long (Suppl. table ST2). The same occurred with the area,  
520 9.4 and 5.3 km<sup>2</sup>, respectively (Suppl. table ST3). Over the different stages, the western  
521 glacier lost 31% of its area and retreated 51% of its total length (Suppl. tables ST2 and  
522 ST3) while there was less shrinkage of the eastern glacier both in area loss (26%) and  
523 length (34%). Figs. 2B and 3B and Suppl. table ST2 show only one reversal during the  
524 general retreating trend, in the stage 15 of the western and the stage 16 of the eastern  
525 Tungnahryggsjökull. The greatest area losses occurred in the transition to the stages 2,  
526 4, 7, 9 and 14 (>3%) on the western glacier while losses between stages in the eastern  
527 glacier were lower except for the transition between the stages 14 and 17, where a  
528 noticeable reduction of the accumulation area was observed in the aerial photos of 1946  
529 and 1985, and the satellite image of 2005 (Fig. 3B). The volumes calculated from the  
530 reconstructed glacier DEM and the corrected bed DEM show that the glaciers reached  
531 ~1.10 km<sup>3</sup> (western) and ~0.47 km<sup>3</sup> (eastern) at their recorded maximum extent  
532 corresponding to their outmost moraines. From the oldest to the most recent stage they  
533 lost 30% and 23% of their ice volume, respectively. The losses between consecutive  
534 stages of the glaciers were in general lower than 3% with the exception of the stages 2,  
535 4, 7, 9 (western) and stage 14 (eastern), where the values ranged from 3% to 10%  
536 (Suppl. table ST3). Only one slight inversion of the volume trend is seen in the stages  
537 15 of the western glacier and in 16 of the eastern glacier.

#### 538 4.3. Equilibrium-Line Altitudes (ELAs)

539 The application of the AAR (0.67) method showed ELAs ranging from 1021 to 1099 m  
540 a.s.l. (western glacier) and from 1032 to 1065 m a.s.l. (eastern glacier) for the different  
541 reconstructed stages. This means an overall rise of 78 and 33 m respectively (Table 1)  
542 from the maximum to the minimum extent recorded. The results from applying the

543 AABR (1.5) show the same trend and similar ELAs, with differences of up to  $\pm 15$  m  
544 compared with those obtained from the AAR. The AABR-ELAs tend to be higher than  
545 the AAR-ELAs, especially in the second half of the reconstructed stages with the most  
546 remarkable differences occurring in the eastern Tungnahryggsjökull (Table 1).  
547 However, the error derived from the uncertainties associated to the applied balance ratio  
548 (BR,  $\pm 0.4$ ) tends to decrease as the glaciers get smaller. The greatest change in the ELA  
549 between consecutive stages is found between the stages 1 and 2 in the western glacier  
550 (+26 m), fully coincident with the largest retreat measured, about 1 km. An interesting  
551 result is that the ELA rise is attenuated in both glaciers from stage 10 onwards, with  
552 stage-to-stage variations close to zero predominating, and with only one inversion (-3  
553 m) occurring in the western glacier between the stages 14 and 15 (Table 1).

#### 554 4.4. Lichenometric dating

555 Altogether 17 lichenometry stations (8 in Vesturdalur and 9 in Austurdalur) were set up  
556 during fieldwork in the two glacier forelands. Their spatial distribution and  
557 correspondence with the different glacial stages are given in Figs. 2 and 3 and Suppl.  
558 table ST4. The table also shows the measurements of the largest *Rhizocarpon*  
559 *geographicum* thalli found during fieldwork in the moraines (stages) to which the  
560 stations correspond. TUE-0 was the only station where no lichen of either species was  
561 found in 2015. Unlike *Porpidia* cf. *soredizodes* thalli, which are present in all the  
562 remaining lichenometry stations, *Rhizocarpon geographicum* thalli suitable for  
563 measuring (ellipsoidal, not coalescent) were only found in stations TUW-2 to TUW-7 in  
564 Vesturdalur, and in TUE-2 to TUE-7 in Austurdalur.

565 The measurements considered the diameter of the smallest circle bounding the thallus  
566 outline as representative of the longest axis (Suppl. figure SF1). The obtained values  
567 ranged from 19.3 to 71.5 mm in Vesturdalur, and from 19.0 to 47.7 mm in Austurdalur

568 (Suppl. table ST4). Only one size inversion (decreasing size with increasing distance to  
569 the current terminus) was detected in Austurdalur in the station TUE-6 (Fig. 3).  
570 *Rhizocarpon geographicum* thalli were absent in the nearest stations (TUW-1 and TUE-  
571 1) and were coalescent in the most distant stations (TUW-8 and TUE-8) in both glacier  
572 forelands. On the other hand, *Porpidia cf. soredizodes* thalli measurements ranged from  
573 18.3 to 148.4 mm in Vesturdalur, and from 16.8 to 141.8 mm in Austurdalur (Suppl.  
574 table ST4). A size inversion of *Porpidia cf. soredizodes* thalli is also observed in TUE-6  
575 and in TUE-7.

576 When the ages of *Rhizocarpon geographicum* lichens are calculated applying a 0.44  
577 mm yr<sup>-1</sup> growth rate and a 10-year colonization lag following Kugelmann (1991), they  
578 range from 54 to 173 years in Vesturdalur, and from 53 to 119 years in Austurdalur. If  
579 longer colonization lags of 15, 20, 25 and 30 years (see Methods section) are applied  
580 tentatively, the oldest ages obtained are ~170-190 years, and the youngest ~40-70 years  
581 (Table 2). In general, the further away the lichenometry stations are, the older are the  
582 ages (Figs. 2 and 3), with the inversions mentioned above. Apparently the lichenometry-  
583 dated moraines are younger than the CRE-dated distal moraines.

584 The absence of *Rhizocarpon geographicum* lichens in 2015 at lichenometry station  
585 TUW-1 (uncovered by the glacier at some time between 1994 and 2000; Suppl. figure  
586 SF2) suggests a colonization lag of at least 15-21 years. In addition, it is only when the  
587 colonization lag is assumed to be longer than 10 years and shorter than 30 years that the  
588 ages obtained at stations TUW-3 and TUE-2 are in good agreement with the ages  
589 deduced from the aerial photos (Table 2).

590 During the 2015 field campaign, the species *Porpidia cf. soredizodes* was absent in  
591 station TUE-0, located on a glacially polished threshold uncovered by the glacier after  
592 2005 (post-stage 17). However, it was found in stations TUW-1 and TUE-1, dated to

593 1994-2000 and 1946-1985 respectively, based on the position of the snouts in the aerial  
594 photos (Suppl. figure SF2). These observations suggest a colonization lag from 10 to  
595 15-21 years, thus shorter than for *Rhizocarpon geographicum*.

#### 596 4.5. <sup>36</sup>Cl CRE dating

597 The detailed geomorphological analysis carried out on the numerous moraine ridges of  
598 both valleys has greatly limited the number of boulders reliable for successfully  
599 applying <sup>36</sup>Cl CRE and lichenometry dating methods. Due to the great intensity of the  
600 slope processes (especially snow avalanches and debris-flows), only a few boulders are  
601 well-preserved, sometimes only one in each moraine ridge that retains its original  
602 glacier location. Thus, it should be highlighted that this issue prevented performing a  
603 statistically valid sampling for both methods (see e.g. Schaefer et al., 2009; Heymann  
604 et al., 2011).

605 During the fieldwork campaigns in the forelands of the western and eastern  
606 Tungnahryggsjökull glaciers, 12 samples from stable and very protrusive moraine  
607 boulders (Suppl. figure SF4) were collected in areas where lichenometric dating was not  
608 suitable because of lichen thalli coalescence, and also 2 samples from a polished ridge  
609 downwards the confluence of Vesturdalur and Austurdalur (Suppl. figure SF5). The  
610 input data for exposure age calculations, namely sample thickness, topographic  
611 shielding factor, major element concentrations of bulk/target fractions, are summarized  
612 in the Suppl. tables ST5, ST6, ST7 and ST8 includes the <sup>36</sup>Cl CRE ages calculated  
613 according to different Ca spallation production rates and the distance to the most recent  
614 glacier terminus position mapped. Table 3 includes the <sup>36</sup>Cl CRE ages converted to CE  
615 dates format presented throughout the text. The dates presented below are based on the  
616 Licciardi et al. (2008) Ca spallation production rate.

617 Aiming to obtain a maximum (oldest) age for the onset of the deglaciation in the valleys  
618 studied, two samples (ELLID-1 and ELLID-2) were extracted from the western sector  
619 of Elliði, a 660-m-high glacially polished crest separating Viðinesdalur and  
620 Kolbeinsdalur valleys (Suppl. figure SF5), and located at 11 km downstream from the  
621 confluence of Vesturdalur and Austurdalur valleys. Both samples yielded dates of  
622  $14300 \pm 1700$  BCE and  $14200 \pm 1700$  BCE.

623 In Vesturdalur, 8 samples were collected from 5 moraines corresponding to 5 of the  
624 stages identified on the geomorphological map (Fig. 2). Samples TUW-9 and TUW-10  
625 were taken from two boulders in the moraine that correspond to the left latero-frontal  
626 edge of the glacier during the stage 7, ~1 km from the 2005 CE (stage 17) glacier  
627 terminus (measured along the flowline from the reconstructed terminus apex); they  
628 yielded consistent dates of  $1590 \pm 100$  CE and  $1640 \pm 90$  CE. Samples TUW-11 and  
629 TUW-12 were extracted from the moraines corresponding to the glacial stages 6 and 5,  
630 at 185 m and 465 m downstream respectively (~1.2 km and ~1.5 km respectively from  
631 the 2005 CE snout), and gave consistent dates  $1480 \pm 120$  CE and  $1450 \pm 100$  CE. The  
632 next  $^{36}\text{Cl}$  samples (TUW-13 and TUW-14) were taken from two adjacent moraine  
633 boulders on the left latero-frontal moraine ridge corresponding to the stage 3, at 264 m  
634 downstream (1.8 km from the 2005 CE snout); they yielded dates of  $1470 \pm 130$  CE and  
635  $670 \pm 210$  CE, which are significantly different from each other. The most distant  
636 samples (TUW-15 and TUW-16) were extracted from the stage 2 moraine, ~400 m  
637 downstream from the moraine ridge corresponding to stage 3 (2.2 km from the 2005 CE  
638 terminus). They yielded dates of  $1460 \pm 110$  CE and  $1220 \pm 190$  CE, respectively, that are  
639 consistent with each other and in chronological order with sample TUW-13 from the  
640 stage 3. However, these ages are not in agreement with the oldest date of TUW-14  
641 ( $670 \pm 210$  CE) from the stage 3.

642 Four  $^{36}\text{Cl}$  samples were taken from two prominent moraines in the Austurdalur valley  
643 (Fig. 3). Samples TUE-9 and TUE-10 were collected on the frontal moraine  
644 corresponding to stage 4 (1 km from the 2005 CE glacier terminus) and yield  
645 significantly different dates of  $740\pm 170$  CE and  $1460\pm 100$  CE. Samples TUE-11 and  
646 TUE-12 were taken from two moraine boulders located on the ridge of the left lateral  
647 moraine that records the maximum ice extent (Fig. 3). Their calculated  $^{36}\text{Cl}$  dates,  
648  $380\pm 200$  CE and  $400\pm 200$  CE, are consistent with each other and in stratigraphic order  
649 with the ages from stage 4.

650 The dates derived from Stone et al. (1996) Ca spallation production rate are similar to  
651 those presented above, only 4% older. Those derived from the Schimmelpfennig et al.  
652 (2011) production rate yielded dates older by 15% on average (Suppl. table ST8). These  
653 small differences do not represent statistical difference given the calculated age  
654 uncertainties.

## 655 5. Discussion

656

### 657 5.1. $^{36}\text{Cl}$ CRE dating

658 The dates obtained in both valleys range from  $380\pm 200$  CE to  $1640\pm 90$  CE and are  
659 significantly younger than the ages from Elliði polished ridge (Suppl. table ST8). T UW-  
660 14 ( $670\pm 210$  CE) could be the only outlier as it is significantly older than the other  
661 sample obtained from the same moraine of the stage 3 (T UW-13;  $1470\pm 130$  CE) and  
662 also older than the samples T UW-15 ( $1460\pm 110$  CE) and T UW-16 ( $1220\pm 190$  CE),  
663 from the moraine of the previous stage 2 (Fig. 2). This would imply assuming nuclide  
664 inheritance for sample T UW-14 due to either remobilization of an earlier exposed  
665 moraine boulder (see Matthews et al., 2017) or to previous exposure periods, but the

666 high geomorphological dynamism of the slopes limits this possibility (Andres et al.,  
667 2019). Another possible interpretation is that the samples T UW-15 and T UW-16 (stage  
668 2) would be the outliers since they may have experienced incomplete exposure due to  
669 post-depositional shielding (Heymann, 2011). The possibility of both samples being  
670 affected by proglacial processes can be ruled out given the distance to the meltwaters  
671 channel or the absence of glacial burst features (see Caseldine, 1985a) in the  
672 surroundings of the sampled boulders. Thus, the ages of samples T UW-14 and T UW-13  
673 would indicate that the moraine of stage 3 was built during two overlapped glacial  
674 advances at  $670\pm 210$  CE and  $1470\pm 130$  CE. In Austurdalur, the interpretation of the  
675 ages is also complex. Samples T UE-9 ( $740\pm 170$  CE) and T UE-10 ( $1460\pm 100$  CE) from  
676 the same moraine are significantly different, but it is difficult to decide whether or not  
677 one of these two samples is an outlier. It is also possible that the younger age indicates  
678 the timing of a further readvance with the snout reaching the same moraine. It would be  
679 necessary to take more samples, but it will be difficult to find other sectors of these  
680 moraines that are not affected by slope processes, especially debris-flows. The  
681 hypothesis of supraglacial debris dumping can be rejected due to the lack of supraglacial  
682 debris or other features indicative of a palaeo debris-covered glacier. Other possibility  
683 to be consider is that older boulders may be incorporated in the formation of push  
684 moraines as has been shown in maritime Scandinavia, and identified to give  
685 overestimated ages for LIA-moraines (Matthews et al., 2017). The asynchronicity of  
686 glacial advances and retreat in both valleys should not be surprising as glaciers can  
687 retreat or advance differently in adjacent valleys due to a number of factors such as  
688 hypsometry, aspect, gradient, etc. Caseldine (1985b) suggested a high climate  
689 sensitivity of the glacier in Vesturdalur due to its steeper wally floor and thinness”,  
690 which could explain a different behaviour of the glacier compared to the eastern glacier.

691 *5.1.1. Pre-LIA glacial advances*

692  $^{36}\text{Cl}$  CRE dating results from glacially polished surfaces on the Elliði crest show an age  
693 of  $14250 \pm 1700$  yr (mean) for the Kolbeinsdalur deglaciation ([Suppl. figure SF5](#)).  
694 However, this should be considered as a minimum age since this probably indicates  
695 when the retreating and thinning glacier uncovered the ridge, and thus the start of the  
696 final deglaciation of the main valley. From this point to the outmost frontal moraines  
697 surveyed in this paper, no glacially polished outcrops or erratic boulders suitable for  
698  $^{36}\text{Cl}$  sampling were found, impeding us to provide further chronological constraints for  
699 the deglaciation pattern of these valleys.

700 Our  $^{36}\text{Cl}$  CRE dating results suggest late Holocene glacial advances prior to the LIA, at  
701 around  $\sim 400$  and  $\sim 700$  CE, in Vesturdalur and Austurdalur, respectively, coinciding  
702 with the Dark Ages Cold Period (DACP) (between 400 and 765 CE) in central Europe,  
703 according to [Helama et al. \(2017\)](#). In fact, recent synthesis about Icelandic lake records  
704 indicate a strong decline in temperature at 500 CE ([Geirsdóttir et al., 2018](#)).

705 The presence of Late Holocene moraines outside the outermost LIA moraines in other  
706 valleys of Tröllaskagi has been suggested through radiocarbon dating and  
707 tephrochronology in the Vatnsdalur (first, between  $4880 \pm 325$  cal. BCE (tephra Hekla 5)  
708 and  $3430 \pm 510$  cal. BCE, and another after  $1850 \pm 425$  cal. BCE; [Stötter, 1991](#)),  
709 Lambárdalur (before  $3915 \pm 135$  cal. BCE; [Wastl and Stötter, 2005](#)), Þverárdalur (before  
710  $3500 \pm 130$  cal. BCE; [Wastl and Stötter, 2005](#)), Kóngsstaðadalur (after  $1945 \pm 170$  cal.  
711 BCE; [Wastl and Stötter, 2005](#)), Barkárdalur (between  $375 \pm 375$  cal. BCE and  $190 \pm 340$   
712 cal. CE and before  $460 \pm 200$  cal. CE; [Häberle, 1991](#)) and Bægisárdalur ( $2280 \pm 205$  cal.  
713 BCE and  $1050 \pm 160$  cal. CE; [Häberle, 1991](#)) valleys. Specifically, our oldest  $^{36}\text{Cl}$  dates  
714 ( $\sim 400$  and  $\sim 700$  CE) coincide with glacial advances that are radiocarbon dated from

715 intra-morainic peat bogs in other valleys in Tröllaskagi and southern Iceland, e.g. the  
716 Barkárdalur II stage (ca. 460 CE) in Subatlantic times (Häberle, 1991, 1994), and given  
717 the uncertainties of our dates (200 yr), also with Drangajökull (NW Iceland) advancing  
718 at the same time (~300 CE; Harning et al., 2018). On the other hand, Meyer and Venzke  
719 (1985) had already suggested the presence of pre-LIA moraines at Klængshóll (eastern  
720 cirque, tributary of Skíðadalur). Caseldine (1987, 1991) proposed a date of 5310±345  
721 cal. BCE as the youngest for a moraine in that cirque, based on tephrochronology  
722 (tephra layer Hekla 5 dated in a similar ground in Gljúfurárdalur) and rock weathering  
723 measurements using the Schmidt hammer technique. Based on the big size of some  
724 moraines in Skíðadalur and Holárdalur, Caseldine (1987, 1991) also supports the  
725 hypothesis of pre-LIA moraines formed during several advances. All this information is  
726 not in agreement with the hypothesis that all the glaciers in Tröllaskagi reached their  
727 maximum ice extent since the Early Holocene during the LIA (Hjort et al., 1985;  
728 Caseldine, 1987, 1991; Caseldine and Hatton, 1994).

729 In south and central and northwest Iceland, the ice caps reached their Late Holocene  
730 maximum advance during the LIA (Brynjólfsson, et al. 2015a; Larsen et al. 2015;  
731 Harning et al., 2016a; Anderson et al., 2018; Geirsdóttir et al., 2018). But also pre-LIA  
732 advances have been identified and dated through radiocarbon and tephrochronology in a  
733 moraine sequence of Kvíárjökull (south-east Vatnajökull), the first of which occurred at  
734 Subatlantic times (before 110±240 cal. BCE) and the second at 720±395 CE (Black,  
735 1990; cited in Guðmundsson, 1997). Considering the uncertainty of our ~400 and ~700  
736 CE dates, these advances likely were coetaneous with other advances reported from  
737 southern Iceland in Kötlujökull (after 450±100 cal. CE, radiocarbon dated and  
738 supported by tephrochronology; Schomaker et al., 2003) and Sólheimajökull (southern  
739 Mýrkdalsjökull, “Ystagil stage”; Dugmore, 1989). In fact, the 669±211 CE advance of

740 western Tungnahryggsjökull (stage 3) also overlaps with the Drangajökull and  
741 Langjökull advances at ~560 CE and 550 CE, respectively (Larsen et al., 2011; Harning  
742 et al., 2016a) during DACP, in response to the summer cooling between ~250 CE and  
743 ~750 CE (Harning et al., 2016a). These advances would correspond to the general  
744 atmospheric cooling in the North Atlantic reflected by widespread glacier advances  
745 (Solomina et al., 2016).

746 The timing of the stage 2 in Vesturdalur is difficult to define because the sample TUW-  
747 16 (1220±190 CE) has almost 200-year uncertainty, and thus overlaps with both the  
748 LIA and the higher temperatures of the Medieval Warm Period (MWP, Lamb, 1965; 950-  
749 1250 CE, see Solomina et al., 2016) not conducive to glacier development as it has been  
750 observed in northwest and central Iceland (Larsen et al., 2011; Harning et al., 2016a).  
751 On the other hand, moraines in Greenland Arctic environments date within the MWP,  
752 based on cosmogenic nuclide dating (Young et al., 2015; Jomelli et al., 2016),  
753 suggesting a cooling in the western North Atlantic while the eastern sector remained  
754 warm. Iceland is located in the middle of this dipole “see-saw” pattern (Rogers and van  
755 Loon, 1979). Thus, the correlations with the glacier fluctuations Greenland or Norway,  
756 are complicated as the climate anomalies in both regions show opposing signs in the  
757 different see-saw modes. To increase the difficulty of interpretation, glaciers of  
758 Tröllaskagi are known to surge occasionally (Brynjólfsson et al., 2012; Ingólfsson et al.,  
759 2016), which could explain additional complexity in the glacial advances pattern, as it  
760 would not be driven by climatic variability. Brynjólfsson et al. (2012) pointed out that  
761 only four surges from three glaciers (Teigarjökull, Búrfellsjökull, Bægisárjökull) have  
762 been reported in the Tröllaskagi peninsula, where over 160 cirque glaciers exist.

763 *5.1.2. LIA glacial advances (15<sup>th</sup>-17<sup>th</sup> centuries)*

764 The remaining  $^{36}\text{Cl}$  ages obtained from Vesturdalur and Austurdalur are within the  
765 1450-1640 CE range (Suppl. table ST8; Table 3) and so correspond to different glacial  
766 advances or standstills during the second third of the LIA during the 15<sup>th</sup>, 16<sup>th</sup> and 17<sup>th</sup>  
767 centuries. According to our results, one of the largest glacier extents of the LIA  
768 culminated in both valleys at the latest around the mid-15<sup>th</sup> century (samples: TUW-12:  
769 1450±100 CE / stage 6; TUE-10: 1460±100 CE / stage 4). This is a very early date  
770 compared to the LIA advances previously dated in Tröllaskagi. Earlier lichenometric  
771 research carried out in nearby valleys report more recent dates for the LIA maximum:  
772 mid-18<sup>th</sup> century in Barkárdalur (Häberle, 1991); early 19<sup>th</sup> century in Bægisárjökull and  
773 Skríðudalur (Häberle, 1991), and in Búrfellsdalur and Vatnsdalur (Kugelmann, 1991,  
774 Fig. 7); mid-19<sup>th</sup> century (1845-1875 CE) in Myrkárjökull, Vindheimajökull (Häberle,  
775 1991), Þverárdalur, Teigardalur, Grýtudalur, Vesturárdalur (Kugelmann, 1991, Fig. 7),  
776 Heiðinnamannadalur and Kvarnárdalur (Caseldine, 1991); and late 19<sup>th</sup> century (1880s-  
777 1890s CE) in Gljúfurárdalur (Caseldine, 1985b, 1991). Caseldine (1991) proposed  
778 1810-1820 CE as the date of the “outer” moraine of Vesturdalur based on a minimum  
779 lichenometric age. According to our  $^{36}\text{Cl}$  moraine ages, the LIA maximum of  
780 Tungnahryggjökull glaciers occurred ~400 years earlier than these dates. This should  
781 not be surprising as Kirkbride and Dugmore (2001) reported lichenometric ages >100  
782 years younger than those derived from tephrochronology in the same landforms. Our  
783 results also give the earliest LIA dates based on moraine dating obtained so far in  
784 Iceland, compared to the previously published dates all obtained through lichenometric  
785 dating: 1740-1760 CE in south-east Iceland (Chenet et al., 2010). In northwestern  
786 Iceland, glaciolacustrine sediments recorded a contemporary expansion of Drangajökull  
787 at ~1400 CE (Harning et al., 2016a). Likewise a first major advance of Langjökull  
788 (western central Iceland; Fig. 1A) between 1450 and 1550 CE has been reported (Larsen

789 [et al., 2011](#)), as well as advances in central Iceland between 1690 and 1740 CE  
790 ([Kirkbride and Dugmore, 2006](#)), based on varve thickness variance together with annual  
791 layer counting and C:N mass ratio, and tephrochronology (geochemical analysis),  
792 respectively.

793 The dates of samples TUV-13, TUV-12 and TUV-11 in Vesturdalur (average date  
794  $1470 \pm 120$  CE; stages 3, 5 and 6) cannot be distinguished statistically if their internal  
795 uncertainty is considered ([Fig. 4](#); [Suppl. table ST8](#)). The spatial scatter of these  
796 sampling sites ([Fig. 2](#)) may indicate frequent and intense terminus fluctuations in a short  
797 time interval. Different ages obtained from the moraines of the stages 3 and 4 in  
798 Vesturdalur and Austurdalur, respectively, may indicate that in the 15<sup>th</sup> century the  
799 glacier termini reached the moraines deposited at  $\sim 700$  CE ([Figs. 2 and 3](#)) and rebuilt  
800 them, which may explain the large size of these moraines. [Caseldine \(1987\)](#) argued that  
801 other moraines in Skíðadalur were formed during more than one advance. Based on the  
802 size of the largest moraines, he also pointed out that many glaciers must have advanced  
803 to positions similar to those of the late 19<sup>th</sup> century earlier in the Neoglacial.

804 The glacier advances in the 15<sup>th</sup> century in Vesturdalur and Austurdalur may have been  
805 the result of different climate forcings during that century: negative radiative forcing  
806 and summer cooling were linked to intense volcanic activity ([Miller et al., 2012](#)), the  
807 low solar activity of the Spörer Minimum (1460-1550 CE; [Eddy, 1976](#)), the sea-  
808 ice/ocean feedback with increased sea ice ([Miller et al., 2012](#)) and the weakening of the  
809 Atlantic Meridional Overturning Circulation (AMOC) ([Zhong et al., 2011](#)). Solar  
810 activity may have played a major role in these glacial advances if we consider that the  
811 climate in the North Atlantic is highly influenced by solar activity variability ([Jiang et al.,](#)  
812 [2015](#)). On the contrary, historical records, although not determinant, suggest a mild  
813 climate for 1430-1550 CE ([Ogilvie and Jonsdóttir, 2000](#)), and especially for 1412-1470

814 CE (Ogilvie, 1984). This would also be compatible with increased precipitation and  
815 hence more winter snow in warm periods (Caseldine and Stötter, 1993; Stötter et al.,  
816 1999; Fernández-Fernández et al., 2017), and also with potential surge activity with  
817 glacial advances not directly linked to specific climate periods (e.g. Brynjólfsson et al.,  
818 2012; Ingólfsson et al., 2016).

819 In Vesturdalur, the dates of samples TUW-9 (1590±100 CE) and TUW-10 (1640±90  
820 CE) are compatible with a cold period from the late 1500s to 1630 CE (Ogilvie and  
821 Jónsson, 2001). Nevertheless, considering the uncertainties of these samples, their dates  
822 also overlap with the Maunder Minimum (1645-1715 CE) (Eddy, 1976), when the LIA  
823 maximum glacial advance occurred in the Alps (Holzhauser et al., 2005).

## 824 *5.2. Lichenometric dating.*

### 825 *5.2.1. <sup>36</sup>Cl CRE dating vs. lichenometric dating. Multiple lichen species dating* 826 *approach.*

827 The contrast between our CRE dating results and earlier lichenometry-based results  
828 published elsewhere evidences the clear underestimation of the latter. This could be  
829 explained either by lichen growth inhibition due to saturation of the rock surface and  
830 competition of other thalli (Wiles et al., 2010; Le Roy et al., 2017) or a colonization lag  
831 longer than assumed up to now, from 10 to 15 years in Tröllaskagi (Kugelmann, 1991;  
832 Caseldine, 1985b, respectively). However, other factors affect the reliability of the  
833 lichen-derived ages, and may explain the differences with CRE dates. One of them is  
834 the reliability of the growth rates and lichenometric calibration curves that are  
835 commonly assumed to be linear (constant) growth in northern Iceland (e.g. Caseldine,  
836 1983, 1985b; Häberle, 1991; Kugelmann, 1991), although it has been demonstrated that  
837 the lichen diameter growth declines with age (see e.g. Winkler, 2003, Fig. 4). This

838 might lead to significant age underestimations for the oldest dates, putting potentially  
839 earlier dates in the 19<sup>th</sup> century. Most of the fixed control points from which lichen  
840 growth rates have been derived in northern Iceland comprise abandoned gravestones,  
841 memorial stones, old bridges and mostly abandoned farmsteads (Caseldine, 1983;  
842 Kugelmann, 1991). Time of death is commonly assumed for gravestones, and  
843 abandonment date for farmsteads. Although the latter is well known on the basis of  
844 historical documentation, the colonization lag sometimes relies on the “the likely  
845 duration” of the deterioration of the buildings after abandonment that depends on the  
846 quality and stability of the constructions (see Kugelmann, 1991), and hence affect the  
847 results. However, it should be highlighted that our approach circumvents this last issue  
848 by combining field observations with historical aerial photographs. In addition, given  
849 that lichen growth of *Rhizocarpon* subgenus depends mostly on available humidity, the  
850 location of the measured lichens has also a potential effect on the results, i.e. to micro-  
851 climatic changes (see Innes, 1985; Hamilton and Whalley, 1995) between the location  
852 of the fixed points and the location on the moraine (crest: dryer and more exposed;  
853 green zone on the proximal slope, etc.). In the literature cited above about lichenometry-  
854 dated LIA advances no detailed information is provided about the location of the lichen  
855 measured for dating purposes, so potential error derived from this issue can not be  
856 assessed. Nevertheless, given that we measured lichens on horizontal flat surfaces  
857 where there is no restriction to the moisture receipt of the lichens, we can consider our  
858 results presented throughout the next sections valid. In any case, such a great difference  
859 of our CRE dates and the previous lichen-derived is more likely to be explained by the  
860 technical limitations of the technique rather than environmental factors.

861 Our field observations and historical aerial photos of known age restricted the dates of  
862 the moraines colonized by *Rhizocarpon geographicum* lichens. This approach would

863 support the dates obtained from the 0.44 mm yr<sup>-1</sup> growth rate of Kugelmann (1991) and  
864 the 20-year colonization lag. This rate is slightly higher than those reported from the  
865 Antarctic Peninsula (0.31 mm yr<sup>-1</sup>; Sancho et al., 2017), but lower than in Tierra del  
866 Fuego (0.63 mm yr<sup>-1</sup>; Sancho et al., 2011). The correlation between the sizes of largest  
867 *Rhizocarpon geographicum* and *Porpidia* cf. *soredizodes* thalli at the same stations  
868 showed a proportionality between the largest thalli of both species: thalli of *Porpidia* cf.  
869 *soredizodes* species grow faster than those of *Rhizocarpon geographicum*. The sizes of  
870 the largest *Rhizocarpon geographicum* thalli were plotted against the sizes of the largest  
871 *Rhizocarpon geographicum* lichens (Fig. 5). The slope of the best-fit linear curve  
872 obtained was around 1.675 (r<sup>2</sup>=0.82) that suggests that *Porpidia* cf. *soredizodes* lichens  
873 grow 1.675 times faster than those of *Rhizocarpon geographicum*. So if we assume 0.44  
874 mm yr<sup>-1</sup> growth rate for *Rhizocarpon geographicum* lichens, a tentative growth rate of  
875 *Porpidia* cf. *soredizodes* would be 0.737 mm yr<sup>-1</sup>. However, this approach should be  
876 taken with caution due to the limited number of lichens (n=7) used of each species.  
877 Aiming to obtain a tentative date (Table 2), this growth rate was applied to the largest  
878 *Porpidia* cf. *soredizodes* lichens found in those stations where no *Rhizocarpon*  
879 *geographicum* lichens could be measured (TUW-1, TUW-8, TUE-1 and TUE-8).

880 Assuming colonization lags of 20 and 15 years for *Rhizocarpon geographicum* and  
881 *Porpidia* cf. *soredizodes* lichens, respectively, and the above-mentioned growth rates,  
882 several glacial advances or standstills are tentatively placed in the 19<sup>th</sup> and 20<sup>th</sup>  
883 centuries, in the context of a general retreat from the most advanced LIA positions, as  
884 discussed in the next section.

#### 885 5.2.2. LIA glacial advances/standstills: 19<sup>th</sup> century

886 Despite the low number of lichenometry stations surveyed and the limitations of this  
887 dating approach discussed in the previous sections, our results are in accordance with

888 the geomorphological logic and with the chronological frame obtained from historical  
889 aerial photos. The ages derived from *Rhizocarpon geographicum* thalli measurements at  
890 lichenometry stations pre-dating 1946 suggest that the western and eastern  
891 Tungnahryggsjökull culminated successive advances/standstills around the 1830s,  
892 1840s, 1860s and 1890s CE (Figs. 2 and 3, Table 2). Ages tentatively estimated from  
893 *Porpidia* cf. *soredizodes* thalli considering its apparently higher growth rate suggest  
894 glacial advances/standstills around the 1800s (Figs. 2 and 3, Table 2). No inconsistency  
895 (age inversions) is detected in the lichenometry-dated moraine sequence, but we  
896 recognise that some age underestimation may occur since: (i) we assume linear growth  
897 when applying a growth rate; and (ii) our 19<sup>th</sup> dates were derived from >40-45 mm-  
898 diameter lichens (Table 2 and Suppl. table ST4), which exceed the size of the biggest  
899 control point from which Kugelmann's growth rate was estimated (Kugelmann, 1991,  
900 Fig. 3). This problem reinforces the need of taking lichen-derived ages as relative. The  
901 interpretation of the chronology in Austurdalur is more complicated: the lichen sizes  
902 measured at the stations TUE-6 (1890s CE, stage 9) and TUE-7 (1880s CE; stage 7)  
903 yield more recent dates than at station TUE-5 (1860s CE; stage 10) despite being  
904 representative of earlier stages (Fig. 3). Given that this anomaly occurs in both lichen  
905 species, it is reasonable to conclude that an environmental factor could have affected the  
906 lichen populations at both stations. It could even indicate a date when the boulders may  
907 have been remobilized by postglacial processes.

908 Our chronology of the 19<sup>th</sup> century glacial advances in both valleys (Table 2) does not  
909 coincide exactly with the phases identified by Kugelmann (1991) in Svarfaðardalur-  
910 Skíðadalur (1810, 1850, 1870-1880, 1890-1900 CE). It also differs appreciably from the  
911 chronology proposed by Caseldine (1985b) in Vesturdalur (moraines of 1868, 1878,  
912 1887, 1898 CE). Nevertheless, it should be borne in mind that we are considering only

913 two glaciers with their own glaciological properties. Moreover, we have estimated the  
914 ages from the growth rate (instead of a specific calibration growth curve), longer  
915 colonization lag based on field observations, and applied to the longest axis  
916 measurements ([Kugelmann, 1991](#)). On the other hand, micro-climatic differences  
917 between the location of fixed points and our lichen measured may occur. However, we  
918 recognise that the comparisons with [Caseldine's \(1985b\)](#) results are quite difficult since:  
919 (i) the moraines dated by Caseldine are poorly located in his mapping (and hard to  
920 identify over aerial photos and our moraine mapping); (ii) we are not able to apply the  
921 same parameters to his measurements, as he used the mean longest axis of the five  
922 largest lichen is not provided (only the average value); and (iii) he recognised the lichen  
923 growth slowdown when dating the outermost moraine, which probably is one of those  
924 dated with  $^{36}\text{Cl}$  in this work.

925 Our results, despite the limitations of the applied method, largely due to the low number  
926 of moraine boulders suitable for its application can be considered compatible and in  
927 good agreement with glacial advances and cold periods during the first third of the 19<sup>th</sup>  
928 century as we show below. [Martin et al. \(1991\)](#) pointed out the existence of a moraine  
929 dated to ca. 1810-1820 CE in “Western Tröllaskagi Tungnahryggsjökull” (ambiguously,  
930 without providing any detail of its location), as well as others of this period in  
931 Svarfaðardalur, Búrfellsdalur and Vatnsdalur. Other dates obtained from more  
932 sophisticated statistical techniques applied to lichenometry dating procedures also  
933 evidenced a glacial advance phase 1810-1820 CE ([Chenet et al., 2010](#)). These advance  
934 phases were coetaneous with significant sea ice persistence in the early 1800s ([Ogilvie  
935 and Jónsson, 2001](#)), decreased solar activity, and strong volcanic eruptions (Dalton  
936 Minimum, 1790-1830 CE; [Wagner et al., 2005](#)). The moraines dated in Vesturdalur to  
937 around 1830 CE (TUW-7: 1830s CE, stage 10) and the early 1890s CE (TUW-5: 1890s

938 CE, stage 12) are in good agreement with the glacial advances in Svarfaðardalur-  
939 Skíðadalur during the 1830s and early 1890s CE (Kugelmann, 1991, Fig. 8), as well as  
940 with the low temperatures and presence of sea ice at these dates (Koch, 1945; Ogilvie,  
941 1996; Ogilvie and Jonsdóttir, 2000; Ogilvie and Jónsson, 2001; Kirkbride, 2002).

#### 942 5.2.3. Post-LIA glacial advances/standstills.

943 Lichen-derived ages from *Rhizocarpon geographicum* thalli suggest the occurrence of  
944 glacial advances or standstills at the first half of the 20<sup>th</sup> century, culminating in 1910s,  
945 1930s, 1940s and 1950s CE, although the 1930s CE date (TUE-3; stage 12) disagrees  
946 with the date inferred from the aerial photos, at some point between 1946 and 1985 CE  
947 (Suppl. figure SF2; Table 2). However, the 1910s CE date in both valleys is in good  
948 agreement with the moraine abandonment during the first two decades of the 20<sup>th</sup>  
949 century; it would be the result of the accumulated effect of the temperature rise since the  
950 latter half of the 19<sup>th</sup> century (Caseldine, 1987; Wanner et al., 2008). Thus, the  
951 subsequent advances would be the response to specific relative thermal minima within a  
952 warmer climate (Stötter et al., 1999). The date of TUW-3 (stage 13) representing the  
953 moraine abandonment in ~1940 CE is in agreement with the overall context of general  
954 glacier retreat as a result of the warmest decades of the 1930s and 1940s CE, which  
955 triggered an intense retreat of the glaciers (Einarsson, 1991; Martin et al., 1991;  
956 Kirkbride, 2002). The advances/standstills dated to the early 1950s CE in both  
957 Tungnahryggsjökull glaciers are likely to be synchronous given the similarity of the  
958 dates obtained (Table 2). They could represent glacial advances in consonance with the  
959 late 1940s – early/mid-1950s CE cooling (Einarsson, 1991; Fernández-Fernández et al.,  
960 2017), recorded both in Akureyri and many other weather stations throughout Iceland.  
961 Caseldine (1983) found a similar chronology in Gljúfurárdalur (Skíðadalur headwater,

962 10 km to the east), with moraine deposition between mid-1910s and 1930, around mid-  
963 1930s and late 1940s-1950 CE.

964 The subsequent trend of the Tungnahryggsjökull glaciers, inferred from aerial  
965 photographs, a satellite image, geomorphological mapping, and glacier reconstruction,  
966 was characterized by continuous retreat and volume loss, in line with the increasing  
967 temperature trend since the end of the LIA. This trend was only reversed between the  
968 mid-1960s and mid-1980s CE by a major cooling event (Einarsson, 1991; Sigurðsson,  
969 2005; Fernández-Fernández et al., 2017). Two moraines have been dated after the 1950s  
970 CE. The date obtained in station TUE-1 (1970s CE; stage 14) agrees with the date  
971 deduced from the 1946 and 1985 aerial photographs (Suppl. figure SF2). However, the  
972 date estimated in station TUW-1 (1970s CE; between stages 15 and 16) is prior to that  
973 obtained from the 1994 and 2000 aerial photographs. The reason for this mismatch may  
974 be a non-linear growth phase of the *Porpidia* cf. *soredizodes* thalli measured (i.e. its real  
975 growth rate may have been lower than the estimated). Nevertheless, more research on  
976 this species is required to use it successfully in lichenometric dating.

977 The aerial photographs from 1994 (stage 15 western Tungnahryggsjökull) and 2000  
978 (stage 16) show a reversal in the trend of both Tungnahryggsjökull glaciers (Suppl.  
979 figure SF2), as the positions of their termini are more advanced than in 1985 (stages 14  
980 and 15; see Fernández-Fernández et al., 2017). These advances in Vesturdalur and  
981 Austurdalur, culminating after 1985 in a period non-conducive to glacier expansion,  
982 may have been linked to above average precipitation for 1988-1995, which prevented a  
983 negative mass balance of the glaciers (Sigurðsson, 2005). The 2000 aerial photo (stage  
984 16) and 2005 SPOT satellite image (stage 17) display the retreat of both glaciers. This  
985 trend was reinforced by the sudden warming initiated in 1995, which triggered  
986 decreased snowfall, negative mass balances for 1996-2000, and retreat of the non-

987 surging glaciers after 2000 (Sigurðsson, 2005). In spite of these glacial fluctuations in  
988 response to the intense climatic fluctuations of the last century, the ELAs estimated in  
989 this paper only show a general rise of 5-10 m (Table 1). This small ELA increase may  
990 be derived from some artifacts of the glacier reconstruction or the attenuating effect of  
991 the increase in winter precipitation suggested by glacier-climate models (Caseldine and  
992 Stötter, 1993; Fernández-Fernández et al., 2017).

993 *5.3. Final remarks: Can the occurrence of pre-LIA glacial advances be confirmed? Was*  
994 *the LIA in northern Iceland the Holocene glacial maximum? Was it a single maximum*  
995 *advance?*

996 Our results demonstrate that Tungnahryggsjökull advanced during Late Holocene glacial  
997 stages prior to the LIA and reached considerably more advanced positions, even though  
998 the Iceland large ice caps reached generally their Late Holocene maximum advance  
999 during the LIA (Larsen et al. 2015, Harning et al., 2016a; Anderson et al., 2018,  
1000 Geirsdóttir et al., 2018). The chronological data presented in the previous sections  
1001 suggests that during the LIA the glaciers overlapped moraines deposited in pre-LIA  
1002 glacial stages. Our results also show LIA advances since the 15<sup>th</sup> century and are thus  
1003 contrary to the traditional proposal of a single maximum LIA advance occurring during  
1004 either mid-18<sup>th</sup> or late-19<sup>th</sup> centuries in Tröllaskagi peninsula, followed by subsequent  
1005 minor readvances in an overall retreating trend (see Caseldine, 1983, 1985b, 1987;  
1006 Kugelmann, 1991; Martin et al., 1991). The use of the <sup>36</sup>Cl production rates from Ca  
1007 spallation reported by Stone et al. (1996) does not lead to major changes in the  
1008 interpretation and conclusions as the changes in the nominal dates (up to 90 yr earlier;  
1009 Table 3) are within the external uncertainty and also overlap with the results presented  
1010 above based on the Licciardi et al. (2008) production rate. Similarly, if we consider the  
1011 results derived by the Schimmelpfennig et al. (2011) production rate, we obtain even

1012 earlier ages, which still overlap with the results derived by the other production rates  
1013 due to a higher external uncertainty (see [Table 3](#)). Although the snow cover duration is  
1014 known to be high in northern Iceland (see [Dietz et al., 2012](#)), quantifying the effect of  
1015 snow cover on sub-surface  $^{36}\text{Cl}$  production is a complex issue: on the one side, snow  
1016 lowers the isotopic production rates related to spallation reactions due to the shielding  
1017 effect on high-energy neutrons ([Benson et al., 2004](#); [Schildgen et al., 2005](#)), and on the  
1018 other side it increases the  $^{36}\text{Cl}$  production rate from thermal neutrons below the rock  
1019 surface, due to the enhancing effect of hydrogen on these low-energy neutrons ([Dunai et](#)  
1020 [al., 2014](#)). Both effects might cancel out depending on the composition of the samples,  
1021 and their quantification is still debated and affected by high uncertainties ([Zweck et al.,](#)  
1022 [2013](#); [Dunai et al., 2014](#); [Delunel et al., 2014](#)). Given this complexity, snow shielding  
1023 was not applied. In any case its effect is unlikely to be higher than the uncertainty  
1024 derived from extracting  $^{36}\text{Cl}$  from whole rock instead of minerals.

1025 Our results are in concordance with several valleys in northern Iceland, but also with the  
1026 results that are being obtained in other sectors of Arctic and North Atlantic region in the  
1027 last years, such as: in Baffin Island (northern Canada), where glaciers reached Late  
1028 Holocene maximum positions prior to the LIA ([Young et al., 2015](#);  $^{10}\text{Be}$  dating), or  
1029 West Greenland, with several advances or stabilizations at  $1450\pm 90$  CE and  $1720\pm 60$   
1030 CE ([Jomelli et al., 2016](#);  $^{36}\text{Cl}$  dating). However, it is striking that the early LIA  
1031 advances of northern Iceland reported in the present paper do not agree with maritime  
1032 Norway with later maximum culminations (see [Nesje et al., 2008](#)) despite being the  
1033 glaciated region most comparable with Iceland in terms of climate and glaciology. Our  
1034 results also agree with farther and southern areas such as the Alps, with maximum  
1035 advances at around 1430 CE ([Schimmelpfennig et al., 2012, 2014a](#));  $^{10}\text{Be}$  dates; and  
1036 Sierra Nevada (Iberian Peninsula), where LIA advances have been reported between the

1037 14<sup>th</sup> and 17<sup>th</sup> centuries (Palacios et al., 2019; <sup>10</sup>Be dates). Our detailed moraine  
1038 mapping, combined with CRE dating in the surveyed valleys, clearly shows a number of  
1039 advances throughout the LIA, in response to the great climatic variability of the region  
1040 with alternating cold and mild/warm periods (Ogilvie, 1984, 1996; Ogilvie and  
1041 Jónsdóttir, 2000; Ogilvie and Jónsson, 2001; Geirsdóttir et al., 2009) as occurred in the  
1042 Alps (e.g. Schimmelpfennig et al., 2014a) or the Iberian mountains (e.g. Oliva et al.,  
1043 2018). The ELA calculations show that the major long-lasting rise of the glacier ELA  
1044 (24-50 m depending on the calculation method) took place prior to 1900s/1910s.

1045 According to the results, the evolution pattern described by Fernández-Fernández et al.  
1046 (2017) for the Tungnahryggsjökull glaciers should be revised as the <sup>36</sup>Cl CRE dates  
1047 from the 15<sup>th</sup> and 17<sup>th</sup> centuries indicate that LIA maximum was reached earlier than  
1048 previously thought. Thus, if we consider the ELA of the earliest LIA dates obtained  
1049 with <sup>36</sup>Cl CRE (i.e. stages 5 and 4 of western and eastern Tungnahryggsjökull), these  
1050 imply ELA depressions (with reference to the 2005 date) of 24-50 m (depending on the  
1051 ELA calculation method), occurring for at least 560 years (Table 1) and not 150 years as  
1052 had been previously assumed (Caseldine and Stötter, 1993; Fernández-Fernández et al.,  
1053 2017).

## 1054 **Conclusions**

1055 (i) This paper highlights the detailed geomorphological analysis of the glacial landforms  
1056 as an essential pre-requisite prior to the application of dating methods on them.  
1057 Nevertheless, this has greatly limited the number of valid moraine boulders to be dated,  
1058 since the vast majority of those were affected by post-glacial processes. This issue which  
1059 has prevented a statistically acceptable sampling and the validation or invalidation of  
1060 the “inconsistent” ages yielded by several boulders, so a conclusive explanation cannot  
1061 be given.

1062 (ii) Applying  $^{36}\text{Cl}$  CRE dating for the first time in the Tröllaskagi peninsula enabled us  
1063 to identify pre-LIA glacial advances in Vesturdalur and Austurdalur. Thus, the western  
1064 and eastern Tungnahryggsjökull glaciers did not reach their Late Holocene maximum  
1065 extent during the LIA. The maximum extent for the eastern glacier was dated to ~400  
1066 CE. For the western glacier a latest date of ~700 CE and an earliest of 16300 years ago  
1067 (when the Elliði crest was deglaciated) have been obtained.

1068 (iii) The LIA maximum in Vesturdalur and Austurdalur was reached by the 15<sup>th</sup> century  
1069 at the latest. A combination of detailed moraine mapping and  $^{36}\text{Cl}$  CRE dating confirm a  
1070 number of glacial advances between the 15<sup>th</sup> and 17<sup>th</sup> centuries, the earliest LIA  
1071 advances dated in Tröllaskagi at present.

1072 (iv) For the recent dates, the complementary use of aerial photographs, a satellite image  
1073 and fieldwork has aided to obtain lichenometry-derived ages tentatively in good  
1074 agreement with the morpho-stratigraphic order of the glacial landforms. It has also  
1075 compensated some of the limitations and error sources of lichenometric dating. Thus, it  
1076 has proved to be a useful tool to assess the colonization lags and the validity of the  
1077 lichenometry-derived ages.

1078 (v) Fieldwork on recently deglaciated surfaces and historical aerial photographs have  
1079 shown clearly that the colonization lag of *Rhizocarpon geographicum* lichen species is  
1080 from 15-21 to 30 years, considerably longer than previously assumed in Tröllaskagi.  
1081 Colonization of the *Porpidia* cf. *soredizodes* species is shorter, between 10 and 21  
1082 years.

1083 (vi) From the measurements carried out in different lichenometry stations, growth of  
1084 *Porpidia* cf. *soredizodes* lichen appeared to be higher than in the case of *Rhizocarpon*  
1085 *geographicum*, and also proportional to that. Its growth rate has been tentatively

1086 estimated for the first time, at around 0.737 mm yr<sup>-1</sup>. However, further research on the  
1087 growth rates of this species is required for its potential use in lichenometric dating as a  
1088 complementary species, since it also shows a shorter colonisation lag than *Rhizocarpon*  
1089 *geographicum*.

## 1090 **Acknowledgements**

1091 This paper was supported by the project CGL2015-65813-R (Spanish Ministry of  
1092 Economy and Competitiveness) and Nils Mobility Program (EEA GRANTS), and with  
1093 the help of the High Mountain Physical Geography Research Group (Complutense  
1094 University Madrid). We thank the Icelandic Association for Search and Rescue, the  
1095 Icelandic Institute of Natural History, the Hólar University College, and David Palacios  
1096 Jr. and María Palacios for their support in the field. José M. Fernández-Fernández  
1097 received a PhD fellowship from the FPU programme (Spanish Ministry of Education,  
1098 Culture and Sport; reference FPU14/06150). The <sup>36</sup>Cl measurements were performed at  
1099 the ASTER AMS national facility (CEREGE, Aix en Provence), which is supported by  
1100 the INSU/CNRS and the ANR through the "Projets thématiques d'excellence" program  
1101 for the "Equipements d'excellence" ASTER-CEREGE action and IRD.

## 1102 **References**

- 1103 Anderson, L.S., Flowers, G.E., Jarosch, A.H., Aðalgeirsdóttir, G.T., Geirsdóttir, Á.,  
1104 Miller, G.H., Harning, D.J., Thorsteinsson, T., Magnússon, E., Pálsson, F., 2018.  
1105 Holocene glacier and climate variations in Vestfirðir, Iceland, from the modeling of  
1106 Drangajökull ice cap. *Quat. Sci. Rev.* 190, 39–56.  
1107 doi:10.1016/j.quascirev.2018.04.024
- 1108 Andrews, J.T., Giraudeau, J., 2003. Multi-proxy records showing significant Holocene  
1109 environmental variability: the inner N. Iceland shelf (Húnaflói). *Quat. Sci. Rev.* 22,  
1110 175–193. doi: 10.1016/S0277-3791(02)00035-5
- 1111 Andrés, N., Palacios, D., Sæmundsson, Þ., Brynjólfsson, S., Fernández-Fernández, J.M.,  
1112 2018. The rapid deglaciation of the Skagafjörður fjord, northern Iceland. *Boreas*.  
1113 doi:10.1111/bor.12341

- 1114 Andrés, N., Tanarro, L.M., Fernández, J.M., Palacios, D., 2016. The origin of glacial  
1115 alpine landscape in Tröllaskagi Peninsula (North Iceland). *Cuad. Investig.*  
1116 *Geográfica* 42, 341–368. doi:10.18172/cig.2935
- 1117 Arróniz-Crespo, M., Pérez-Ortega, S., De Los Ríos, A., Green, T.G.A., Ochoa-Hueso,  
1118 R., Casermeiro, M.Á., De La Cruz, M.T., Pintado, A., Palacios, D., Rozzi, R.,  
1119 Tysklind, N., Sancho, L.G., 2014. Bryophyte-cyanobacteria associations during  
1120 primary succession in recently deglaciated areas of Tierra del Fuego (Chile). *PLoS*  
1121 *One* 9, 15–17. doi:10.1371/journal.pone.0096081
- 1122 Barker, S., Knorr, G., Vautravers, M.J., Diz, P., Skinner, L.C., 2010. Extreme  
1123 deepening of the Atlantic overturning circulation during deglaciation. *Nat. Geosci.*  
1124 3, 567–571. doi:10.1038/ngeo921
- 1125 Benn, D.I., Hulton, N.R.J., 2010. An Excel™ spreadsheet program for reconstructing  
1126 the surface profile of former mountain glaciers and ice caps. *Comput. Geosci.* 36,  
1127 605–610. doi:10.1016/j.cageo.2009.09.016
- 1128 Benson, L., Madole, R., Phillips, W., Landis, G., Thomas, T., Kubik, P., 2004. The  
1129 probable importance of snow and sediment shielding on cosmogenic ages of north-  
1130 central Colorado Pinedale and pre-Pinedale moraines. *Quat. Sci. Rev.* 23, 193–206.  
1131 doi:10.1016/j.quascirev.2003.07.002
- 1132 Bergþórsson, P., 1969. An Estimate of Drift Ice and Temperature in Iceland in 1000  
1133 Years. *Jökull* 19, 94-101.
- 1134 Bickerton, R.W., Matthews, J.A., 1992. On the accuracy of lichenometric dates: an  
1135 assessment based on the “Little Ice Age” moraine sequence of Nigardsbreen,  
1136 southern Norway.” *Holocene* 2, 227–237. doi:10.1177/095968369200200304
- 1137 Björnsson, H., 1978. Surface area of glaciers in Iceland. *Jökull* 28, 31.
- 1138 Black, T.A., 1990. The Holocene fluctuation of the Kvíárjökull glacier, southeastern  
1139 Iceland. Unpublished MA thesis. University of Colorado.
- 1140 Bradwell, T., 2004a. Lichenometric dating in southeast Iceland: The size- frequency  
1141 approach. *Geogr. Ann. Ser. A Phys. Geogr.* 86, 31–41. doi:10.1111/j.0435-  
1142 3676.2004.00211.x
- 1143 Bradwell, T., 2004b. Annual Moraines and Summer Temperatures at  
1144 Lambatungnajökull, Iceland. *Arctic, Antarct. Alp. Res.* 36, 502–508.  
1145 [https://doi.org/10.1657/1523-0430\(2004\)036\[0502:AMASTA\]2.0.CO;2](https://doi.org/10.1657/1523-0430(2004)036[0502:AMASTA]2.0.CO;2)
- 1146 Bradwell, T., 2001. A new lichenometric dating curve for Southeast Iceland. *Geogr.*  
1147 *Ann. Ser. A Phys. Geogr.* 83, 91–101. doi:10.1111/j.0435-3676.2001.00146.x
- 1148 Bradwell, T., Armstrong, R.A., 2006. Growth rates of *Rhizocarpon geographicum*  
1149 lichens: a review with new data from Iceland. *J. Quat. Sci.* 22, 311–320.  
1150 doi:10.1002/jqs.1058

- 1151 Brugger, K.A., 2006. Late Pleistocene climate inferred from the reconstruction of the  
1152 Taylor River glacier complex, southern Sawatch Range, Colorado. *Geomorphology*  
1153 75, 318–329. doi:10.1016/j.geomorph.2005.07.020
- 1154 Brynjólfsson, S., Ingólfsson, Ó., Schomacker, A., 2012. Surge fingerprintings of cirque  
1155 glaciers at Tröllaskagi peninsula, North Iceland. *Jökull* 62, 153–168.
- 1156 Brynjólfsson, S., Schomacker, A., Guðmundsdóttir, E.R., Ingólfsson, Ó., 2015a. A 300-  
1157 year surge history of the Drangajökull ice cap, northwest Iceland, and its maximum  
1158 during the Little Ice Age. *The Holocene* 25(7), 1076-1092. doi:  
1159 10.1177/0959683615576232
- 1160 Brynjólfsson, S., Schomacker, A., Ingólfsson, Ó., Keiding, J.K., 2015b. Cosmogenic  
1161 <sup>36</sup>Cl exposure ages reveal a 9.3 ka BP glacier advance and the Late Weichselian-  
1162 Early Holocene glacial history of the Drangajökull region, northwest Iceland. *Quat.*  
1163 *Sci. Rev.* 126, 140–157. doi:10.1016/j.quascirev.2015.09.001
- 1164 Caseldine, C., 1987. Neoglacial glacier variations in northern Iceland: Examples from  
1165 the Eyjafjörður area. *Arct. Alp. Res.* 19, 296–304.
- 1166 Caseldine, C., 1983. Resurvey of the margins of Gljúfurárjökull and the chronology of  
1167 recent deglaciation. *Jökull* 33, 111–118.
- 1168 Caseldine, C., Hatton, J., 1994. Environmental change in Iceland. *Münchener Geogr.*  
1169 *Abhandlungen. R. B Bd. B* 12 41–62.
- 1170 Caseldine, C., Stotter, J., 1993. “Little Ice Age” glaciation of Tröllaskagi peninsula,  
1171 northern Iceland: climatic implications for reconstructed equilibrium line altitudes  
1172 (ELAs).” *Holocene* 3, 357–366. doi:10.1177/095968369300300408
- 1173 Caseldine, C.J., 1991. Lichenometric dating, lichen population studies and Holocene  
1174 glacial history in Tröllaskagi, Northern Iceland, in: Maizels, J.K., Caseldine, C.  
1175 (Eds.), *Environmental Change in Iceland: Past and Present. Glaciology and*  
1176 *Quaternary Geology, Vol 7.* Springer, Dordrecht, pp. 219–233. doi:10.1007/978-  
1177 94-011-3150-6\_15
- 1178 Caseldine, C.J., 1990. A review of dating methods and their application in the  
1179 development of a Holocene glacial chronology for Northern Iceland, in: *Gletscher-*  
1180 *Und Landschaftsgeschichtliche Untersuchungen in Nordisland.* pp. 59–82.
- 1181 Caseldine, C.J., 1985a. Survey of Gljúfurárjökull and features associated with a glacier  
1182 burst in Gljúfurárdalur, Northern Iceland. *Jökull* 35, 61-68.
- 1183 Caseldine, C.J., 1985b. The Extent of Some Glaciers in Northern Iceland during the  
1184 Little Ice Age and the Nature of Recent Deglaciation. *Geogr. J.* 151, 215–227.  
1185 doi:10.2307/633535
- 1186 Chen, T., Robinson, L.F., Burke, A., Southon, J., Spooner, P., Morris, P.J., Ng, H.C.,  
1187 2015. Synchronous centennial abrupt events in the ocean and atmosphere during the  
1188 last deglaciation. *Science* 349, 1537–1541. doi:10.1126/science.aac6159

- 1189 Chenet, M., Roussel, E., Jomelli, V., Grancher, D., 2010. Asynchronous Little Ice Age  
1190 glacial maximum extent in southeast Iceland. *Geomorphology* 114, 253–260.  
1191 doi:10.1016/j.geomorph.2009.07.012
- 1192 Coquin, J., Mercier, D., Bourgeois, O., Cossart, E., Decaulne, A., 2015. Gravitational  
1193 spreading of mountain ridges coeval with Late Weichselian deglaciation: Impact on  
1194 glacial landscapes in Tröllaskagi, northern Iceland. *Quat. Sci. Rev.* 107, 197–213.  
1195 doi:10.1016/j.quascirev.2014.10.023
- 1196 Cossart, E., Mercier, D., Decaulne, A., Feuillet, T., Jónsson, H.P., Sæmundsson, Þ.,  
1197 2014. Impacts of post-glacial rebound on landslide spatial distribution at a regional  
1198 scale in northern Iceland (Skagafjörður). *Earth Surf. Process. Landforms* 39, 336–  
1199 350. doi:10.1002/esp.3450
- 1200 Crochet, P., Jóhannesson, T., Jónsson, T., Sigurðsson, O., Björnsson, H., Pálsson, F.,  
1201 Barstad, I., 2007. Estimating the Spatial Distribution of Precipitation in Iceland  
1202 Using a Linear Model of Orographic Precipitation. *J. Hydrometeorol.* 8, 1285–  
1203 1306. doi:10.1175/2007JHM795.1
- 1204 Dahl, S.O., Nesje, A., 1992. Paleoclimatic implications based on equilibrium-line  
1205 altitude depressions of reconstructed Younger Dryas and Holocene cirque glaciers  
1206 in inner Nordfjord, western Norway. *Palaeogeogr. Palaeoclimatol. Palaeoecol.* 94,  
1207 87–97. doi:10.1016/0031-0182(92)90114-K
- 1208 Decaulne, A., 2016. Lichenometry in Iceland, results and application. *Géomorphologie*  
1209 *Reli. Process. Environ.* 22, 77–91. doi:10.4000/geomorphologie.11291
- 1210 Decaulne, A., Saemundsson, T., 2006. Geomorphic evidence for present-day snow-  
1211 avalanche and debris-flow impact in the Icelandic Westfjords. *Geomorphology* 80,  
1212 80–93. doi:10.1016/J.GEOMORPH.2005.09.007
- 1213 Delunel, R., Boulès, D.L., van der Beek, P.A., Schlunegger, F., Leya, I., Masarik, J.,  
1214 Paquet, E., 2014. Snow shielding factors for cosmogenic nuclide dating inferred  
1215 from long-term neutron detector monitoring. *Quat. Geochronol.* 24, 16–26. doi:  
1216 10.1016/J.QUAGEO.2014.07.003
- 1217 Dietz, A.J., Wohner, C., Kuenzer, C., 2012. European Snow Cover Characteristics  
1218 between 2000 and 2011 Derived from Improved MODIS Daily Snow Cover  
1219 Products. *Remote Sens.* 4, 2432–2454. doi:10.3390/rs4082432
- 1220 Dong, G., Zhou, W., Yi, C., Zhang, L., Li, M., Fu, Y., Zhang, Q., 2017. Cosmogenic  
1221 <sup>10</sup>Be surface exposure dating of ‘Little Ice Age’ glacial events in the Mount  
1222 Jaggang area, central Tibet. *The Holocene* 27(10), 1516-1525.  
1223 doi:10.1177/0959683617693895
- 1224 Dugmore, A.J., 1989. Tephrochronological studies of Holocene glacial fluctuations in  
1225 South Iceland, in: *Glacier Fluctuations and Climatic Change*. pp. 37–55.  
1226 doi:10.1007/978-94-015-7823-3\_3

- 1227 Dunai, T.J., 2010. *Cosmogenic Nuclides*. Cambridge University Press, Cambridge.  
1228 doi:10.1017/CBO9780511804519
- 1229 Dunai, T.J., Binnie, S.A., Hein, A.S., Paling, S.M., 2014. The effects of a hydrogen-rich  
1230 ground cover on cosmogenic thermal neutrons: Implications for exposure dating.  
1231 *Quat. Geochronol.* 22, 183–191. doi:10.1016/J.QUAGEO.2013.01.001
- 1232 Eddy, J.A., 1976. The Maunder Minimum. *Science* 192 (4245), 1189–1202.  
1233 doi:10.1126/science.192.4245.1189
- 1234 Einarsson, M.Á., 1984. Climate of Iceland. In van Loon, H. (Eds.), *World Survey of*  
1235 *Climatology: 15: Climates of the Oceans*. Elsevier, Amsterdam, pp. 673-697.
- 1236 Einarsson, M.A., 1991. Temperature conditions in Iceland 1901-1990. *Jökull* 41, 1–20.
- 1237 Etzelmüller, B., Farbrót, H., Guðmundsson, Á., Humlum, O., Tveito, O.E., Björnsson,  
1238 H., 2007. The regional distribution of mountain permafrost in Iceland. *Permafrost*.  
1239 *Periglac. Process.* 18, 185–199. doi:10.1002/ppp.583
- 1240 Evans, D.J.A., Archer, S., Wilson, D.J.H., 1999. A comparison of the lichenometric and  
1241 Schmidt hammer dating techniques based on data from the proglacial areas of some  
1242 Icelandic glaciers. *Quat. Sci. Rev.* 18, 13–41. doi:10.1016/S0277-3791(98)00098-5
- 1243 Fernández-Fernández, J.M., Andrés, N., 2018. Methodological Proposal for the  
1244 Analysis of the Evolution of Glaciers Since the Little Ice Age and Its Application in  
1245 the Tröllaskagi Peninsula (Northern Iceland). *Cuad. Investig. Geográfica Geogr.*  
1246 *Res. Lett.* No 44, 69–97. doi:10.18172/cig.3392
- 1247 Fernández-Fernández, J.M., Andrés, N., Sæmundsson, Þ., Brynjólfsson, S., Palacios, D.,  
1248 2017. High sensitivity of North Iceland (Tröllaskagi) debris-free glaciers to climatic  
1249 change from the ‘Little Ice Age’ to the present. *The Holocene* 27, 1187–1200.  
1250 doi:10.1177/0959683616683262
- 1251 Feuillet, T., Coquin, J., Mercier, D., Cossart, E., Decaulne, A., Jónsson, H.P.,  
1252 Sæmundsson, Þ., 2014. Focusing on the spatial non-stationarity of landslide  
1253 predisposing factors in northern Iceland. *Prog. Phys. Geogr.* 38, 354–377.  
1254 doi:10.1177/0309133314528944
- 1255 Fink, D., Vogt, S., Hotchkis, M., 2000. Cross-sections for <sup>36</sup>Cl from Ti at Ep=35–150  
1256 MeV: Applications to in-situ exposure dating. *Nucl. Instruments Methods Phys.*  
1257 *Res. Sect. B Beam Interact. with Mater. Atoms* 172, 861–866. doi:10.1016/S0168-  
1258 583X(00)00200-7
- 1259 Flowers, G.E., Björnsson, H., Geirsdóttir, Á., Miller, G.H., Black, J.L., Clarke, G.K.C.,  
1260 2008. Holocene climate conditions and glacier variation in central Iceland from  
1261 physical modelling and empirical evidence. *Quat. Sci. Rev.* 27, 797–813.  
1262 doi:10.1016/J.QUASCIREV.2007.12.004
- 1263 Gardner, A.S., Moholdt, G., Cogley, J.G., Wouters, B., Arendt, A.A., Wahr, J., Berthier,  
1264 E., Hock, R., Pfeffer, W.T., Kaser, G., Ligtenberg, S.R.M., Bolch, T., Sharp, M.J.,

- 1265 Hagen, J.O., Van Den Broeke, M.R., Paul, F., 2013. A reconciled estimate of  
1266 glacier contributions to sea level rise: 2003 to 2009. *Science* 340, 852–857.  
1267 doi:10.1126/science.1234532
- 1268 Geirsdóttir, Á., Miller, G.H., Axford, Y., Sædis Ólafsdóttir, 2009. Holocene and latest  
1269 Pleistocene climate and glacier fluctuations in Iceland. *Quat. Sci. Rev.* 28, 2107–  
1270 2118. doi:10.1016/j.quascirev.2009.03.013
- 1271 Geirsdóttir, Á., Miller, G. H., Andrews, J. T., Harning, D. J., Anderson, L. S.,  
1272 Thordarson, T., 2018. The onset of Neoglaciation in Iceland and the 4.2 ka event.  
1273 *Clim. Past Discuss.*, doi:10.5194/cp-2018-130. Manuscript under review
- 1274 Gordon, J.E., Sharp, M., 1983. Lichenometry in dating recent glacial landforms and  
1275 deposits, southeast Iceland. *Boreas* 12, 191–200. doi:10.1111/j.1502-  
1276 3885.1983.tb00312.x
- 1277 Grove, J.M., 1988. *The Little Ice Age*. Routledge, London.
- 1278 Guðmundsson, H.J., 1997. A review of the Holocene environmental history of Iceland.  
1279 *Quat. Sci. Rev.* 16, 81–92. doi:10.1016/S0277-3791(96)00043-1
- 1280 Häberle, T., 1994. Glacial, Late Glacial and Holocene History of the Hörgárdalur Area,  
1281 Tröllaskagi, Northern Iceland, in: Stöttter, J., Wilhelm, F. (Eds.), *Environmental*  
1282 *Change in Iceland*. Münchener Geographische Abhandlungen, Reihe B, pp. 133–  
1283 145.
- 1284 Häberle, T., 1991. Holocene Glacial History of the Hörgárdalur Area, Tröllaskagi,  
1285 Northern Iceland, in: Maizels, J.K., Caseldine, C. (Eds.), *Environmental Change in*  
1286 *Iceland: Past and Present*. Glaciology and Quaternary Geology, Vol 7. Springer,  
1287 Dordrecht, pp. 193–202. doi:10.1007/978-94-011-3150-6\_13
- 1288 Hamilton, S.J., Whalley, W.B., 1995. Rock glacier nomenclature: A re-assessment.  
1289 *Geomorphology* 14, 73–80. doi:10.1016/0169-555X(95)00036-5
- 1290 Harning, D.J., Geirsdóttir, Á., Miller, G.H., 2018. Punctuated Holocene climate of  
1291 Vestfirðir, Iceland, linked to internal/external variables and oceanographic  
1292 conditions. *Quat. Sci. Rev.* 189, 31–42. doi:10.1016/j.quascirev.2018.04.009
- 1293 Harning, D.J., Geirsdóttir, Á., Miller, G.H., Anderson, L., 2016a. Episodic expansion of  
1294 Drangajökull, Vestfirðir, Iceland, over the last 3 ka culminating in its maximum  
1295 dimension during the Little Ice Age. *Quat. Sci. Rev.* 152, 118–131.  
1296 <https://doi.org/10.1016/j.quascirev.2016.10.001>
- 1297 Harning, D.J., Geirsdóttir, Á., Miller, G.H., Zalzal, K., 2016b. Early Holocene  
1298 deglaciation of Drangajökull, Vestfirðir, Iceland. *Quat. Sci. Rev.* 153, 192–198.  
1299 doi:10.1016/j.quascirev.2016.09.030
- 1300 Harris, T., Tweed, F.S., Knudsen, Ó., 2004. A polygenetic landform at Stígá,  
1301 Öräfajökull, southern Iceland. *Geogr. Ann. Ser. A Phys. Geogr.* 86, 143–154.  
1302 doi:10.1111/j.0435-3676.2004.00220.x

- 1303 Helama, S., Jones, P.D., Briffa, K.R., 2017. Dark Ages Cold Period: A literature review  
1304 and directions for future research. *The Holocene* 27, 1600–1606.  
1305 doi:10.1177/0959683617693898
- 1306 Heyman, J., Stroeven, A.P., Harbor, J.M., Caffee, M.W., 2011. Too young or too old:  
1307 Evaluating cosmogenic exposure dating based on an analysis of compiled boulder  
1308 exposure ages. *Earth Planet. Sci. Lett.* 302, 71–80. doi:10.1016/j.epsl.2010.11.040
- 1309 Hjort, C., Ingólfsson, Ó., Norðdahl, H., 1985. Late Quaternary geology and glacial  
1310 history of Hornstrandir, Northwest Iceland: a reconnaissance study. *Jökull* 35, 9–  
1311 29.
- 1312 Holzhauser, H., Magny, M., Zumbuühl, H.J., 2005. Glacier and lake-level variations in  
1313 west-central Europe over the last 3500 years. *The Holocene* 15, 789–801.  
1314 doi:10.1191/0959683605hl853ra
- 1315 Hooker, T.N., Brown, D.H., 1977. A photographic method for accurately measuring the  
1316 growth of crustose and foliose saxicolous lichens. *Lichenol.* 9, 65–75.  
1317 doi:10.1017/S0024282977000073
- 1318 Hughes, P.D., Woodward, J.C., van Calsteren, P.C., Thomas, L.E., Adamson, K.R.,  
1319 2010. Pleistocene ice caps on the coastal mountains of the Adriatic Sea. *Quat. Sci.*  
1320 *Rev.* 29, 3690–3708. doi:10.1016/j.quascirev.2010.06.032
- 1321 Icelandic Meteorological Office, 2018. Climatological data. Available  
1322 <http://en.vedur.is/climatology/data/> (accessed 13 April 2018).
- 1323 Ingólfsson, Ó., Benediktsson, Í.Ö., Schomacker, A., Kjær, K., Brynjólfsson, S., Jónsson,  
1324 S.A., Korsgaard, N.J., Johnson, M., 2016. Glacial geological studies of surge type  
1325 glaciers in Iceland – Research status and future challenges. *Earth Science Reviews*  
1326 152, 37–69.
- 1327 Innes, J.L., 1985. Lichenometry, *Progress in Physical Geography*.  
1328 doi:10.1177/030913338500900202
- 1329 Ivy-Ochs, S., Synal, H.-A., Roth, C., Schaller, M., 2004. Initial results from isotope  
1330 dilution for Cl and <sup>36</sup>Cl measurements at the PSI/ETH Zurich AMS facility. *Nucl.*  
1331 *Instruments Methods Phys. Res. Sect. B Beam Interact. with Mater. Atoms* 223–  
1332 224, 623–627. doi:10.1016/j.nimb.2004.04.115
- 1333 Ipsen, H.A., Principato, S.M., Grube, R.E., Lee, J.F., 2018. Spatial analysis of cirques  
1334 from three regions of Iceland: implications for cirque formation and palaeoclimate.  
1335 *Boreas* 47, 565–576. doi:10.1111/bor.12295
- 1336 Jacob, T., Wahr, J., Pfeffer, W.T., Swenson, S., 2012. Recent contributions of glaciers  
1337 and ice caps to sea level rise. *Nature* 482, 514–518. doi:10.1038/nature10847
- 1338 Jaksch, K., 1984. Das Gletshervorfeld des Vatnajökull am Oberflauf des Djúpá,  
1339 Südisland. *Jökull* 34, 97–103.

- 1340 Jaksch, K., 1975. Das Gletschervorfeld des Sólheimajökull. *Jökull* 25, 34–38.
- 1341 Jaksch, K., 1970. Beobachtungen in den Gletschervorfeldern des Sólheima und  
1342 Siðujökull im Sommer 1970. *Jökull* 20.
- 1343 James, W.H.M., Carrivick, J.L., 2016. Automated modelling of spatially-distributed  
1344 glacier ice thickness and volume. *Comput. Geosci.* 92, 90–103.  
1345 doi:10.1016/j.cageo.2016.04.007
- 1346 Janke, J.R., Bellisario, A.C., Ferrando, F.A., 2015. Classification of debris-covered  
1347 glaciers and rock glaciers in the Andes of central Chile. *Geomorphology* 241, 98–  
1348 121. doi:10.1016/j.geomorph.2015.03.034
- 1349 Jiang, H., Muscheler, R., Björck, S., Seidenkrantz, M.S., Olsen, J., Sha, L., Sjolte, J.,  
1350 Eiríksson, J., Ran, L., Knudsen, K.L., Knudsen, M.F., 2015. Solar forcing of  
1351 Holocene summer sea-surface temperatures in the northern North Atlantic. *Geology*  
1352 43, 203–206. doi:10.1130/G36377.1
- 1353 Jóhannesson, T., Sigurðsson, O., 1998. Interpretation of glacier variations in Iceland  
1354 1930-1995. *Jökull* 45, 27–33.
- 1355 Jóhannesson, H., Sæmundsson, K., 1989. Geological map of Iceland. 1:500.000.  
1356 Bedrock. Icelandic Institute of Natural History, Reykjavik.
- 1357 Jomelli, V., Lane, T., Favier, V., Masson-Delmotte, V., Swingedouw, D., Rinterknecht,  
1358 V., Schimmelpfennig, I., Brunstein, D., Verfaillie, D., Adamson, K., Leanni, L.,  
1359 Mokadem, F., Aumaître, G., Bourlès, D.L., Keddadouche, K., 2016. Paradoxical  
1360 cold conditions during the medieval climate anomaly in the Western Arctic. *Sci.*  
1361 *Rep.* 6, 32984. <https://doi.org/10.1038/srep32984>
- 1362 Jónsson, O., 1976. Berghlaup. Ræktunarfélag Norðurlands, Akureyri.
- 1363 Kirkbride, M.P., 2002. Icelandic climate and glacier fluctuations through the  
1364 termination of the “Little Ice Age”. *Polar Geogr.* 26, 116–133.  
1365 doi:10.1080/789610134
- 1366 Kirkbride, M.P., 2011. Debris-covered glaciers. In: Singh, V.P., Singh, P., Haritashya,  
1367 U.K. (Eds.), *Encyclopedia of Snow, Ice and Glaciers: Encyclopedia of Earth Series*.  
1368 Springer, Netherlands, pp. 180–182. doi:10.1007/978-90-481-2642-2\_622
- 1369 Kirkbride, M.P., Dugmore, A.J., 2006. Responses of mountain ice caps in central  
1370 Iceland to Holocene climate change. *Quat. Sci. Rev.* 25, 1692–1707.  
1371 doi:10.1016/j.quascirev.2005.12.004
- 1372 Kirkbride, M.P., Dugmore, A.J., 2001. Can lichenometry be used to date the “Little Ice  
1373 Age” glacial maximum in Iceland? *Clim. Change* 48, 151–167.  
1374 doi:10.1023/A:1005654503481

- 1375 Knight, J., Harrison, S., Jones, D.B., 2018. Rock glaciers and the geomorphological  
1376 evolution of deglaciating mountains. *Geomorphology* 311, 127–142.  
1377 doi:10.1016/j.geomorph.2018.09.020
- 1378 Koblet, T., Gärtner-Roer, I., Zemp, M., Jansson, P., Thee, P., Haeberli, W., Holmlund,  
1379 P., 2010. Reanalysis of multi-temporal aerial images of Storglaciären, Sweden  
1380 (1959-99); Part 1: Determination of length, area, and volume changes. *Cryosph.* 4,  
1381 333–343. doi:10.5194/tc-4-333-2010
- 1382 Koch, L., 1945. The East Greenland Ice. *Medd. Grøn.* 130, 1–374.
- 1383 Kugelmann, O., 1991. Dating Recent Glacier Advances in the Svarfaðardalur-  
1384 Skíðadalur Area of Northern Iceland by Means of a New Lichen Curve, in:  
1385 Maizels, J.K., Caseldine, C. (Eds.), *Environmental Change in Iceland: Past and*  
1386 *Present. Glaciology and Quaternary Geology, Vol 7.* Springer, Dordrecht, pp. 203–  
1387 217. doi:10.1007/978-94-011-3150-6\_14
- 1388 Lamb, H.H., 1965. The early medieval warm epoch and its sequel. *Palaeogeogr.*  
1389 *Palaeoclimatol. Palaeoecol.* 1, 13–37. doi:10.1016/0031-0182(65)90004-0
- 1390 Larsen, D.J., Miller, G.H., Geirsdóttir, Á., Thordarson, T., 2011. A 3000-year varved  
1391 record of glacier activity and climate change from the proglacial lake Hvítárvatn,  
1392 Iceland. *Quat. Sci. Rev.* 30, 2715–2731. doi:10.1016/j.quascirev.2011.05.026
- 1393 Larsen, D.J., Geirsdóttir, Á., Miller, G.H., 2015. Precise chronology of Little Ice Age  
1394 expansion and repetitive surges of Langjökull, central Iceland. *Geology* 43, 167–  
1395 170. <https://doi.org/10.1130/G36185.1>
- 1396 Le Roy, M., Deline, P., Carcaillet, J., Schimmelpfennig, I., Ermini, M., 2017. <sup>10</sup>Be  
1397 exposure dating of the timing of Neoglacial glacier advances in the Ecrins-Pelvoux  
1398 massif, southern French Alps. *Quat. Sci. Rev.* 178, 118–138.  
1399 doi:10.1016/j.quascirev.2017.10.010
- 1400 Li, Y., Li, Y., Harbor, J., Liu, G., Yi, C., Caffee, M.W., 2016. Cosmogenic<sup>10</sup>Be  
1401 constraints on Little Ice Age glacial advances in the eastern Tian Shan, China.  
1402 *Quat. Sci. Rev.* 138, 105–118. doi:10.1016/j.quascirev.2016.02.023
- 1403 Licciardi, J.M., Denoncourt, C.L., Finkel, R.C., 2008. Cosmogenic<sup>36</sup>Cl production  
1404 rates from Ca spallation in Iceland. *Earth Planet. Sci. Lett.* 267, 365–377.  
1405 doi:10.1016/j.epsl.2007.11.036
- 1406 Licciardi, J.M., Kurz, M.D., Curtice, J.M., 2007. Glacial and volcanic history of  
1407 Icelandic table mountains from cosmogenic<sup>3</sup>He exposure ages. *Quat. Sci. Rev.* 26,  
1408 1529–1546. doi:10.1016/j.quascirev.2007.02.016
- 1409 Licciardi, J.M., Kurz, M.D., Curtice, J.M., 2006. Cosmogenic<sup>3</sup>He production rates from  
1410 Holocene lava flows in Iceland. *Earth Planet. Sci. Lett.* 246, 251–264.  
1411 doi:10.1016/j.epsl.2006.03.016

- 1412 Maizels, J.K., Dugmore, A.J., 1985. Lichenometric dating and tephrochronology of  
1413 sandur deposits, Sólheimajökull area, southern Iceland. *Jökull* 35, 69–77.
- 1414 Marrero, S.M., Phillips, F.M., Caffee, M.W., Gosse, J.C., 2016. CRONUS-Earth  
1415 cosmogenic  $^{36}\text{Cl}$  calibration. *Quat. Geochronol.* 31, 199–219.  
1416 doi:10.1016/j.quageo.2015.10.002
- 1417 Martin, H.E., Whalley, W.B., Caseldine, C., 1991. Glacier Fluctuations and Rock  
1418 Glaciers in Tröllaskagi, Northern Iceland, with Special Reference to 1946–1986, in:  
1419 Maizels, J.K., Caseldine, C. (Eds.), *Environmental Change in Iceland: Past and*  
1420 *Present*. Springer Netherlands, Dordrecht, pp. 255–265. doi:10.1007/978-94-011-  
1421 3150-6\_17
- 1422 Marzeion, B., Cogley, J.G., Richter, K., Parkes, D., 2014. Attribution of global glacier  
1423 mass loss to anthropogenic and natural causes. *Science* 345, 919–921.  
1424 doi:10.1126/science.1254702
- 1425 Matthews, J.A., Shakesby, R.A., Fabel, D., 2017. Very low inheritance in cosmogenic  
1426 surface exposure ages of glacial deposits: A field experiment from two Norwegian  
1427 glacier forelands. *Holocene* 27, 1406–1414. doi:10.1177/0959683616687387
- 1428 Merchel, S., Bremser, W., Alfimov, V., Arnold, M., Aumaître, G., Benedetti, L.,  
1429 Bournès, D.L., Caffee, M., Fifield, L.K., Finkel, R.C., Freeman, S.P.H.T.,  
1430 Martschini, M., Matsushi, Y., Rood, D.H., Sasa, K., Steier, P., Takahashi, T.,  
1431 Tamari, M., Tims, S.G., Tosaki, Y., Wilcken, K.M., Xu, S., 2011. Ultra-trace  
1432 analysis of  $^{36}\text{Cl}$  by accelerator mass spectrometry: an interlaboratory study. *Anal.*  
1433 *Bio- anal. Chem.* doi:10.1007/s00216-011-4979-2.
- 1434 Meyer, H.H., Venzke, J.F., 1985. Der Klængshóll-Kargletscher in Nordisland. *Natur*  
1435 *and Museum* 115, 29–46.
- 1436 Miller, G.H., Geirsdóttir, Á., Zhong, Y., Larsen, D.J., Otto-Bliesner, B.L., Holland,  
1437 M.M., Bailey, D.A., Refsnider, K.A., Lehman, S.J., Southon, J.R., Anderson, C.,  
1438 Björnsson, H., Thordarson, T., 2012. Abrupt onset of the Little Ice Age triggered  
1439 by volcanism and sustained by sea-ice/ocean feedbacks. *Geophys. Res. Lett.* 39, 1–  
1440 5. doi:10.1029/2011GL050168
- 1441 National Land Survey of Iceland, 2018. Aerial photo collection. Available  
1442 <https://www.lmi.is/landupplýsingar/loftmyndasafn-2-2/> (accessed 5 July 2018).
- 1443 Nesje, A., Bakke, J., Dahl, S.O., Lie, Ø., Matthews, J.A., 2008. Norwegian mountain  
1444 glaciers in the past, present and future. *Glob. Planet. Change* 60, 10–27.  
1445 doi:10.1016/j.gloplacha.2006.08.004
- 1446 Ogilvie, A., 1996. Sea-ice conditions off the coasts of Iceland A. D. 1601-1850 with  
1447 special reference to part of the Maunder Minimum period (1675-1715). *AmS-Varia*  
1448 25, 9–12.

- 1449 Ogilvie, A.E.J., 1984. The past climate and sea-ice record from Iceland, Part 1: Data to  
1450 A.D. 1780. *Clim. Change* 6, 131–152. doi:10.1007/BF00144609
- 1451 Ogilvie, A.E.J., Jónsdóttir, I., 2000. Sea ice, climate, and Icelandic fisheries in the  
1452 eighteenth and nineteenth centuries. *Arctic* 53, 383–394. doi:10.14430/arctic869
- 1453 Ogilvie, A.E.J., Jónsson, T., 2001. “Little Ice Age” Research: a perspective from  
1454 Iceland. *Clim. Change* 48, 9–52.
- 1455 Oliva, M., Ruiz-Fernández, J., Barriendos, M., Benito, G., Cuadrat, J.M., Domínguez-  
1456 Castro, F., García-Ruiz, J.M., Giralt, S., Gómez-Ortiz, A., Hernández, A., López-  
1457 Costas, O., López-Moreno, J.I., López-Sáez, J.A., Martínez-Cortizas, A., Moreno,  
1458 A., Prohom, M., Saz, M.A., Serrano, E., Tejedor, E., Trigo, R., Valero-Garcés, B.,  
1459 Vicente-Serrano, S.M., 2018. The Little Ice Age in Iberian mountains. *Earth-  
1460 Science Rev.* 177, 175–208. doi:10.1016/j.earscirev.2017.11.010
- 1461 Orwin, J.F., Mckinzey, K.M., Stephens, M.A., Dugmore, A.J., 2008. Identifying  
1462 moraine surfaces with similar histories using lichen size distributions and the U2  
1463 statistic, Southeast Iceland. *Geogr. Ann. Ser. A Phys. Geogr.* 90 A, 151–164.  
1464 doi:10.1111/j.1468-0459.2008.00168.x
- 1465 Osborn, G., McCarthy, D., LaBrie, A., Burke, R., 2015. Lichenometric dating: Science  
1466 or pseudo-science? *Quat. Res. (United States)* 83, 1–12.  
1467 doi:10.1016/j.yqres.2014.09.006
- 1468 Osmaston, H., 2005. Estimates of glacier equilibrium line altitudes by the Area ×  
1469 Altitude, the Area × Altitude Balance Ratio and the Area × Altitude Balance Index  
1470 methods and their validation. *Quat. Int.* 138–139, 22–31.  
1471 doi:10.1016/j.quaint.2005.02.004
- 1472 Palacios, D., Gómez-Ortiz, A., Alcalá-Reygosa, J., Andrés, N., Oliva, M., Tanarro,  
1473 L.M., Salvador-Franch, F., Schimmelpfennig, I., Fernández-Fernández, J.M.,  
1474 Léanni, L., 2019. The challenging application of cosmogenic dating methods in  
1475 residual glacial landforms: The case of Sierra Nevada (Spain). *Geomorphology*  
1476 325, 103–118. doi:10.1016/j.geomorph.2018.10.006
- 1477 Paterson, W.S.B., 1994. *The Physics of Glaciers*, 3<sup>rd</sup> Edition. Pergamon/Elsevier,  
1478 London.
- 1479 Pellitero, R., Rea, B.R., Spagnolo, M., Bakke, J., Hughes, P., Ivy-Ochs, S., Lukas, S.,  
1480 Ribolini, A., 2015. A GIS tool for automatic calculation of glacier equilibrium-line  
1481 altitudes. *Comput. Geosci.* 82, 55–62. doi:10.1016/j.cageo.2015.05.005
- 1482 Pellitero, R., Rea, B.R., Spagnolo, M., Bakke, J., Ivy-Ochs, S., Frew, C.R., Hughes, P.,  
1483 Ribolini, A., Lukas, S., Renssen, H., 2016. GlaRe, a GIS tool to reconstruct the 3D  
1484 surface of palaeoglaciers. *Comput. Geosci.* 94, 77–85.  
1485 doi:10.1016/j.cageo.2016.06.008

- 1486 Principato, S.M., Geirsdóttir, Á., Jóhannsdóttir, G.E., Andrews, J.T., 2006. Late  
 1487 Quaternary glacial and deglacial history of eastern Vestfirðir, Iceland using  
 1488 cosmogenic isotope ( $^{36}\text{Cl}$ ) exposure ages and marine cores. *J. Quat. Sci.* 21, 271–  
 1489 285. doi:10.1002/jqs.978
- 1490 Rea, B.R., 2009. Defining modern day Area-Altitude Balance Ratios (AABRs) and their  
 1491 use in glacier-climate reconstructions. *Quat. Sci. Rev.* 28, 237–248.  
 1492 doi:10.1016/j.quascirev.2008.10.011
- 1493 Reimer PJ, Bard E, Bayliss A, Beck JW, Blackwell PG, Bronk Ramsey C, Buck CE,  
 1494 Cheng H, Edwards RL, Friedrich M, Grootes PM, Guilderson TP, Hafliðason H,  
 1495 Hajdas I, Hatté C, Heaton TJ, Hoffmann DL, Hogg AG, Hughen KA, Kaiser KF,  
 1496 Kromer B, Manning SW, Niu M, Reimer RW, Richards DA, Scott EM, Southon  
 1497 JR, Staff RA, Turney CSM, van der Plicht J. 2013. IntCal13 and Marine13  
 1498 radiocarbon age calibration curves 0–50,000 years cal BP. *Radiocarbon*  
 1499 55(4):1869–1887.
- 1500 Roca-Valiente, B., Hawksworth, D.L., Pérez-Ortega, S., Sancho, L.G., Crespo, A.,  
 1501 2016. Type studies in the *Rhizocarpon geographicum* group (Rhizocarpaceae,  
 1502 lichenized Ascomycota). *Lichenologist* 48, 97–110.  
 1503 doi:10.1017/S002428291500050X
- 1504 Rogers, J.C., Van Loon, H., 1979. The Seesaw in Winter Temperatures between  
 1505 Greenland and Northern Europe. Part II: Some Oceanic and Atmospheric Effects in  
 1506 Middle and High Latitudes. *Mon. Weather Rev.* 107, 509–519. doi:10.1175/1520-  
 1507 0493(1979)107<0509:TSIWTB>2.0.CO;2
- 1508 Russell, A.J., Knight, P.G., Van Dijk, T.A.G.P., 2001. Glacier surging as a control on  
 1509 the development of proglacial, fluvial landforms and deposits, Skeiðarársandur,  
 1510 Iceland. *Glob. Planet. Change* 28, 163–174. doi:10.1016/S0921-8181(00)00071-0
- 1511 Sancho, L.G., Pintado, A., Navarro, F., Ramos, M., De Pablo, M.A., Blanquer, J.M.,  
 1512 Raggio, J., Valladares, F., Green, T.G.A., 2017. Recent Warming and Cooling in  
 1513 the Antarctic Peninsula Region has Rapid and Large Effects on Lichen Vegetation.  
 1514 *Sci. Rep.* 7, 5689. <https://doi.org/10.1038/s41598-017-05989-4>
- 1515 Sancho, L.G., Palacios, D., Green, T.G.A., Vivas, M., Pintado, A., 2011. Extreme high  
 1516 lichen growth rates detected in recently deglaciaded areas in Tierra del Fuego. *Polar*  
 1517 *Biol.* 34, 813–822. <https://doi.org/10.1007/s00300-010-0935-4>
- 1518 Sæmundsson, K., Kristjánsson, L., McDougall, I., Watkins, N.D., 1980. K-Ar dating,  
 1519 geological and paleomagnetic study of a 5-km lava succession in northern Iceland.  
 1520 *J. Geophys. Res. Solid Earth* 85, 3628–3646. doi:10.1029/JB085iB07p03628
- 1521 Sæmundsson, Þ., Morino, C., Helgason, J.K., Conway, S.J., Pétursson, H.G., 2018. The  
 1522 triggering factors of the Móafellshyrna debris slide in northern Iceland: Intense  
 1523 precipitation, earthquake activity and thawing of mountain permafrost. *Sci. Total*  
 1524 *Environ.* 621, 1163–1175. doi:10.1016/J.SCITOTENV.2017.10.111

- 1525 Schaefer, J.M., Denton, G.H., Kaplan, M., Putnam, A., Finkel, R.C., Barrell, D.J.A.,  
 1526 Andersen, B.G., Schwartz, R., Mackintosh, A., Chinn, T., Schlüchter, C., 2009.  
 1527 High-frequency Holocene glacier fluctuations in New Zealand differ from the  
 1528 northern signature. *Science* 324, 622–625. doi:10.1126/science.1169312
- 1529 Schildgen, T.F., Phillips, W.M., Purves, R.S., 2005. Simulation of snow shielding  
 1530 corrections for cosmogenic nuclide surface exposure studies. *Geomorphology* 64,  
 1531 67–85. doi:10.1016/j.geomorph.2004.05.003
- 1532 Schimmelpfennig, I., 2009. Cosmogenic <sup>36</sup>Cl in Ca and K rich minerals: analytical  
 1533 developments, production rate calibrations and cross calibration with <sup>3</sup>He and  
 1534 <sup>21</sup>Ne. Ph. D. Thesis, Université Aix-Marseille III, France. <http://tel.archives-ouvertes.fr/tel-00468337/fr>
- 1536 Schimmelpfennig, I., Benedetti, L., Finkel, R., Pik, R., Blard, P.H., Bourlès, D.,  
 1537 Burnard, P., Williams, A., 2009. Sources of in-situ <sup>36</sup>Cl in basaltic rocks.  
 1538 Implications for calibration of production rates. *Quat. Geochronol.* 4, 441–461.  
 1539 doi:10.1016/j.quageo.2009.06.003
- 1540 Schimmelpfennig, I., Benedetti, L., Garreta, V., Pik, R., Blard, P.H., Burnard, P.,  
 1541 Bourlès, D., Finkel, R., Ammon, K., Dunai, T., 2011. Calibration of cosmogenic  
 1542 <sup>36</sup>Cl production rates from Ca and K spallation in lava flows from Mt. Etna (38°N,  
 1543 Italy) and Payun Matru (36°S, Argentina). *Geochim. Cosmochim. Acta* 75, 2611–  
 1544 2632. doi:10.1016/j.gca.2011.02.013
- 1545 Schimmelpfennig, I., Schaefer, J.M., Akçar, N., Ivy-Ochs, S., Finkel, R.C., Schlüchter,  
 1546 C., 2012. Holocene glacier culminations in the Western Alps and their hemispheric  
 1547 relevance. *Geology* 40, 891–894. doi:10.1130/G33169.1
- 1548 Schimmelpfennig, I., Schaefer, J.M., Akçar, N., Koffman, T., Ivy-Ochs, S., Schwartz,  
 1549 R., Finkel, R.C., Zimmerman, S., Schlüchter, C., 2014a. A chronology of Holocene  
 1550 and Little Ice Age glacier culminations of the Steingletscher, Central Alps,  
 1551 Switzerland, based on high-sensitivity beryllium-10 moraine dating. *Earth Planet.*  
 1552 *Sci. Lett.* 393, 220–230. doi:10.1016/j.epsl.2014.02.046
- 1553 Schimmelpfennig, I., Schaefer, J.M., Putnam, A.E., Koffman, T., Benedetti, L., Ivy-  
 1554 Ochs, S., Team, A., Schlüchter, C., 2014b. <sup>36</sup>Cl production rate from K-spallation  
 1555 in the European Alps (Chironico landslide, Switzerland). *J. Quat. Sci.* 29, 407–413.  
 1556 doi:10.1002/jqs.2720
- 1557 Schomacker, A., Krüger, J., Larsen, G., 2003. An extensive late Holocene glacier  
 1558 advance of Kötlujökull, central south Iceland. *Quat. Sci. Rev.* 22, 1427–1434.  
 1559 doi:10.1016/S0277-3791(03)00090-8
- 1560 Schomacker, A., Brynjólfsson, S., Andreassen, J.M., Gudmundsdóttir, E.R., Olsen, J.,  
 1561 Odgaard, B.V., Håkansson, L., Ingólfsson, O., Larsen, N.K., 2016. The Drangajökull  
 1562 ice cap, northwest Iceland, persisted into the early-mid Holocene. *Quat. Sci. Rev.*  
 1563 148, 66–84.

- 1564 Sigurðsson, O., 1998. Glacier variations in Iceland 1930-1995. *Jökull* 45, 27–33.
- 1565 Sigurðsson, O., 2005. 10. Variations of termini of glaciers in Iceland in recent centuries  
1566 and their connection with climate, in: *Developments in Quaternary Science*. pp.  
1567 241–255. doi:10.1016/S1571-0866(05)80012-0
- 1568 Sigurðsson, O., Jónsson, T., Jóhannesson, T., 2007. Relation between glacier-termini  
1569 variations and summer temperature in Iceland since 1930. *Ann. Glaciol.* 46, 170–  
1570 176. doi:10.3189/172756407782871611
- 1571 Sissons, J.B., 1974. A Late-Glacial Ice Cap in the Central Grampians, Scotland. *Trans.*  
1572 *Inst. Br. Geogr.* 95. doi:10.2307/621517
- 1573 Solomina, O.N., Bradley, R.S., Jomelli, V., Geirsdottir, A., Kaufman, D.S., Koch, J.,  
1574 McKay, N.P., Masiokas, M., Miller, G., Nesje, A., Nicolussi, K., Owen, L.A.,  
1575 Putnam, A.E., Wanner, H., Wiles, G., Yang, B., 2016. Glacier fluctuations during  
1576 the past 2000 years. *Quat. Sci. Rev.* 149, 61–90.  
1577 doi:10.1016/j.quascirev.2016.04.008
- 1578 Stone, J.O., 2000. Air pressure and cosmogenic isotope production. *J. Geophys. Res.*  
1579 *Solid Earth* 105, 23753–23759. doi:10.1029/2000JB900181
- 1580 Stone, J.O., Allan, G.L., Fifield, L.K., Cresswell, R.G., 1996. Cosmogenic chlorine-36  
1581 from calcium spallation. *Geochim. Cosmochim. Acta* 60, 679–692.  
1582 doi:10.1016/0016-7037(95)00429-7
- 1583 Stone, J.O., Fifield, K., Vasconcelos, P., 2005. Terrestrial chlorine-36 production from  
1584 spallation of iron, in: *Abstract of 10th International Conference on Accelerator*  
1585 *Mass Spectrometry*. Berkeley, CA.
- 1586 Stötter, J., 1991. New Observations on the Postglacial Glacial History of Tröllaskagi,  
1587 Northern Iceland, in: Maizels, J.K., Caseldine, C. (Eds.), *Environmental Change in*  
1588 *Iceland: Past and Present. Glaciology and Quaternary Geology, Vol 7*. Springer,  
1589 Dordrecht, pp. 181–192. doi:10.1007/978-94-011-3150-6\_12
- 1590 Stötter, J., 1990. Geomorphologische und landschaftsgeschichtliche Untersuchungen im  
1591 Svarfaðardalur-Skiðadalur, Tröllaskagi, N-Island. *Münchener Geogr.*  
1592 *Abhandlungen* 9.
- 1593 Stötter, J., Wastl, M., Caseldine, C., Häberle, T., 1999. Holocene palaeoclimatic  
1594 reconstruction in northern Iceland: Approaches and results. *Quat. Sci. Rev.* 18,  
1595 457–474. doi:10.1016/S0277-3791(98)00029-8
- 1596 Tanarro, L.M., Palacios, D., Andrés, N., Fernández-Fernández, J.M., Zamorano, J.J.,  
1597 Sæmundsson, Þ., Brynjólfsson, S., 2019. Unchanged surface morphology in debris-  
1598 covered glaciers and rock glaciers in Tröllaskagi peninsula (northern Iceland). *Sci.*  
1599 *Total Environ.* 648, 218–235. <https://doi.org/10.1016/j.scitotenv.2018.07.460>

- 1600 Thompson, A., Jones, A., 1986. Rates and causes of proglacial river terrace formation in  
1601 southeast Iceland: an application of lichenometric dating techniques. *Boreas* 15,  
1602 231–246. doi:10.1111/j.1502-3885.1986.tb00928.x
- 1603 Van der Veen, C.J., 1999. *Fundamentals of glacier dynamics*. Balkema, Rotterdam.
- 1604 Wagner, S., Zorita, E., 2005. The influence of volcanic, solar and CO<sub>2</sub> forcing on the  
1605 temperatures in the Dalton Minimum (1790-1830): A model study. *Clim. Dyn.* 25,  
1606 205–218. doi:10.1007/s00382-005-0029-0
- 1607 Wanner, H., Beer, J., Bütikofer, J., Crowley, T.J., Cubasch, U., Flückiger, J., Goosse,  
1608 H., Grosjean, M., Joos, F., Kaplan, J.O., Küttel, M., Müller, S.A., Prentice, I.C.,  
1609 Solomina, O., Stocker, T.F., Tarasov, P., Wagner, M., Widmann, M., 2008. Mid- to  
1610 Late Holocene climate change: an overview. *Quat. Sci. Rev.* 27, 1791–1828.  
1611 doi:10.1016/j.quascirev.2008.06.013
- 1612 Wastl, M., Stötter, J., 2005. 9. Holocene glacier history, in: *Developments in*  
1613 *Quaternary Science*. pp. 221–240. doi:10.1016/S1571-0866(05)80011-9
- 1614 Wiles, G.C., Barclay, D.J., Young, N.E., 2010. A review of lichenometric dating of  
1615 glacial moraines in Alaska. *Geogr. Ann. Ser. A Phys. Geogr.* 92, 101–109.  
1616 doi:10.1111/j.1468-0459.2010.00380.x
- 1617 Winkler, S., 2003. A new interpretation of the date of the “Little Ice Age” glacier  
1618 maximum at Svartisen and Okstindan, northern Norway. *Holocene* 13, 83–95.  
1619 doi:10.1191/0959683603hl573rp
- 1620 Xiao, X., Zhao, M., Knudsen, K.L., Sha, L., Eiríksson, J., Gudmundsdóttir, E., Jiang,  
1621 H., Guo, Z., 2017. Deglacial and Holocene sea–ice variability north of Iceland and  
1622 response to ocean circulation changes. *Earth Planet. Sci. Lett.* 472, 14–24.  
1623 doi:10.1016/J.EPSL.2017.05.006
- 1624 Young, N.E., Schweinsberg, A.D., Briner, J.P., Schaefer, J.M., 2015. Glacier maxima in  
1625 Baffin Bay during the Medieval Warm Period coeval with Norse settlement. *Sci.*  
1626 *Adv.* 1. doi:10.1126/sciadv.1500806
- 1627 Zhong, Y., Miller, G.H., Otto-Bliesner, B.L., Holland, M.M., Bailey, D.A., Schneider,  
1628 D.P., Geirsdóttir, A., 2011. Centennial-scale climate change from decadal-paced  
1629 explosive volcanism: a coupled sea ice-ocean mechanism. *Clim. Dyn.* 37, 2373–  
1630 2387. doi:10.1007/s00382-010-0967-z
- 1631 Zweck, C., Zreda, M., Desilets, D., 2013. Snow shielding factors for cosmogenic  
1632 nuclide dating inferred from Monte Carlo neutron transport simulations. *Earth*  
1633 *Planet. Sci. Lett.* 379, 64–71. doi:10.1016/J.EPSL.2013.07.023
- 1634

1635 **Figure captions.**

1636 Figure 1. Location of the Tungnahryggsjökull glaciers and their forelands (C)  
1637 (Vesturdalur and Austurdalur) in the context of Iceland (A) and the Tröllaskagi  
1638 peninsula (B). The red boxes in panels A and B are panels B and C, respectively. The  
1639 figure also includes the location of the place names mentioned throughout the paper.  
1640 This figure is available in colour in the online version.

1641 Figure 2. Geomorphological map of the Vesturdalur foreland. (A) General view of the  
1642 Western Tungnahryggsjökull foreland. (B) Detailed moraine mapping and glacier  
1643 margin geometry reconstructed throughout the different glacial stages identified, and  
1644  $^{36}\text{Cl}$  CRE and lichenometric dating results (both are expressed in ages and calendar  
1645 years). Note that stages 13, 14, 15 and 16 correspond to the years 1946, 1985, 1994 and  
1646 2000. The surface-contoured glacier (white) corresponds to the year 2005 (stage 17).  
1647 The abbreviations “Rg” and “Ps” in lichenometry stations indicate that the estimated  
1648 dates are derived from the *Rhizocarpon geographicum* and *Porpidia sore dizodes*  
1649 lichens, respectively, and the number correspond to the longest axis of the largest lichen  
1650 measured. This figure is available in colour in the online version.

1651 Figure 3. Geomorphological map of the Austurdalur foreland. (A) General view of the  
1652 Eastern Tungnahryggsjökull foreland. (B) Detailed moraine mapping and glacier margin  
1653 geometry reconstructed throughout the different glacial stages identified, and  $^{36}\text{Cl}$  CRE  
1654 and lichenometric dating results (both are expressed in ages and calendar years). Note  
1655 that stages 11, 15 and 16 correspond to the years 1946, 1985 and 2000. The surface-  
1656 contoured glacier (white) corresponds to the year 2005 (stage 17). The abbreviations  
1657 “Rg” and “Ps” in lichenometry stations indicate that the estimated dates are derived  
1658 from the *Rhizocarpon geographicum* and *Porpidia sore dizodes* lichens, respectively,

1659 and the number correspond to the longest axis of the largest lichen measured. This  
1660 figure is available in colour in the online version.

1661 Figure 4.  $^{36}\text{Cl}$  CRE ages and internal (analytical) uncertainty at  $1\sigma$  level of the samples  
1662 from Vesturdalur and Austurdalur. Note that the samples clustering around 500 yr (15<sup>th</sup>  
1663 century) in Austurdalur are indistinguishable. Distance to the terminus (year 2005) is  
1664 measured along the flowline from the reconstructed snout apex of the phase where the  
1665 samples were collected. This figure is available in colour in the online version.

1666 Figure 5. Correlation between largest thalli (longest axis) of species *Rhizocarpon*  
1667 *geographicum* and *Porpidia* cf. *soredizodes* in several lichenometry stations. With the  
1668 aim of avoiding those lichens potentially affected for any environmental factor  
1669 disturbing their normal growth, the largest lichens used come from those lichenometry  
1670 stations where no lichen size decrease with increasing distance to the terminus was  
1671 observed (i.e., TUV-2, TUV-4, TUV-5, TUV-6, TUV-2, TUE-4 and TUE-5). From  
1672 the measurements, it appears that *Porpidia* cf. *soredizodes* lichens grow faster than  
1673 those of *Rhizocarpon geographicum*.

1674

1675 **Table captions**

1676 Table 1. Glacial Equilibrium-Line Altitudes (ELAs) calculated over  
1677 Tungnahryggsjökull glaciers through the application of the AAR and AABR methods  
1678 over the 3D glacier reconstructions.

1679 Table 2. Surface ages estimated from [Kugelmann's \(1991\)](#) 0.44 mm yr<sup>-1</sup> growth rate for  
1680 different colonization lags. The ages obtained from *Rhizocarpon geographicum* lichens  
1681 discussed throughout the text are those derived from a 20-yr colonization lag. The  
1682 figures in italics correspond to ages tentatively inferred from the largest *Porpidia*  
1683 *soredizodes* lichen, assuming a 0.737 mm yr<sup>-1</sup> growth rate and a 15-year colonization  
1684 lag (see section 5.2.1).

1685 Table 3. <sup>36</sup>Cl CRE ages converted to CE/BCE dates according to the different <sup>36</sup>Cl  
1686 production rates from Ca spallation. Uncertainties include the analytical and production  
1687 rate error.

1688 **Supplementary figures captions**

1689 SF1. Examples of *Rhizocarpon geographicum* group and *Porpidia soledizodes* thalli  
1690 measured over scaled field photos from the lichenometric station TUW-3. The lines  
1691 refer to the minimum circle (white) bounding the thalli outlines (yellow) and the  
1692 diameter of the circle (black). Note the contrasted size of the largest thalli in the  
1693 different species.

1694 SF2. Location of the lichenometry stations in relation to the glacier snout position  
1695 shown in the different aerial photographs and the satellite image. The lines refer to the  
1696 glacier margin outlined over the aerial photo at a specific date (red) and at the previous  
1697 date with aerial photo available (green dashed line). The points display the location of  
1698 the lichenometry stations. The aerial photos provide the dating control for the validation  
1699 of the lichenometric dates.

1700 SF3. Glacier surface reconstruction for the CRE- and lichenometry-dated glacial stages.

1701 SF4. Examples of moraine boulders sampled for  $^{36}\text{Cl}$  CRE dating in Vesturdalur  
1702 (“TUW” samples) and Austurdalur (“TUE” samples) and their dates derived from the  
1703 [Licciardi et al. \(2008\)](#)  $^{36}\text{Cl}$  production rate from Ca spallation.

1704 SF5. Location and BCE dates of the  $^{36}\text{Cl}$  samples from the Elliði crest.

1705 **Supplementary tables captions.**

1706 ST1. Correspondence between glacial stages mapped over historical aerial photos and  
1707 the dates.

1708 ST2. Glacier length and snout position variations measured along the flowline.

1709 ST3. Glacier extent and volume variations calculated from 2D and 3D glacier  
1710 reconstructions.

1711 ST4. Size of the largest lichen at the lichenometry stations in the forelands of the  
1712 western and eastern Tungnahryggsjökull glaciers.

1713 ST5. Geographic sample locations, topographic shielding factor, sample thickness and  
1714 distance from terminus.

1715 ST6. Chemical composition of the bulk rock samples before chemical treatment. The  
1716 figures in *italic* correspond to the average values of the bulk samples analysed and were  
1717 those used for the age-exposure calculations of the samples without bulk chemical  
1718 composition analysis.

1719 ST7. Concentrations of the  $^{36}\text{Cl}$  target elements Ca, K, Ti and Fe, determined in splits  
1720 taken after the chemical pre-treatment (acid etching).

1721 ST8.  $^{36}\text{Cl}$  analytical data and CRE dating results according to different  $^{36}\text{Cl}$  production  
1722 rates from Ca spallation.  $^{36}\text{Cl}/^{35}\text{Cl}$  and  $^{35}\text{Cl}/^{37}\text{Cl}$  ratios were inferred from measurements  
1723 at the ASTER AMS facility. The numbers in *italic* correspond to the internal  
1724 (analytical) uncertainty at  $1\sigma$  level.

**Table 1**[Click here to download Table: Table\\_1.docx](#)

| Stage | W Tungnahryggsjökull |          |                       |          | E Tungnahryggsjökull |          |                       |          |
|-------|----------------------|----------|-----------------------|----------|----------------------|----------|-----------------------|----------|
|       | <i>AAR (0.67)</i>    | $\Delta$ | <i>AABR (1.5±0.4)</i> | $\Delta$ | <i>AAR (0.67)</i>    | $\Delta$ | <i>AABR (1.5±0.4)</i> | $\Delta$ |
| 1     | 1021                 | -        | 1006 +25/-20          | -        | 1032                 | -        | 1027 ±20              | -        |
| 2     | 1047                 | +26      | 1032 ±20              | +26      | 1032                 | 0        | 1032 ±15              | +5       |
| 3     | 1052                 | +5       | 1037 +20/-15          | +5       | 1034                 | +2       | 1034 ±15              | +2       |
| 4     | 1054                 | +2       | 1049 +20/-15          | +12      | 1037                 | +3       | 1037 ±15              | +3       |
| 5     | 1059                 | +5       | 1059 ±15              | +10      | 1041                 | +4       | 1041 ±15              | +4       |
| 6     | 1067                 | +8       | 1062 +20/-10          | +3       | 1042                 | +1       | 1042 ±15              | +1       |
| 7     | 1072                 | +5       | 1072 +15/-10          | +10      | 1046                 | +5       | 1046 ±15              | +5       |
| 8     | 1076                 | +4       | 1081 ±15              | +9       | 1047                 | +1       | 1052 ±15              | +6       |
| 9     | 1082                 | +6       | 1087 +15/-10          | +6       | 1054                 | +7       | 1054 +15/-10          | +2       |
| 10    | 1086                 | +4       | 1091 +15/-10          | +4       | 1055                 | +1       | 1060 +15/-10          | +6       |
| 11    | 1094                 | +8       | 1099 +15/-10          | +8       | 1061                 | +6       | 1071 ±10              | +11      |
| 12    | 1094                 | 0        | 1099 +15/-5           | 0        | 1060                 | -1       | 1070 ±10              | -1       |
| 13    | 1094                 | 0        | 1099 +15/-5           | 0        | 1061                 | +1       | 1071 +15/-10          | +1       |
| 14    | 1100                 | +6       | 1110 ±10              | +11      | 1060                 | -1       | 1075 ±10              | +4       |
| 15    | 1102                 | +2       | 1107 +15/-5           | -3       | 1061                 | +1       | 1076 +15/-10          | +1       |
| 16    | 1098                 | -4       | 1108 +10/-5           | +1       | 1061                 | 0        | 1076 ±10              | 0        |
| 17    | 1099                 | +1       | 1109 +15/-5           | +1       | 1065                 | +4       | 1080 ±10              | +4       |

**Table 1. Glacial Equilibrium-Line Altitudes (ELAs) calculated over Tungnahryggsjökull glaciers through the application of the AAR and AABR methods over the 3D glacier reconstructions. Delta ( $\Delta$ ) is referred to the change with respect to the previous stage.**

Table 2

[Click here to download Table: Table\\_2.docx](#)

| Glacier foreland        | Lichen station | Glacial stage | Date deduced from photographic evidence | Surface date from growth rate |                 |                |                 |                |
|-------------------------|----------------|---------------|---|-------------------------------|-----------------|----------------|-----------------|----------------|
|                         |                |               |   | 10-yr col. lag                | 15-yr col. lag. | 20-yr col. lag | 25-yr col. lag. | 30-yr col. lag |
| W<br>Tungnahryggsjökull | TUW-1          | 15-16         | 1994-2000                               | <i>1980*</i>                  | <i>1975*</i>    | <i>1970*</i>   | <i>1965*</i>    | <i>1960*</i>   |
|                         | TUW-2          | 13-15         | 1946-1994                               | 1961                          | 1956            | 1951           | 1946            | 1941*          |
|                         | TUW-3          | 12-13         | <1946                                   | 1950*                         | 1945            | 1940           | 1935            | 1930           |
|                         | TUW-4          | 12            | <1946                                   | 1925                          | 1920            | 1915           | 1910            | 1905           |
|                         | TUW-5          | 11            | <1946                                   | 1904                          | 1899            | 1894           | 1889            | 1884           |
|                         | TUW-6          | 10            | <1946                                   | 1854                          | 1849            | 1844           | 1839            | 1834           |
|                         | TUW-7          | 9             | <1946                                   | 1842                          | 1837            | 1832           | 1827            | 1822           |
|                         | TUW-8          | 8             | <1946                                   | <i>1804</i>                   | <i>1799</i>     | <i>1794</i>    | <i>1789</i>     | <i>1784</i>    |
| E<br>Tungnahryggsjökull | TUE-0          | post-17       | 2005<                                   | -                             | -               | -              | -               | -              |
|                         | TUE-1          | 14            | 1946-1985                               | <i>1982</i>                   | <i>1977</i>     | <i>1972</i>    | <i>1967</i>     | <i>1962</i>    |
|                         | TUE-2          | 13            | 1946-1985                               | 1962                          | 1957            | 1952           | 1947            | 1942*          |
|                         | TUE-3          | 12            | 1946-1985                               | 1943*                         | 1938*           | 1933*          | 1928*           | 1923*          |
|                         | TUE-4          | 11            | <1946                                   | 1925                          | 1920            | 1915           | 1910            | 1905           |
|                         | TUE-5          | 10            | <1946                                   | 1879                          | 1874            | 1869           | 1864            | 1859           |
|                         | TUE-6          | 9             | <1946                                   | 1901**                        | 1896**          | 1891**         | 1886**          | 1881**         |
|                         | TUE-7          | 7             | <1946                                   | 1896**                        | 1891**          | 1886**         | 1881**          | 1876**         |
|                         | TUE-8          | 7             | <1946                                   | <i>1813</i>                   | <i>1808</i>     | <i>1803</i>    | <i>1798</i>     | <i>1793</i>    |

**Comment [JM1]:** Asumiendo que el sector del frente en el que se encuentra el bloque, ha permanecido estático, estable desde 1946

Table 2. Surface exposure ages estimated from Kugelmann's (1991)  $0.44 \text{ mm yr}^{-1}$  growth rate for different colonization lags. The stars indicate that either the date does not agree with the date deduced from aerial photos (\*) or the date is incoherent with the moraine chronostratigraphy (\*\*). The figures in italics correspond to dates tentatively inferred from the largest *Porpidia soledizodes* lichen, assuming a  $0.737 \text{ mm yr}^{-1}$  growth rate and a 10-year colonization lag.

**Table 3**[Click here to download Table: Table\\_3.docx](#)**Table 3.  $^{36}\text{Cl}$  CRE ages converted to CE/BCE dates according to the different  $^{36}\text{Cl}$  production rates from Ca spallation. Uncertainties include the analytical and production rate error.**

| Sample name  | Dates (CE/BCE)  |   |   |
|--|---|---|---|
|  | <a href="#">Licciardi et al. (2008)</a><br>Ca spallation prod. rate | <a href="#">Stone et al. (1996)</a> Ca<br>spallation prod. rate | <a href="#">Schimmelpfennig et al. (2011)</a> Ca<br>spallation prod. rate |
| <i>Moraine boulders at Vesturdalur (W Tungnahryggsjökull foreland)</i> |   |   |   |
| TUW-9  | 1590 ± 100  | 1570±100  | 1520±120  |
| TUW-10   | 1640±90   | 1620±90   | 1580±110  |
| TUW-11   | 1480±120  | 1470±120  | 1420±140  |
| TUW-12   | 1450±100  | 1430±110  | 1370±120  |
| TUW-13   | 1470±130  | 1450±130  | 1400±150  |
| TUW-14   | 670±210   | 620±210   | 500±250   |
| TUW-15   | 1460±110  | 1430±110  | 1370±120  |
| TUW-16   | 1220±190  | 1200±190  | 1130±210  |
| <i>Moraine boulders at Austurdalur (E Tungnahryggsjökull foreland)</i> |   |   |   |
| TUE-9  | 740±170   | 660±170   | 510±210   |
| TUE-10   | 1460±100  | 1430±100  | 1360±120  |
| TUE-11   | 380±200   | 290±200   | 110±250   |
| TUE-12   | 400±200   | 320±190   | 150±240   |
| <i>Glacially polished ridge Elliði</i>                                 |   |   |   |
| ELLID-1  | 14300±1700  | 14900±1600  | 16600±2100  |
| ELLID-2  | 14200±1700  | 14800±1700  | 16500±2100  |

Figure 1  
[Click here to download high resolution image](#)

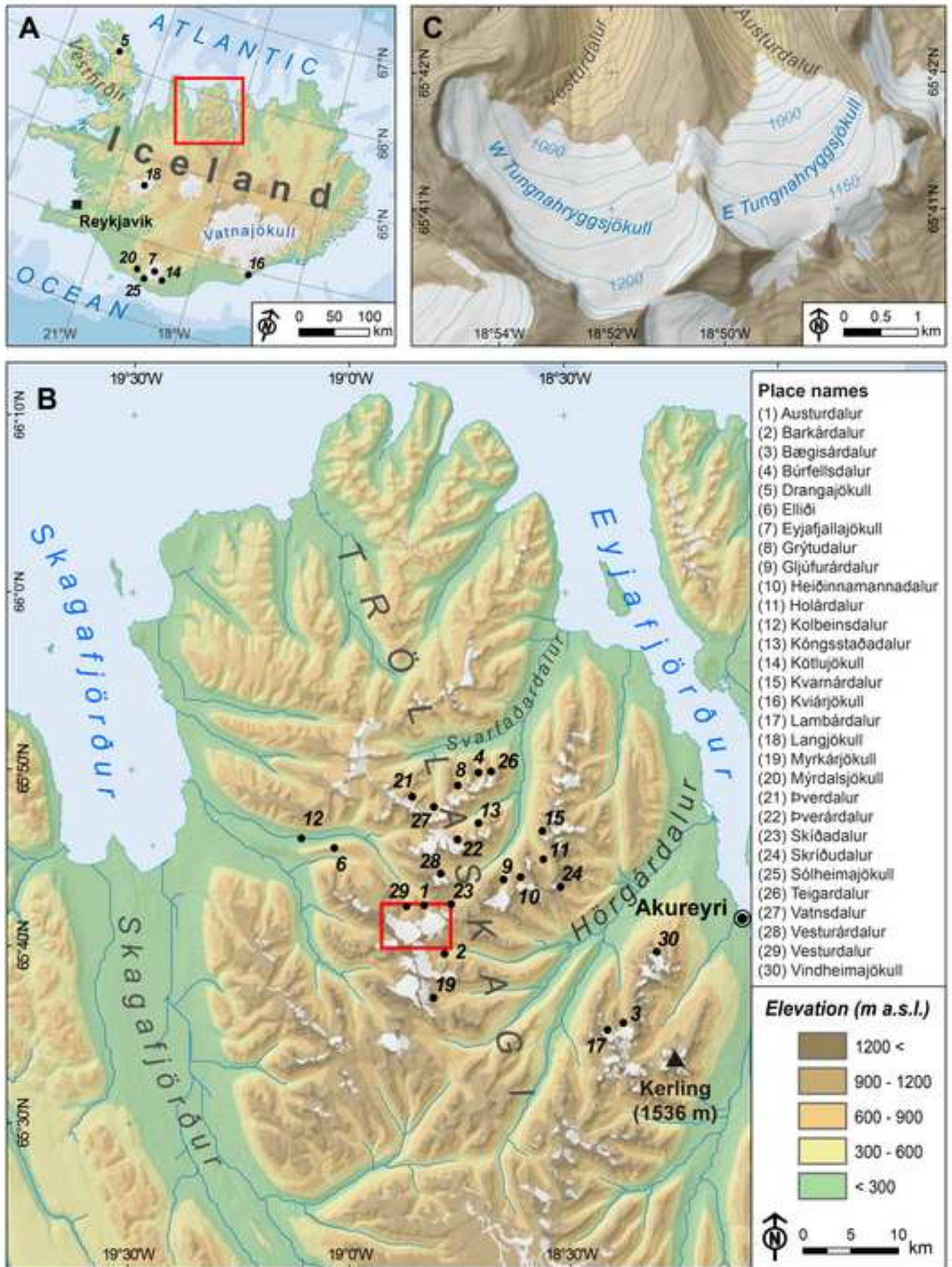


Figure 2

[Click here to download high resolution image](#)

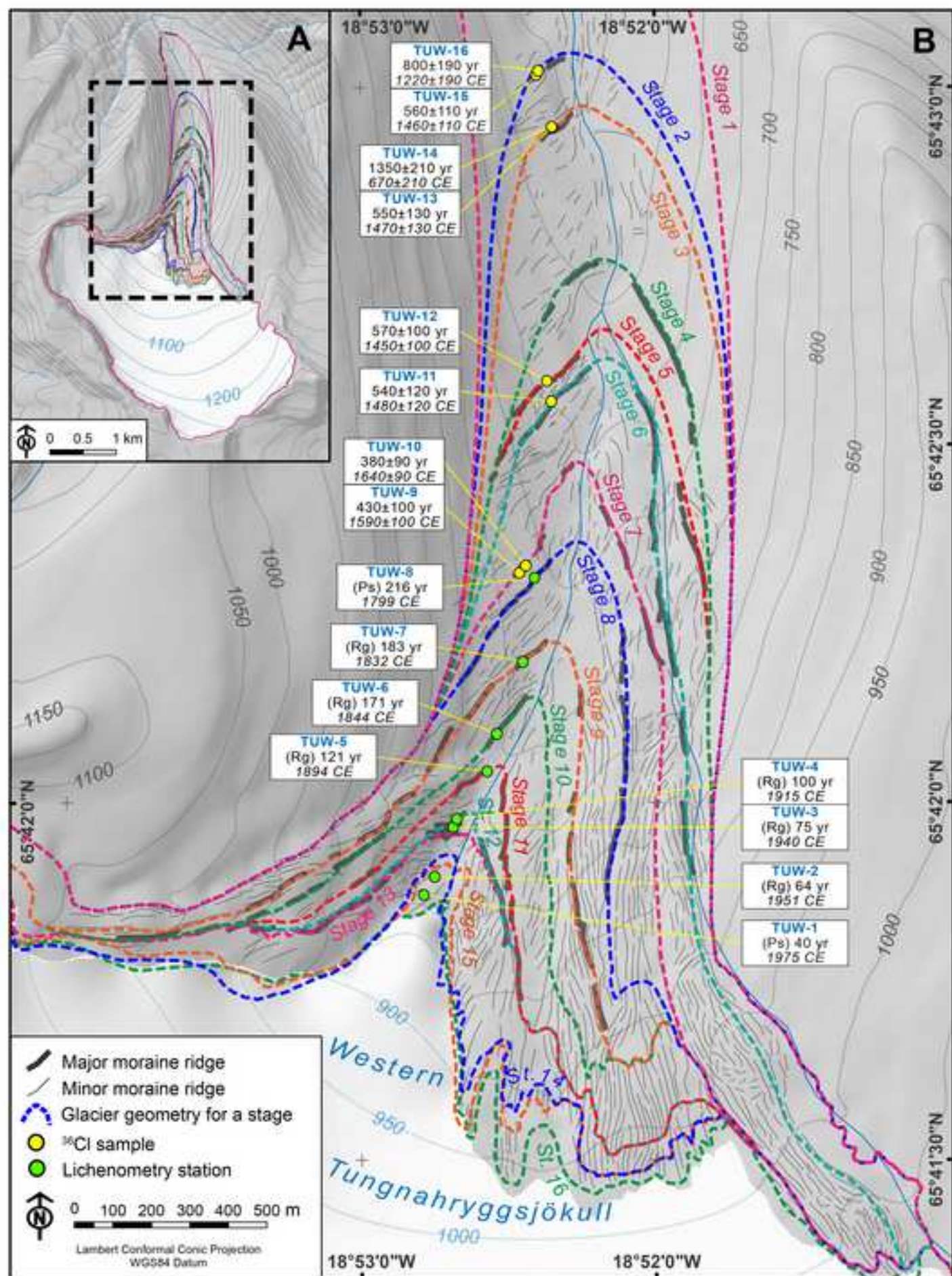


Figure 3  
[Click here to download high resolution image](#)

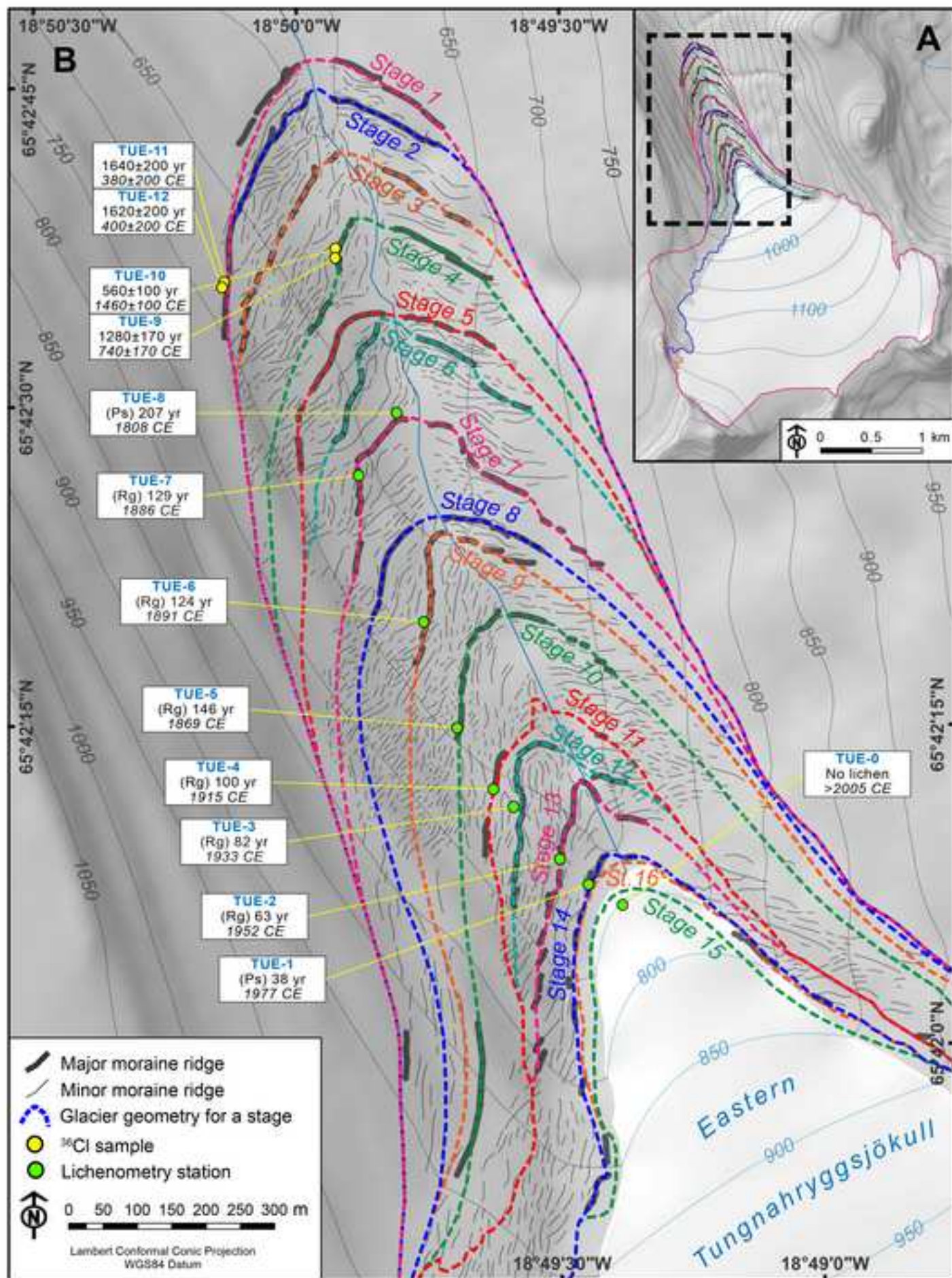


Figure 4  
[Click here to download high resolution image](#)

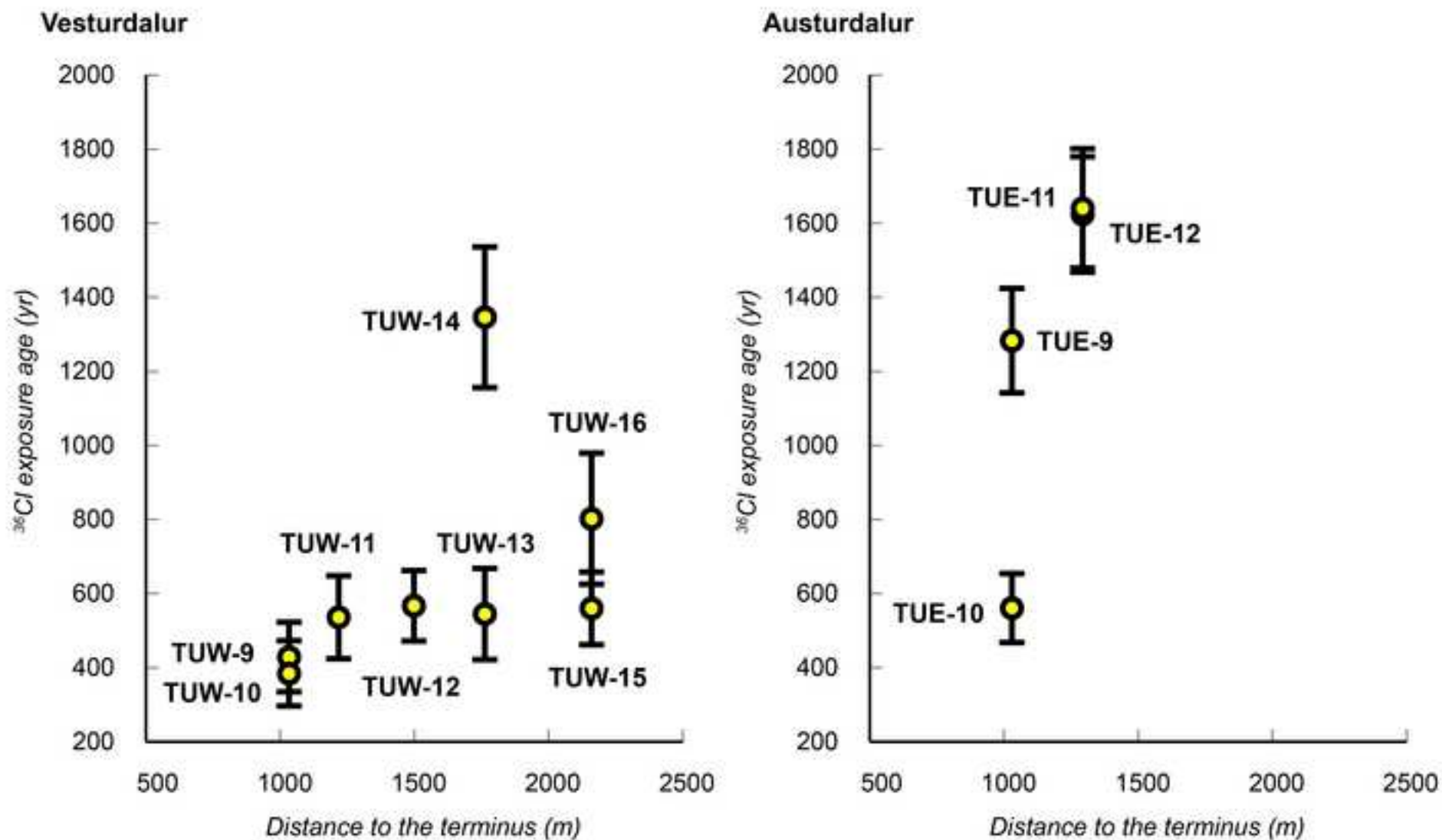
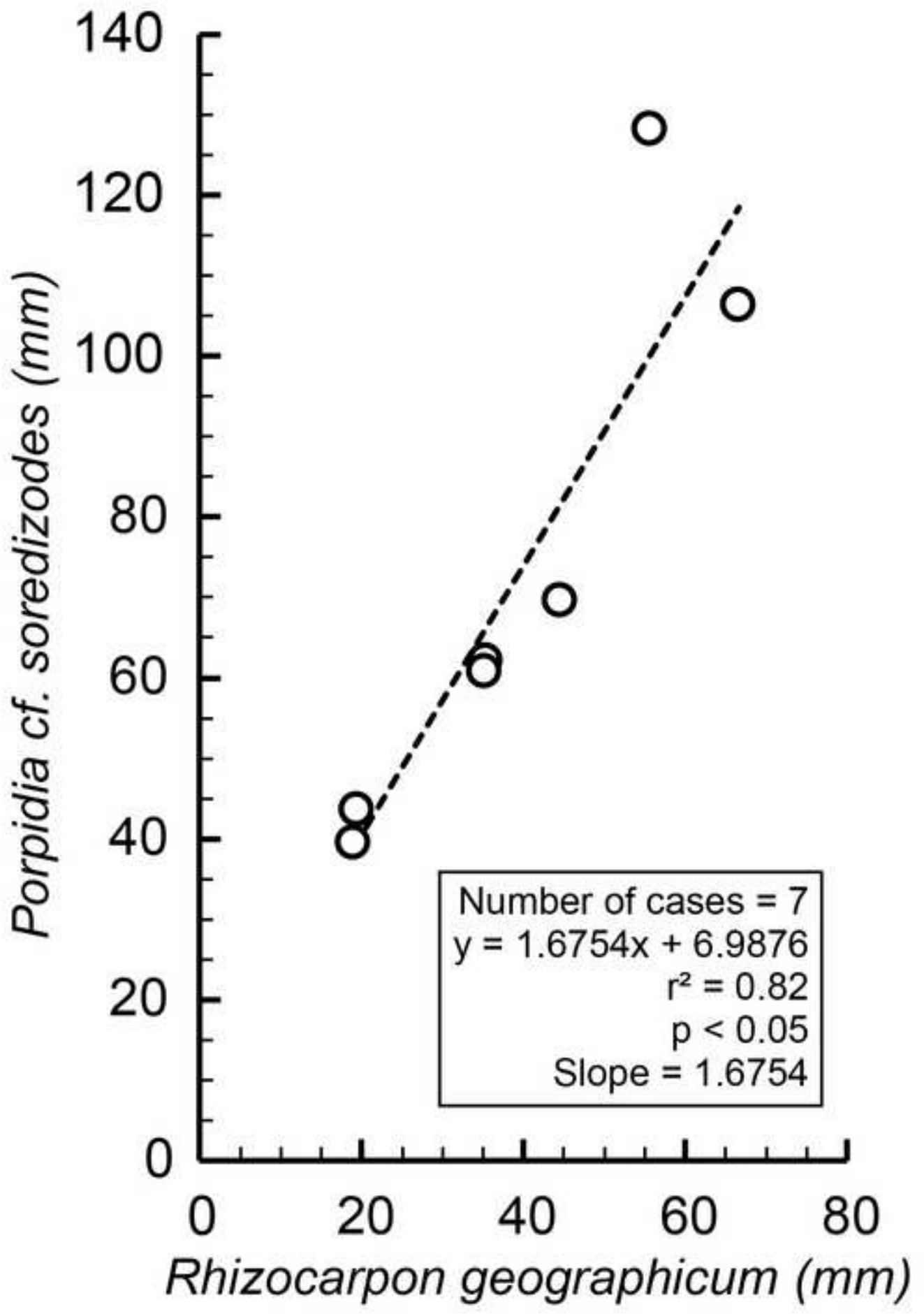


Figure 5  
[Click here to download high resolution image](#)



**Supplementary figure SF1**

[Click here to download Supplementary material for on-line publication only: Supp\\_data\\_S1.jpg](#)

**Supplementary figure SF2**

[Click here to download Supplementary material for on-line publication only: Supp\\_data\\_S2.jpg](#)

**Supplementary figure SF3**

[Click here to download Supplementary material for on-line publication only: Supp\\_data\\_S3.jpg](#)

**Supplementary figure SF4**

[Click here to download Supplementary material for on-line publication only: Supp\\_data\\_S4.jpg](#)

**Supplementary figure SF5**

[Click here to download Supplementary material for on-line publication only: Supp\\_data\\_S5.jpg](#)

**Supplementary table ST1**

[Click here to download Supplementary material for on-line publication only: Supp\\_table\\_ST1.docx](#)

**Supplementary table ST2**

[Click here to download Supplementary material for on-line publication only: Supp\\_table\\_ST2.docx](#)

**Supplementary table ST3**

[Click here to download Supplementary material for on-line publication only: Supp\\_table\\_ST3.docx](#)

**Supplementary table ST4**

[Click here to download Supplementary material for on-line publication only: Supp\\_table\\_ST4.docx](#)

**Supplementary table ST5**

[Click here to download Supplementary material for on-line publication only: Supp\\_table\\_ST5.docx](#)

**Supplementary table ST6**

[Click here to download Supplementary material for on-line publication only: Supp\\_table\\_ST6.docx](#)

**Supplementary table ST7**

[Click here to download Supplementary material for on-line publication only: Supp\\_table\\_ST7.docx](#)

**Supplementary table ST8**

[Click here to download Supplementary material for on-line publication only: Supp\\_table\\_ST8.docx](#)